In compliance with the
Canadian Privacy Legislation
some supporting forms
may have been removed from
this dissertation.

While these forms may be included
in the document page count,
their removal does not represent
any loss of content from the dissertation.

The University of Alberta

ALTERATIONS IN CARDIAC FATTY ACID OXIDATION INDUCED BY NUTRITIONAL DEFICIENCY AND *IN VIVO* GENE TRANSFER

by

Emily Louise Manning

A thesis submitted to the Faculty of Graduate Studies and Research in partial fulfillment of the requirements
for the degree of Master of Science

Department of Pharmacology

Edmonton, Alberta

Fall 2003

National Library
of Canada

Acquisitions and
Bibliographic Services

395 Wellington Street
Ottawa ON K1A 0N4
Canada

Bibliothèque nationale
du Canada

Acquisisitons et
services bibliographiques

395, rue Wellington
Ottawa ON K1A 0N4
Canada

Your file Votre référence
ISBN: 0-612-87823-6
Our file Notre référence
ISBN: 0-612-87823-6

The author has granted a non-exclusive licence allowing the National Library of Canada to reproduce, loan, distribute or sell copies of this thesis in microform, paper or electronic formats.

The author retains ownership of the copyright in this thesis. Neither the thesis nor substantial extracts from it may be printed or otherwise reproduced without the author's permission.

L'auteur a accordé une licence non exclusive permettant à la Bibliothèque nationale du Canada de reproduire, prêter, distribuer ou vendre des copies de cette thèse sous la forme de microfiche/film, de reproduction sur papier ou sur format électronique.

L'auteur conserve la propriété du droit d'auteur qui protège cette thèse. Ni la thèse ni des extraits substantiels de celle-ci ne doivent être imprimés ou aturement reproduits sans son autorisation.

Canada

University of Alberta

Library Release Form

Name of Author: Emily Manning

Title of Thesis: Alterations in Cardiac Fatty Acid Oxidation Induced by Nutritional Deficiency and *in vivo* Gene Transfer.

Degree: Master of Science

Year This Degree Granted: Fall 2003

Permission is hereby granted to the University of Alberta Library to reproduce single copies of this thesis and to lend or sell such copies for private, scholarly or scientific research purposes only.

The author reserves all other publication and other rights in association with the copyrights in the thesis, and except as herein before provided, neither the thesis nor any substantial portion thereof may be printed or otherwise reproduced in any material form whatever without the author's prior written permission.

Date Submitted: July 22 2003

UNIVERSITY OF ALBERTA

FACULTY OF GRADUATE STUDIES AND RESEARCH

The undersigned certify that they have read, and recommend to the Faculty of Graduate Studies and Research for acceptance, a thesis entitled Alterations in Cardiac Fatty Acid Oxidation Induced by Nutritional Deficiency and *in vivo* Gene Transfer, submitted by Emily Louise Manning in partial fulfillment of the requirements for the degree of Master of Science.

Dr. Gary Lopaschuk (Supervisor)

Dr. Jason Dyck

Dr. Peter Light

Date: July 16, 2003

ABSTRACT

The heart derives the majority of its energy requirements from the oxidation of fatty acids and glucose. During states of nutritional deficiency, cardiac reliance of the oxidation of fatty acids increases at the expense of glucose oxidation. Since a key rate-limiting step of fatty acid oxidation is carnitine palmitoylcarnitine type 1 (CPT-1) which is regulated by malonyl CoA levels, we examined whether the expression levels of the enzymes that regulate the levels malonyl CoA are increased during nutritional deficiency. We demonstrate that the increase in fatty acid oxidation noted during fasting is not noted in the presence of an increased expression of acetyl CoA carboxylase (ACC), malonyl CoA decarboxylase (MCD) or 5' AMP activated protein kinase (AMPK). Additionally, we examined whether *in vivo* intracoronary delivery of constitutively active AMPK would result in increased fatty acid oxidation. However, due to the low efficiency of gene delivery noted following intracoronary delivery, we were unable to determine the metabolic effects of this over-expression and the study evolved to one where different gene delivery techniques were examined for efficiency of gene delivery to the myocyte.

ACKNOWLEDGEMENTS

I would like to thank my parents and sister for their unconditional love, support and encouragement during the pursuit of my Master's Degree. Without their support, I would never have accomplished this task.

I am additionally grateful to my supervisor Dr. Gary Lopaschuk for taking a chance on me, allowing me to pursue my degree in his laboratory and funding me through the process.

I would also like to thank the other members of my supervisory committee, Dr. Jason Dyck and Dr. Peter Light, for their constant input and support of my thesis.

I would like to thank Dr. Martin Spoor for all his help in teaching me the technical aspects of surgery.

A special note of gratitude must be given to Dr. Ken Walsh and Dr. Kaori Sato at the Boston University Medical Center for so kindly inviting me down to learn the intracoronary gene delivery technique.

I am particularly grateful to my fellow graduate students and technicians in Dr. Lopaschuk's lab, the Cardiovascular Research Group and the Pharmacology Department, especially Teresa Hopkins, Mary Collinson, Jason Iden, Jay Jaswal, Clifford Folmes, Arzu Besiki, Judith Altarejos, Mike Kuang and Amy Barr. Without the help and friendship of these people, I would have not been able to complete my Masters, or remain sane during the process.

I would like to thank all the members of the Cardiovascular Research Group and MMRL - I can not imagine having a better working and learning environment.

Thank you to Lynn Eisner and Dr. Wilma Suarez-Pinzon for helping me with the cardiac myocyte isolation technique, heart fixation and embedding techniques.

Finally, I would like to thank all my non-scientifically inclined friends for their support, especially my fabulous roomies at the Barry-ManHole - Charlotte and Joanne. I also appreciate the support of my friends Niki, Trish, Jen, Ryan, Mike, Dennis, Vanessa, Samir and everyone else who listened to my ideas and nodded approvingly, regardless of whether they understood the ideas or not. I love you all.

DEDICATION

This thesis is dedicated entirely to my parents, Carol and Robert Manning. I cannot even begin to express my gratitude to you. You have always supported and encouraged my dreams while providing suggestions on how to achieve them. Mom, I am so grateful that you were constantly supportive of me and my research. Dad, I so greatly appreciate that you took such sincere interest in my research and even managed to get the scientific lingo down.

I have said it once and I will say it again – in return for the 'full parental support', I promise to provide you with full access to the finest nursing homes. And yes, I will make sure they have a BBC cable feed.

I love you both so much.

TABLE OF CONTENTS

1. INTRODUCTION 1
- Cardiac Metabolism 2
- Fasting Effects on Cardiac Metabolism 6
- PPARα and Its Role in Regulating Fatty Acid Oxidation 6
- Gene Therapy 8
- Cardiovascular Gene Therapy 9
- Intracoronary Gene Delivery Technique 11
- Direct Myocardial Injection Technique 13
- Adenovirus as Gene Vector 15
- Adenovirus Replication and Early Transcription Genes 16
- Adenovirus Infection of Cardiac Myocytes 17
- Reporter Genes 20
- Green Fluorescent Protein 20
- AMPK as an Experimental Gene 24
- Endothelial Barrier 26
- Hypothesis and Objectives 27
- References 29

2. METHODS AND MATERIALS 45
- Materials 46
- Methods 47
  - Animals 47
  - Preparation of Hearts for Working Heart Model 48
  - Assessment of Mechanical Function of the Isolated Working Rat Heart 51
  - Assessment of Fatty Acid Oxidation in the Isolated Working Rat Heart 51
  - Wet to Dry Weight Ratio Determination 52
  - Malonyl CoA Decarboxylase Activity Assay 52

Tissue Triacylglycerol Determination 54
[^{3}H] Palmitate Incorporation into Endogenous TG Stores 55
Fatty Acid Uptake into the Heart 55
Plasma Measurements 56
Tissue CoA Extractions 57
Recombinant Adenoviral Formation 57
Sub-cloning DNA and Cutting of Shuttle Vector 57
Generation of Recombinant Adenoviral Plasmids 58
Homologous Recombination 59
Sceening for Recombinants 59
Production of Adenovirus in Mammalian Cells 59
Testing of Virus 60
Large Scale Adenovirus Production 61
Cesium Chloride Gradient 62
Dialysis 62
Adenovirus Storage 63
Titering of Virus 63
Preparation of Rats for Surgery 64
Intubation and Ventilation 64
Thoracotomy 65
Preparation of Hearts for Viral Gene Delivery 66
Intracoronary Viral Gene Delivery 69
Intracoronary Delivery with Histamine 69
Direct Myocardial Gene Delivery 70
Suturing and Post-Surgical Care 73
Assessment of Cardiac Protein Expression 74
Immunoblot Analysis 74
Determination of Protein Expression 75
Densitometric Analysis 75
Cardiac Myocyte Isolation 77
Solution Preparation 77
Equipment Preparation 78
Rat Preparation 78
Cardiac Myocyte Isolation 79
Additional Examination of Direct Injection Hearts 80

Preparation of Heart Slices for GFP Fluorescence Analysis 80
Histological Analysis of GFP 80
Statistics 81
References 82

3. The Fasting-Induced Increase of PPARα Expression and Fatty Acid Oxidation Does Not Occur in Conjunction with Altered Expression of Malonyl CoA Decarboxylase, Acetyl CoA Carboxylase or 5' AMP-Activated Protein Kinase 85
Abstract 86
Introduction 88
Methods 90
Fasting Protocol 90
Heart Perfusion Protocol 90
Plasma Measurements 90
Tissue Extractions 90
Immunoblotting 91
MCD Activity 91
Statistics 91
Results 92
Perfusion Results from Control vs. Fasted Rats 92
Contribution of Acetyl CoA to TCA Cycle 92
MCD Activity Levels from Perfused Hearts 93
PPARα Expression Levels 93
Triacylglycerol Tissue Levels of Perfused Hearts 93
Plasma Triacylglyerol Levels 94
CoA Tissue Levels 95
Protein Expression Levels 95
Discussion 108
References 120

4. Cardiac *in vivo* Gene Therapy: A Cautionary Tale 127
Abstract 128
Introduction 131
Methods 134
Preparation of Recombinant Adenovirus 134
Animals 134
Surgical Procedure 134
Intracoronary Gene Delivery 134
Direct Myocardial Gene Delviery 134
Perfusions of Infected Hearts 135
Assessent of Cardiac Protein Expression 135
Cardiac Myocyte Isolation 135
In situ Visualization of GFP Expression 135
Preparation of Heart Slices for GFP Fluorescence Analysis 136
Statstics 136
Results 137
Perfusion Data 137
Determination of Myocardial GFP Content 137
Determination of Myocardial c-myc Content 137
Myocardial Akt Protein Content 138
Comparison of GFP Expression from Delivery Groups 138
Cardiac Myocyte Isolation 139
In situ Heart Fluorescent Microscopy 141
Localization of GFP Fluorescence in Heart Slices 142
Surgical Mortality 143
Discussion 165
Summary 182
References 183

5. DISCUSSION, LIMITATIONS AND FUTURE DIRECTIONS 188
Discussion and Conclusions 189
Limitations 191
Future Directions 193
References 195

LIST OF FIGURES

Figure 1-1. Overview of cardiac metabolism 5

Figure 1-2. Uptake and internalization of the adenovirus into the cells via the Coxsackie and Adenovirus Receptor (CAR) 19

Figure 1-3. The 3D structure of green fluorescent protein (GFP) 23

Figure 2-1. Rat anatomy 1 67

Figure 2-2. Rat anatomy 2 68

Figure 2-3. Method of intracoronary gene delivery 71

Figure 2-4. Method of direct myocardial gene delivery 72

Figure 3-1. Glucose and palmitate oxidation rates in isolated working hearts from control and 72 hour fasted rats 98

Figure 3-2. Acetyl CoA contribution to TCA cycle from glucose and palmitate oxidation 99

Figure 3-3. MCD expression and activity levels in hearts from control and 72 hour fasted rats 100

Figure 3-4. PPARα expression in hearts from control and 72 hour fasted rats . 101

Figure 3-5. ACC1 (265 kDa isoform) and ACC2 (280kDa isoform) expression in hearts from control and 72 hour fasted rats 105

Figure 3-6. Phospho-ACC1 (265 kDa isoform) and Phospho-ACC2 (280kDa isoform) expression in hearts from control and 72 hour fasted rats 106

Figure 3-7. AMPK and phospho-AMPK expression in hearts from control and 72 hour fasted rats 107

Figure 4-1. Glucose and palmitate oxidation rates in isolated working hearts from Ad-GFP and Ad-caAMPK-GFP infected hearts 145

Figure 4-2. Immunoblot of Ad-GFP and Ad-caAMPK-GFP infected hearts following perfusion 146

Figure 4-3. Immunoblot determining expression of c-myc in Ad-GFP and Ad-caAMPK-GFP infected hearts 147

Figure 4-4. Akt Expression in hearts infected with Ad-Akt1 148

Figure 4-5. Immunoblot results of Akt expression following intracoronary delivery of Ad-Akt1 149

Figure 4-6. Immunoblot of hearts infected with Ad-GFP using different gene delivery technique 150

Figure 4-7. Myocytes isolated from the left ventricle of a heart infected via the intracoronary gene delivery technique (without histamine) 151

Figure 4-8. Myocytes isolated from the left ventricle of a heart infected using the intracoronary gene delivery technique in the presence of histamine 152

Figure 4-9. Representative picture of myocytes isolated from the left ventricle of the heart infected via direct myocardial injection 153

Figure 4-10. Myocytes isolated from a visually confirmed area that was infected via the direct myocardial infection gene delivery technique 154

Figure 4-11. Comparison of gene delivery techniques via quantification of the percentage of myocytes infected 155

Figure 4-12. *In situ* visualization of heart infected with Ad-GFP through the intracoronary technique (with histamine) 157

Figure 4-13. *In situ* visualization of heart infected with Ad-GFP following direct myocardial injection 158

Figure 4-14. *In situ* visulalization of site directly injected with Ad-GFP 159

Figure 4-15. *In situ* visualization of aorta 160

Figure 4-16. Heart slices taken from an intracoronary infected heart and an uninfected control 161

Figure 4-17. Heart slice taken from a heart infected via the intracoronary technique (in the presence of histamine)..... 162

Figure 4-18. Slices taken from the hearts infected by the direct myocardial injection technique 163

LIST OF TABLES

Table 2.1. Immunoblotting Protocol 76

Table 3.1. Perfusion Functional Parameters of Control and Fasted Rats 97

Table 3.2. Tissue TG, Fatty Acid Uptake and ^{3}H-Palmitate Incorporation into Endogenous TG Stores in Control and Fasted Rats 102

Table 3.3. Plasma TG and Fatty Acid Levels in Control and Fasted Hearts 103

Table 3.4. Malonyl CoA and Acetyl CoA Measurements of Control and Fasted Hearts 104

Table 4.1. Perfusion Functional Parameters of Hears Infected Intracornarily with Ad-GFP and Ad-caAMPK-GFP 144

Table 4.2. Percentage of Myocytes Infected - Comparison of Different Gene Delivery Techniques 156

Table 4.3. Experimental Fate of Hearts Infected Through Different Gene Delivery Techniques 164

SYMBOLS AND ABBREVIATIONS

1° Ab ..... primary antibody
2° Ab ..... secondary antibody
α ..... alpha
β ..... beta
γ ..... gamma
°C ..... degrees celcius
% ..... percent
x g ..... times gravity – centrifugation speed
ACC ..... acetyl CoA carboxylase
Acetyl CoA ..... acetyl coenzyme A
ACS ..... acyl coA synthetase
AMP ..... adenosine monophoshate
AMPK ..... 5' AMP activated protein kinase
ANOVA ..... analysis of variance
ATP ..... adenosine triphosphate
BPM ..... beats per minute
BSA ..... bovine serum albumin
[^{14}C] ..... ^{14}Carbon
caAMPK ..... constitutively active AMPK
$CaCl_2$ ..... calcium chloride
cAMP ..... cyclic adenosine monophosphate
cDNA ..... complementary deoxyribonucleic acid
Ci ..... Curie(s)
CO_2 ..... carbon dioxide
CoA ..... coenzyme A
CPT-1 ..... Carnitine palmitoyltransferase type 1
CPT-2 ..... Carnitine palmitoyltransferase type 2
CsCl ..... cesium chloride
d ..... day(s)
Da ..... Dalton (1 atomic mass unit)

ddH_2O ..... double distilled water
DTT ..... dithiothreitol
DNA ..... deoxyribonucleic acid
E. coli ..... *Escherichia coli*
EDTA ..... ethylenediaminetetraacetic acid di-sodium salt
e.g. ..... *exempli gratia* (Latin, 'for example')
EGTA ..... ethylene glycol-bis(β-aminoethylether)-N,N,N',N'-tetraacetic acid
eq. ..... Equation
et al. ..... et alii (Latin, 'and others')
FABP ..... fatty acid binding protein
FAT/CD36 ..... fatty acid transporter
g ..... gram(s)
GFP ..... Green Fluorescent Protein
GLUT-4 ..... glucose transporter-4
h ..... hour(s)
$[^3H]$ ..... ^{3}Hydrogen (Tritium)
H_2O ..... water
H_3PO_4 ..... phosphoric acid
HCl ..... hydrochloric acid
HEPES ..... 4-(2-hydroxyethyl) piperazine-1-ethane sulphonic acid
Hg ..... mercury
HPLC ..... high performance liquid chromatography
hr ..... hour
i.e. ..... *id est* (Latin, 'that is')
KAT ..... 3-ketoacyl thiolase
kb ..... kilobase(s)
KCl ..... potassium chloride
KCN ..... potassium cyanide
K_2HPO_4 ..... potassium phoshate dibasic
KH ..... Krebs–Henseleit
KH_2PO_4 ..... Potassium phosphate
kg ..... kilogram
l ..... litre(s)
LB broth ..... Luria-Bertani broth
LCAD ..... long chain acyl dehydrogenase

m ..... metre(s)
M ..... moles·l^{-1}
MAb ..... monoclonal antibody
Malonyl CoA ..... malonyl coenzyme A
MCAD ..... medium chain acyl dehydrogenase
MCD ..... malonyl CoA decarboxylase
MEM ..... modified Eagle's media
mg ..... milligram
$MgCl_2$ ..... magnesium chloride
$MgSO_4$ ..... magnesium sulphate
min ..... minute(s)
ml ..... milliliter
mM ..... millimolar
mmHg ..... millimeters of mercury
mol ..... moles
mRNA ..... messenger ribonucleic acid
n ..... number of animals
n ..... number of samples
N_2 ..... nitrogen
NaCl ..... sodium chloride
$NaCO_3$ ..... sodium carbonate
NaF ..... sodium fluoride
$NaHCO_3$ ..... sodium bicarbonate
nmol ..... nano mole
NaOH ..... sodium hydroxide
O_2 ..... molecular oxygen
OD ..... optical density
PAb ..... polyclonal antibody
pg. ..... page
PFK-1 ..... phosphofructokinase-1
PFK-2 ..... phosphofructokinase-2
pfu. ..... plaque forming units
PKC ..... protein kinase C
pmol ..... picomol
pp. ..... pages

PPARα .....peroxisome proliferator activated receptor alpha
rpm ..... revolutions per minute
RT ..... room temperature
SD ..... standard deviation of the mean
SDS-PAGE.....sodium dodecylsulphate polyacrylamide gel electrophoresis
sec ..... second(s)
SEM ..... standard error of the mean
TBS ..... tris buffered saline
TCA.....tricarboxylic acid
TG ..... triacylglycerol
TNFα.....tumor necrosis factor alpha
tris HCl ..... tris[hydroxymethyl]-amino methane hydrochloride
µl .....microliter
µmol ..... micromole
µU ..... microunit
UV..... ultra violet
V..... Volt(s)
vs. ..... versus

Mathematical prefixes.....

M.....mega (10^{6})
k ..... kilo (10^{3})
c.....centi (10^{-1})
m ..... milli (10^{-3})
µ .....micro (10^{-6})
n ..... nano (10^{-9})
p .....pico (10^{-12})

CHAPTER 1. INTRODUCTION

CHAPTER 1 - INTRODUCTION

Cardiac Metabolism

The heart derives its energy mainly from the oxidation of glucose and fatty acids. During respiration, glucose is transported into the adult heart primarily via the glucose transporter-4 (GLUT-4) and activated by hexokinase to glucose-6-phosphate. Glucose-6-phosphate then enters the glycolysis pathway. The key rate-limiting step of the glycolytic pathway is phosphofructokinase-1 (PFK-1) which converts fructose-6-phosphate to fructose-1,6-bisphosphate. The endpoint of glycolysis is pyruvate (2 molecules per glucose molecule) that is converted to acetyl CoA by the pyruvate dehydrogenase (PDH) complex, a series of enzymes in the mitochondrial membrane. In the mitochondrial matrix, acetyl CoA then enters into the tricarboxylic acid (TCA) cycle. NADH and $FADH_2$ produced from the TCA cycle are used in the process of oxidative phosphorylation (electron transport chain) which results in the production of the high-energy phosphate, ATP. Fats are also oxidized to acetyl CoA, which like the acetyl CoA derived from glucose catabolism, enters the TCA cycle with the same energy producing fate as the acetyl CoA derived from glucose oxidation.

Fatty acids are carried hematogenously to the cell attached to albumin or by lipoproteins such as very-low-density-lipoproteins (VLDL) and chylomicrons, which bind the fats as triacylglycerols (3 fatty acids anchored to a glycerol back-bone). Lipoprotein lipase present in the endothelial cells of the vascular wall cleave the fatty

acid groups from the glycerol scaffolding, following which the fatty acids diffuse through the interstitial space, from the endothelium to the cardiac myocytes, and attach to fatty acid transporting proteins present on the cell surface. Fatty acids enter the myocyte via one of 3 mechanisms: either via diffusion, fatty acid transport protein (FATP) or fatty acid translocase (FAT/CD36). Once in the cytosol, fatty acids are activated energetically (requires ATP) by acyl CoA synthetase (ACS), which catalyzes the addition of CoA-SH to the fatty acid moiety to form fatty acyl CoA. Fatty acyl CoA can undergo passage into the mitochondria for catabolic processing (CoA removal followed by re-addition of the CoA moiety in order to pass through mitochondrial membrane to matrix).

In the normoxic heart, fatty acid oxidation usually accounts for 60-70% of the energy requirements (Neely et al. 1973). In order for activated long-chain fatty acids (fatty acyl CoA) to be oxidized within cardiac myocytes for ATP production, they have to be transported into the mitochondria from the cytoplasm for processing. A key enzyme involved in transporting fatty acids into the mitochondria is carnitine palmitoyltransferase-1 (CPT-1) (McGarry et al. 1989). Since CPT-1 regulates the entry of fatty acids into the mitochondria, it is a key rate-limiting step in cardiac fatty acid metabolism (Kantor et al. 2001). The transporting ability of CPT-1 is tightly regulated by malonyl CoA, a 3 carbon activated compound formed by the carboxylation of acetyl CoA by acetyl coenzyme A carboxylase (ACC) (see Kantor et al. 2001 for review). It has been shown that malonyl CoA levels in the heart are the key regulator of CPT-1 function, rather than alterations in the sensitivity of CPT-1 to

malonyl CoA inhibition, such as has been shown in hepatic tissue (McGarry et al. 1978 and Saggerson 1986). Thus, the cellular levels of malonyl CoA is a strong dictator of rates of fatty acid oxidation since malonyl CoA inhibits CPT-1, which is a key regulator of fatty acid oxidation. (refer to Figure 1-1 for cardiac metabolism schematic).

ACC has already been mentioned as a regulator of malonyl CoA levels; however, there is another enzyme that is responsible for controlling levels of malonyl CoA. Malonyl coenzyme A decarboxylase (MCD) is responsible for decarboxylating malonyl CoA to form acetyl CoA (Kolattukudy et al. 1981 and Dyck et al. 1998). Since the activation of MCD decreases malonyl CoA levels, the inhibition this molecule has on CPT-1 decreases, and thus fatty acids could be transported into the mitochondria to allow for fatty acid oxidation. Another enzyme that has been suggested as an important regulator of cardiac fatty acid oxidation is 5' adenosine monophosphate-activated protein kinase (AMPK). AMPK is essentially a stress activated fuel gauge that is activated when there are low levels of energy within the cells, as determined by high AMP levels (See ref: Hardie et al. 1997 for full review). One target enzyme of AMPK is ACC. AMPK acts on ACC by phosphorylating ACC and, consequently inactivating the enzyme (Sim et al. 1988 and Kudo et al. 1996). The inactivation of ACC by AMPK would result in inhibition of the formation of malonly CoA from acetyl CoA. This lower level of malonyl CoA would allow for a disinhibition of CPT-1 and result in an increase of fatty acid oxidation.

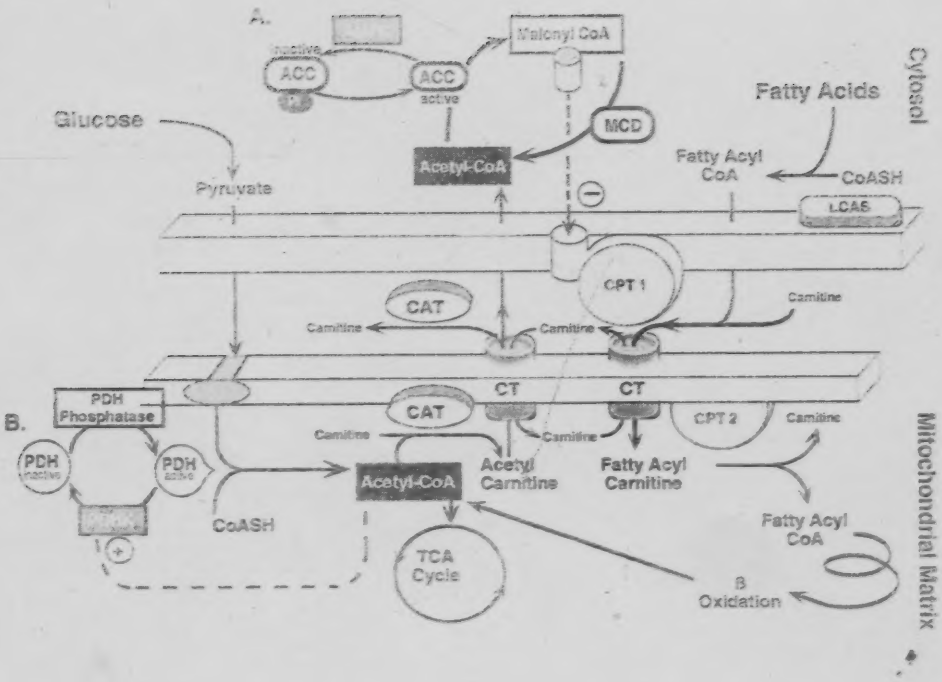

Figure 1-1. Overview of cardiac metabolism. The key mechanisms governing the regulation of fatty acid oxidation (A) and glucose oxidation (B) are outlined in the above schematic. (Figure taken from Kantor et al. 1999).

Fasting Effects on Cardiac Metabolism

During fasting, the contribution of fatty acids to cardiac energy production increases (Van der Lee et al. 2001 and Suzuki et al. 2002). It has been suggested that during fasting, up to 90% of myocardial ATP is derived from oxidation of fatty acids (Kantor et al. 2001). Dyck et al. in 2000 demonstrated that in the livers of fasted rats, MCD activity is increased while the total MCD protein amount is not affected. The increase in MCD activity as noted in the livers of fasted rats by Dyck et al. 2000 was also shown in cardiac tissue following fasting by Young et al. (2001); however, this group also noted an increase in MCD mRNA. Regardless of whether or not the increase in MCD activity is associated with an increase in MCD protein level, it had been shown on separate occasions that fasting in rats results in an increase in cardiac and hepatic MCD activity (Dyck et al 2000 and Young et al. 2001). This increase in cardiac MCD activity could explain, in part, why there is a significant increase in cardiac fatty acid oxidation following fasting.

PPARα and Its Role in Regulating Fatty Acid Oxidation

The family of peroxisome proliferator activated receptors (PPARs) have been shown to play a key role in lipid metabolism and homeostasis (see Barger et al. 2000 for review). One member of this family of nuclear hormone receptors is PPARα, which is a lipid-activated nuclear receptor that induces the transcription of a number of genes involved in lipid metabolism (Gulick et al. 1994, Brandt et al. 1998, Van der Lee et al. 2000, Escher et al. 2001, Campbell et al. 2002). PPARα is activated by free fatty

acids. The activated PPARα then induces the transcription of genes by forming a heterotrimer complex with the retinoid X receptor (RXR) and a coactivator. This heterotrimer complex then binds to sequence-specific target elements (PPAR response element – PPRE) and the transcription of the PPAR target gene is induced (See Barger et al. 2000 for full review). It has been previously shown that PPARα expresses in cells with high catabolic rates of fatty acid oxidation (Escher et al. 2001) and, as such, its role in facilitating increased levels of fatty acid oxidation is becoming established. Additionally, PPARα has also been suggested to play a role in decreasing glucose transport into the cell and its usage within the cell (Wu et al. 1999). PPARα expression increases significantly during severe fasting (Leone et al. 1999) and, therefore, PPARα may play a significant role in the up-regulation of fatty acid oxidation that is noted in these nutritionally deprived animals.

PPARα induces a number of genes involved in the facilitation of fatty acid oxidation. One of the genes that has been suggested to be up-regulated by PPARα is MCD. Young et al. (2001) demonstrated that pharmacologic PPARα activation by WY-14643 resulted in an increase in MCD activity and expression. Additionally, in PPARα knockout mice, the cardiac expression and activity of MCD decreased (Campbell et al. 2002). Therefore, an additional mechanism by which PPARα regulates an increase in fatty acid oxidation may be through an increase in expression and activity of MCD. Additionally, other enzymes that have been shown to effect the regulation of fatty acid oxidation may be regulated by PPARα. Such enzymes include

fatty acid transport protein (FATP), fatty acyl translocase (FAT/CD36), acyl CoA synthetase (ACS), muscle-specific carnitine palmitoyltransferase-1 (CPT-1), acyl dehydrogenase (both MCAD and LCAD) and 3-ketoacyl-CoA thiolase (3-KAT) (Motojima et al. 2000, van Bilsen et al. 1997, van der Lee et al. 2000, Brandt et al. 1998, Djouadi et al. 1999, Gulick et al. 1994 and Barger et al. 2001). Thus, PPARα plays a diverse role in the regulation of cardiac lipid metabolism through the regulation of transcription of a variety of enzymes involved in the use of fatty acids. Therefore, there is a possibility that PPARα could be also regulating the increase in fatty acid oxidation noted during fasting by controlling the expression of enzymes involved in the regulation of fatty acid oxidation such as MCD, ACC and AMPK.

Gene Therapy

Gene therapy, in its simplest term, can be defined as the transfer of nucleic acids to somatic cells resulting in a therapeutic effect (Yla-Herttuala et. al 2000 and Rubanyi 2001). It is this ability to alter the genetic blueprint of the cell that could potentially remove the need for drug intervention to treat certain diseases that has set the scientific world scrambling to harness gene therapy. If successful, the results of these experiments could alter the future course of medical treatments. One of the main organs of interest in the study of gene therapy is the heart since, in North America and many other developed nations, cardiovascular disease is the major cause of morbidity and mortality (see 'cvinfobase' reference). Therefore, if advances could be made in this field of research, the effects could be experimentally and clinically beneficial.

Cardiovascular Gene Therapy

In vivo cardiac gene transfer can facilitate the elucidation of the function of the delivered gene within the proper context of its physiological function. Much insight can be gained from the overexpression of wild-type genes or by the suppression of other genes by using dominant-negative constucts. Gene therapy has been suggested for treatment of cardiovascular diseases such as heart failure and ischaemic heart disease and the initial studies examining gene therapy for treatment of such diseases has demonstrated initial promise (Giordano et al. 1996, Patel et al. 1999, Laham et al. 1999, Eckhart et al. 2000, Shah et al. 2000 and Hammond 2001).

One of the appealing uses of cardiac *in vivo* gene therapy has been for treatment of ischaemic heart disease through promotion of therapeutic angiogenesis by delivery of genes coding for angiogens (Giordano et al. 1996, Patel et al. 1999 and Laham et al. 1999). Angiogenesis generation for treatment of ischaemic heart disease has become a very attractive avenue of research for cardiac gene delivery since a significant portion of patients with this disease cannot undergo current treatments such as coronary artery bypass grafting or percutaneous transluminal coronary angioplasty (Khurana et al. 2001). Initial studies examining the effectiveness of delivering angiogenic cytokines such as VEGF and FGF have shown promise for treatment of ischaemic heart disease since delivery of these angiogens results in increased blood flow to the ischaemic area of the heart, increased contraction within the ischemic area and even collateral developent of blood vessels around the

ischaemic area (Giordano et al. 1996, Patel et al. 1999, Laham et al. 1999 and Hammond 2001). Thus, initial studies examining the effectiveness of using gene delivery techniques to treat ischaemic heart disease have been promising and it has been suggested that gene therapy may be the best treatment to promote therapeutic angiogenesis in cases of myocardial ishemia (Yla-Herttuala et al. 2000). Therefore, there appears to be much potenitial for treatment of ischaemic heart diseases through the use of cardiac *in vivo* gene therapy.

Another potential use for cardiac *in vivo* gene therapy has been suggested for the treatment of heart failure. Heart failure represents a final common pathway of several pathophysiologic processes including hypertension and coronary artery disease (Koch 2002). One of the changes that appears to occur within the heart is alteration to the β-Adernergic receptor (βAR) system which results in cardiac dysfunction (Eckhart et al. 2000). Various groups have tried to augment cardiac function *in vivo* by targetting βAR signalling components (Eckhart et al. 2000). Maurice et al. (1999) was the first group to demonstrate that intracoronary delivery of the β_2-AR transgene to the rabbit heart using an adenoviral transgene resulted in an augmentation of cardiac contractility. The group showed an increase in βAR expression and a significant enhancement of cardiac contraction both at baseline and in response to isoproternol. Other groups also demonstrated the improvement of cardiac function induced by the delivery of the βAR transgene (Shah et al. 2000) and, therefore, the possibility of using gene delivery for treatment of heart failure was becoming established.

Therefore, initial studies examining the possibility for treatment of certain cardiovascular diseases were promising. These studies have paved the way for examination of many different cardiovascular diseases. Using *in vivo* gene therapy, the effects of delivering many different genes of interest could be examinied to elucidate the effects of the expression of the gene under physiological relevant conditions.

Intracoronary Gene Delivery Technique

The intracoronary gene delivery technique was first developed by Barr et al. in 1994 and has become a foundational technique in the realm of cardiac *in vivo* gene transfer upon which many experimental protocols have been performed and developed. Barr's original studies examined the delivery of recombinant adenovirus through the coronary vasculature, via the right internal carotid artery and noted this delivery technique's possible usage for treatment of cardiomyopathy. The idea behind the delivery of a virus through the coronary arteries is one that is quite simple. The myocardium is the area containing the cardiac myocytes and is richly supplied by capillaries branching from the coronary arteries. Therefore, if the virus could be directed through the coronary arteries, it would theoretically have access to all areas of the myocardium and, thus, homogenous cardiac gene delivery could be achieved.

Barr et al. (1994) original technique, which determined the efficiency of myocyte infection to be upwards of 30% was advanced by Hajjar et al. (1998) by using the same idea of coronary virus delivery. However, the method of delivery derived by

Hajjar's group was slightly altered. Their altered technique is performed through opening the chest via thoracotamy, thus revealing the heart and then advancing a catheter up through the apex of the heart, through the left ventricle, past the aortic valve, thus aligning the catheter tip with the opening of the coronary arteries. The pulmonary artery and the aorta are then clamped and the viral solution is administered. Theoretically, the success of this technique lies in the cross-clamping of the aorta and the pulmonary artery since it would result in an increased perfusion pressure down the coronaries allowing maximal opening of the capillaries and thus optimization of the myocardial area to virus exposure (Hajjar et. al 1998). Additionally, the cross-clamping causes a decrease in heart rate which allows for increased diastole and therefore, increased time for viral infection in the myocardium. It has been demonstrated during diastole, that the left ventricular end-diastolic pressure is not significantly increased during cross-clamping since blood return to the left ventricle is blocked. Therefore, perfusion of the virus into the myocytes could occur at relatively low downstream pressures and the myocardium could be efficiently infected homogenously (Hajjar et al. 1998).

Finally, the benefit of cross-clamping lies in the decrease of blood in the coronary arteries. This is important since red blood cells have been suggested to have inhibitory effects on viral delivery (Hajjar et al. 1998). Further supportive evidence was lent to the intracoronary *in vivo* gene delivery technique when studies showed that the optimal temperature for viral delivery to infect cells is 37°C, the body temperature of

rats (Donahue et al. 1997). Thus, the natural environment in which the delivery is performed is actually optimal for viral delivery to the myocytes to occur.

Since its initial use other groups have utilized the technique to examine how the alterations of genes within the myocytes could alter cardiac function (Miao et al. 2000, Taniyama et al. 2002). Hajjar et al. (1998) published research demonstrating the detrimental functional effects in the heart following over-expression of phospholamban in myocytes through intracoronary *in vivo* delivery of this gene via the adenoviral vector. Miao et al. (2000) demonstrated that the over-expression of Akt in myocytes following adenoviral, intracoronary gene delivery protected the myocardium from ischemia-reperfusion injury. Therefore, the evidence supporting the feasibilty of this delivery technique for altering the genetic blueprint within the cardiac myocytes has become well established through multiple publications and the technique is viewed as an efficient and effective means of cardiac *in vivo* gene therapy.

Direct myocardial injection of virus

The direct injection of plasmid DNA to the heart was initially performed by Acsadi et al. (1991) as a pioneering experiment to determine whether cardiac myocytes could express delivered DNA. This first direct injection technique demonstrated success of gene transfer to the rat heart, although confirmed to 100 myocytes in the whole heart. Subsequent to this initial study, many other groups have used this delivery technique using various delivery vectors including adenovirus vectors. The subsequent studies

showed that using adenovirus vectors resulted in a higher efficiency of gene delivery to the myocytes (French et al. 1994). The appeal to using this direct injection is that it was a simple technique of directly delivering genetic information to a specific location of the heart. The intracoronary technique exposes the entire heart to the viral transgene, whereas the direct injection technique can deliver to a specific area. Studies examining the effect of genes involved in angiogenesis have focused on using this delivery technique since ischaemic areas can be targeted for gene transfer (Laham et al. 1998, Kornowski et al. 2000 and Morishita 2002). However, the appeal of this technique to some groups is the drawback to other groups. Since the expression of the gene is localized to the area that it is injected, this direct injection technique does not allow for homogenous delivery of the gene to the heart, such as would be required for studies examining changes of function induced by the delivery of various experimental genes (Hajjar et al. 1998 and Shah et al. 2000). The direct injection technique renders focal areas of infection adjacent to the injection site of the virus. Although this technique may be appealing to some groups, other groups chose not to use this technique since it would not allow for the homogenous delivery desired by many experimental protocols.

Adenovirus as a Gene Vector

Adenoviruses were initially discovered in 1953 (Rowe 1953) and since their discovery, much has been elucidated about these viruses which make them good candidates as vectors for gene delivery. Adenoviruses originate in both birds (aviadenovirus) and humans (mastadenovirus) and they replicate and are assembled in the nucleus of the cell (with the exception of the viral coat proteins) (Ginsberg 1996). The type of adenovirus that is most commonly used for gene delivery is that derived from humans and are of serotype 5, which refers mainly to immunological criteria (Graham et al. 1997, Becker et al. 1994 and Russell 2000). The adenovirus possesses a double-stranded DNA and an icosahedral outer particle shape that makes them very structurally stable (Russell 2000). Additionally, adenoviruses can be grown to high titers, maintain their infectivity well and are relatively easy to handle (Ginsberg 1996 and Kovesdi et al. 1997). In specific regard to infection of cardiac myocytes, the adenovirus offers good infection rates to non-replicating cells such as myocytes (Russell 2000). It is for these reasons that adenoviruses have been used as gene vectors in many experimental *in vitro* and *in vivo* gene therapy models (Becker et al. 1994 and Ginsberg 1996).

Adenovirus Replication and Early Transcription Genes

Except for the synthesis of viral proteins, viral replication occurs entirely within the cellular nucleus (Ginsberg 1996). Before the adenoviral DNA can replicate, a number of early genes must be expressed. These early transcript regions are named the E1, E2, E3 and E4 and it is important to understand what each of these regions are responsible for if there is to be understanding of how the virus replicates. The E1 region is critical in the viral replication process because this region is essential to efficiently express the other early transcript regions (Ginsberg 1996). Mutations in the E1 region render the virus replicationally deficient and thus, this region is a good location to mutate and insert new genetic information. The E2 genes are essential for viral DNA synthesis. Therefore, if the E2 region is absent, the DNA can not replicate and thus the late genes required for formation of structural proteins will not be expressed. The E3 region is termed the nonessential region because it is not necessary for viral replication (Graham et al. 1997). The E3 region is important in the pathogenesis of the virus and its life history. However, although this early transgene region is not necessary to replication, it is important to retain this region because it protects the virus from important cellular functions. It has been shown that if the E3 region is deleted the inflammatory response is markedly increased due to increased levels of cytotoxic cells such as tumor necrosis factor alpha (TNF-α) and polymorphonuclear infiltration (Hierholzer 1988, Rosenfeld 1992 and Ginsberg 1996). Finally, the E4 region is important in the induction of inflammatory response.

It has been shown if the E4 region is deleted, inflammation is significantly reduced. However, by far the most frequently mutated area of the adenoviral genome is the E1 region since the deletion of this region allows for a gene of substantial size to be recombinated into the viral genome (Iilan et al. 1997). Additionally, deletion of this region allows for certain control of viral propagation by restricting the replication of the virus to certain cell types (Kovesdi et al. 1997).

Adenoviral Infection of Cardiac Myocytes.

The adenovirus infects its target cell with its genetic information by means of its fiber coat proteins. These proteins attach to receptors on the cell surface called the coxsackie and adenovirus receptor (CAR) which have been detected on cells isolated from the pancreas, brain, heart, small intestine, testes, prostate, liver and lungs (Tomko et al. 1997). The viral fiber knob protein mediates attachment to the CAR that then allows for an area of the penton base, termed the RGD (arginine-glycine-aspartate) tripeptide motif, to bind to integrins ($\alpha v\beta 3$ and $\alpha v\beta 5$) in the cell membrane surface. This attachment allows for internalization of the virus into an endosomal carrier system (Rubayani 2001)(Figure 1-2). Once transported into the cell via clatharin-mediated endocytosis into the cell, the virus is transported to the nucleus through endosomes with the help of microtubules and lysosomes (Russell 2000). Nuclear signal peptides in the viral coat protein then facilitate the translocation of the

virus into the nucleus via nuclear pores. This finely orchestrated process of delivering the virus to the nucleus takes about 60 minutes (Rubayani 2001)

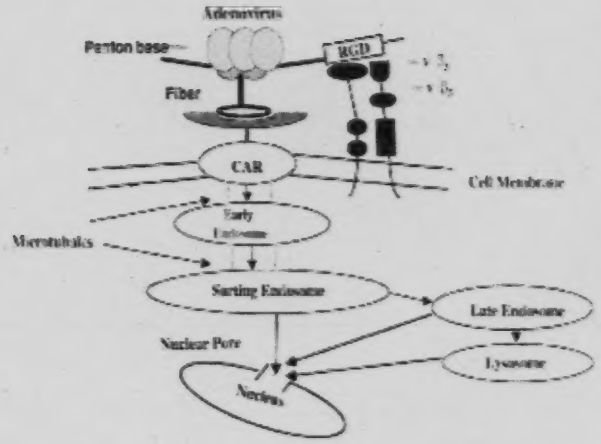

Figure 1-2. Uptake and internalization of the adenovirus into cardiac myocytes via the Coxsackie and Adenovirus Receptor (CAR). (Figure taken from Rubayani 2000).

Reporter genes

Detecting the presence of the delivered gene can be difficult. If the gene being delivered is one that is already present endogenously, then the determination of success of efficient gene transfer can be difficult and imprecise. However, this problem can be overcome by delivering a gene coding for a protein that is not already present *in vivo*. This gene can be termed a reporter gene because often its sole purpose is identifying the efficiency and ability of the cell to be infected rather than having a physiological effect. Reporter genes that are currently used in *in vivo* gene delivery experiments are lac Z` (coding for β-galactosidase) (Wright et al. 2001) and green fluorescent protein (Neyroud et al. 2002) which can be detected via staining and light, respectively. An ideal reporter gene would be one that could be co-expressed with the experimental gene of interest so that confirmation of gene delivery could be performed. Additionally, the ability to co-express the reporter gene with the experimental gene allows the delivery of the reporter gene alone to be used as a control for the experiments being performed.

Green Fluorescent Protein

The first recorded note of green fluorescent protein (GFP) occurred in first century AD when Pliny the Elder noticed jellyfish in the Bay of Naples fluorescing a brilliant green color (Cubitt et al. 1995). As the understanding of this fascinating protein increases, the palatability of GFP as a reporter gene for gene therapy has also increased. GFP is known to be involved in the bioluminescene of Cnidaria, an

evolutionary lower phylum within the metazoa (Prasher 1995). Although GFP has been noted in many different species of marine invertebrates, the two best-characterized forms of GFP are derived from a Pacific Northwest jellyfish, *Aequorea victoria*, and a sea pansy off the Georgian coastline, *Renilla reniformis* (Cubitt et al. 1995). In the marine animals mentioned above, GFP fluoresces by transmutasing blue chemiluminescence from a phytoprotein, aequorin for jellyfish and luciferase for the sea pansy, into green light (Prasher 1995).

Aequorea GFP, derived from the jellyfish, has become the GFP of choice as a reporter gene for gene expression and protein localization in gene therapy experiments (Chalfie et al. 1994 and Li et al. 1997). GFP is a fluorescent monomeric protein of 27-kDa and 238 amino acids long (Cubitt et al. 1995, Prasher 1995, Li et al. 1997, Reid et al. 1997). GFP's largest absorbance peak is at 395nm with a smaller peak at 475nm, and the emission maximum is at 508nm (Heim et al. 1996). This wavelength of light, although provided from a protein within the jellyfish through calcium-aided energy transfer, can be mimicked through the excitation of GFP with light of the specified 475 nm wavelength. It is in this way that GFP is detectable in gene therapy experiments when being used as a reporter gene.

GFP represents a new shape of protein, termed the beta-can. On the outside, 11 anti-parallel beta stands arrange cylindrically. Inside this compact structure, an alpha-helix surrounding the chromophore is present (Ormo et al. 1996 and Yang et al. 1996 and Youvan 1996). It is the very nature of the single-domain structure that allows it to be a protein that is not only resistant to denaturation and protein length-alteration

(Yang et al. 1996), but also fusion to other proteins both C- and N-terminally (Chalfie 1995). It is for all these reasons, that GFP is a reporter protein of choice in many gene therapy experiments. (See Figure 1-3 for schematic of GFP protein).

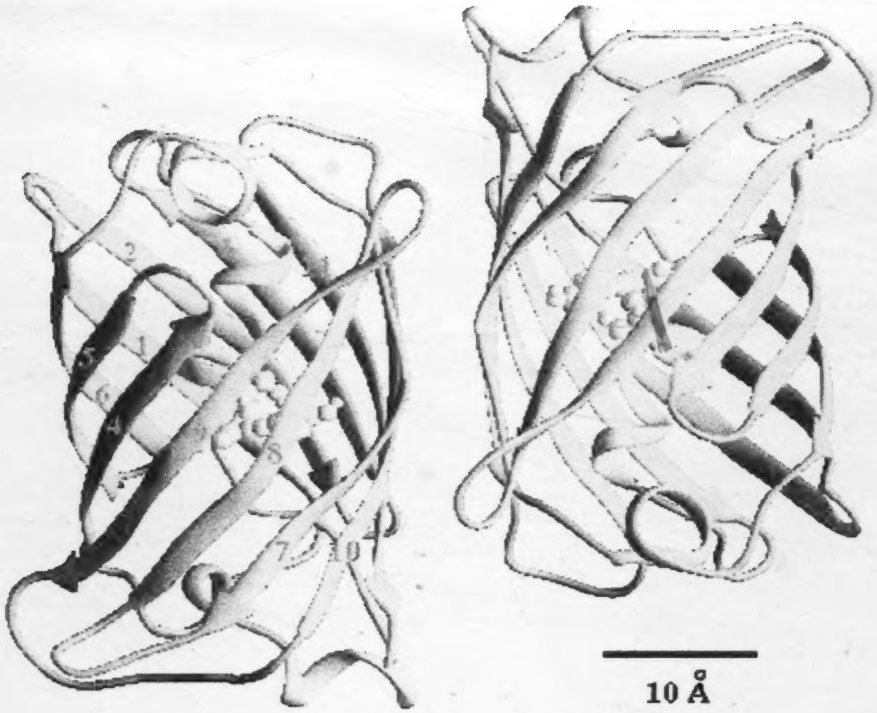

Figure 1-3. The 3D structure of green fluorescent protein (GFP). GFP represents a new shape of protein termed the 'beta-can'. The depiction on the left and right both represent GFP but they show different dimers of the protein. The green portion of the above picture represents the 11 ß-sheets which form the outside of the cylinder. The blue segments represent the α-helices which form the bottom and top of the ß-can. The folding motif of ß-sheets of the outside and α-helices on the inside form the scaffolding for the fluorophore which is represented by the yellow on the diagram These fluorphores are located in the geometric center of the can formation. (This diagram was taken from the paper found online at http://www-bioc.rice.edu/Bioch/Phillips/Papers/gfpbio.html and was written by Yang et al. (year not stated).

AMPK as an Experimental Gene

AMPK is a member of the very diverse serine/threonine protein kinase family (Beri et al. 1994) specifically within the SNF-1 subfamily (Stapleton et al. 1995). AMPK is closely structurally related to PKC and shares common substrates such as ACC and HMG-CoA reductase (Hardie et al. 1992 and Sullivan et al. 1994). Mammalian AMPK is a heterotrimer composed of three subunits: the catalytic α subunit and the scaffolding and regulatory β and γ subunits (Dyck et al. 1996).

AMPK is essentially a metabolic fuel gauge which senses the ratio of AMP : ATP within the cell (Davies et al. 1995, Stein et al. 2000 and Hayashi et al. 2000). AMP is an indicator of low energy levels within the cell and activates AMPK in an allosteric fashion by phosphorylating AMPK at the threonine 172 residue on the catalytic α subunit (Stein et al. 2000 and Hawley et al. 1996) to alter fuel usage within the cell. AMPK affects fatty acid oxidation within the cell by phosphorylating and inhibiting ACC, which, thus, does not allow for the conversion of acetyl CoA to malonyl CoA (Hawley et al. 1996 and Winder et al. 1997). Malonyl CoA is a potent inhibitor of CPT-1, which is the first step in transporting long-chain fatty acids into the mitochondria for β-oxidation (Gao et al. 1994). Therefore, since AMPK phosphorylates and inhibits ACC, malonyl CoA levels would be decreased and inhibition of fatty acid transport would be relieved. Thus, AMPK contributes to an increase in fatty acid oxidation within the cell to produce ATP and 'fill-up' the energy content of the cell.

AMPK also plays a role in the regulation of glucose metabolism to increase the energy status of the cell. AMPK activation promotes GLUT-4 tanslocation to the myocyte's sarcolema (Russell et al. 1999). This results in increased transport of glucose into the cell for use. Additionally, the use of glucose for glycolysis is facilitated by AMPK which phosphorylates phosphofructokinase-2 (PFK-2), a potent activator of glycolysis (Marsin et al. 2000).

Therefore, AMPK plays a regulatory role in up-regulating both fatty acid and glucose metabolism to replenish cellular ATP content. However, it is AMPK's regulatory role on cellular fatty acid oxidation that attracted our group to use it as an experimental gene in cardiac *in vivo* gene transfer studies. It was proposed that the delivery of AMPK to the heart would be an initial step in determining the metabolic effects of over-expressing this enzyme. Since AMPK activity is regulated *in vivo* through phosphorylation by various mechanisms (Davies et al. 1995) for studies examining the over-expression of AMPK *in vivo*, a transgene coding for the active form of AMPK would have to be delivered to the cardiac myocytes. Prior experimentation *in vitro* in our lab using cultures isolated myocytes that have been infected using a constitutively active form of AMPK co-expressing the reporter gene GFP (caAMPK-GFP) demonstrated an increase in fatty acid oxidation relative to control (unpublished data). Therefore, a constitutively active form of AMPK, which is not under control from the various cellular mechanisms but rather always active when expressed (see below), could theoretically be delivered *in vivo* to elucidate the effects of AMPK on the heart and its metabolism under physiological conditions.

(Constitutively active AMPK is not under the phosphorylation control by cellular mechanisms. Replacing the threonine residue at the 172 site of the catalytic α subunit with an aspartic acid residue renders the AMPK constitutively active (Stein et al. 2000)).

Endothelial barrier

All vasculature is protected by endothelial cells which regulate the ability of blood-borne components to enter the tissues of the organ supplied by the vasculature. For blood-delivered virus, such as for the intracoronary delivery technique, to infect myocytes in the heart, the diffusion of the virus through the endothelium is necessary. In order to increase the ability of the virus to infect tissues, it has been shown that the use of a microvascular permeability agent increases the ability of the virus to get across the endothelial barrier in the coronary vasculature to infect the cardiac myocytes (Greelish et al. 1999 and Neyroud et al. 2002). The microvascular permeability agents tested have been ones such as serotonin, bradykinin and histamine (Neyroud et al. 2002 and Yla-Herttuala et al. 2000) and it has been shown that use of these agents increase the ability of the virus to infect the cells of interest. Additionally, decreasing the level of calcium in the perfusate has been shown to increase the ability of the virus to infect the myocytes (Neyroud et al. 2002). Therefore, it has been suggested that the delivery of a microvasculature permeability agent in a low-calcium buffer may aid in the vasculature-mediated delivery of the virus to the myocytes (Donahue et al. 1997 and Neyroud et al. 2002).

HYPOTHESIS AND OBJECTIVES

During severe periods of fasting, cardiac metabolism changes so that fatty acid oxidation is increased relative to glucose oxidation. Although these changes have been previously documented, that which induces this increase in fatty acid oxidation is not fully understood. One hypothesis for the increase in fatty acid oxidation has been suggested to be the increase in MCD and AMPK expression and activity that is noted in conjunction with the alteration of cardiac fuel usage during fasting. Additionally, an increase in the expression of PPARα has been noted in fasted animals. Therefore, we set out to determine whether this increase in PPARα expression was associated with an increase in expression of enzymes involved in the regulation of fatty acid metabolism. Specifically, we determined whether if during fasting, expression levels of MCD, ACC and AMPK changed since alterations in the expression of levels of these enzymes could account for the increase in fatty acid oxidation noted during fasting.

It had been previously shown that fasting induces changes in cardiac metabolism such that fatty acid oxidation and MCD activity increase. Therefore, we decided to examine the effects of over-expressing MCD and constitutively active AMPK *in vivo* to determine whether this over-expression elicited alterations in cardiac fatty acid metabolism. Therefore, by using a pre-established method of gene delivery, we hypothesized that intracoronary *in vivo* gene delivery to the heart would be efficient in

over-expressing MCD and AMPK. Through this over-expression, we also hypothesized that we would note an increase in fatty acid oxidation in these hearts relative to the controls.

Therefore, the objectives of this study were two-fold. Firstly, we set out to determine how nutritional deficiency (fasting) induces enzymatic expression changes that could result in the alteration in cardiac metabolism noted during fasting. Secondly, we set out to determine whether changes in levels of specific constitutively active enzymes involved in regulation of cardiac metabolism could be induced through *in vivo* gene delivery of the transgene coding for these enzymes (MCD and AMPK), thus attempting to mimic the alterations induced by fasting without the nutritional deficiency associated with the fasting protocol.

The rationale for these studies is that in pathological cases such as diabetes and ischemic heart disease, there is a marked increase in fatty acid oxidation that results in functional deficiency of the heart. Therefore, if we can mimic this increase through fasting to examine an experimental model of increasing fatty acid oxidation in the heart, and we can duplicate these metabolic effects by over-expressing the enzymes, such as MCD whose activity has been shown to increase during fasting, there could be potential application for the treatment of certain diseases. This could theoretically be performed in future experiments by down-regulating levels of these enzymes, through use of the dominant negative constructs for the enzymes, to examine whether this decrease rescues the heart from the elevated levels of fatty acid oxidation associated with cardiac dysfunction.

REFERENCES

Acsadi G, Jiao SS, Jani A, Duke D, Williams P, Chong W, Wolff JA. Direct gene transfer and expression into rat heart *in vivo*. *New Biol.* 1991 Jan;3(1):71-81.

Barger PM, Kelly DP. PPAR signaling in the control of cardiac energy metabolism. *Trends Cardiovasc Med.* 2000 Aug;10(6):238-45.

Barr E, Carroll J, Kalynych AM, Tripathy SK, Kozarsky K, Wilson JM, Leiden JM. Efficient catheter-mediated gene transfer into the heart using replication-defective adenovirus. *Gene Ther.* 1994 Jan;1(1):51-8.

Becker TC, Noel RJ, Coats WS, Gomez-Foix AM, Alam T, Gerard RD, Newgard CB. Use of recombinant adenovirus for metabolic engineering of mammalian cells. *Methods Cell Biol.* 1994;43 Pt A:161-89.

Beri RK, Marley AE, See CG, Sopwith WF, Aguan K, Carling D, Scott J, Carey F. Molecular cloning, expression and chromosomal localization of human AMP-activated protein kinase. *FEBS Lett.* 1994 Dec 12;356(1):117-21.

Brandt JM, Djouadi F, Kelly DP. Fatty acids activate transcription of the muscle carnitine palmitoyltransferase I gene in cardiac myocytes via the peroxisome proliferator-activated receptor alpha. *J Biol Chem.* 1998 Sep 11;273(37):23786-92.

Campbell FM, Kozak R, Wagner A, Altarejos JY, Dyck JR, Belke DD, Severson DL, Kelly DP, Lopaschuk GD. A role for peroxisome proliferator-activated receptor alpha (PPARalpha) in the control of cardiac malonyl-CoA levels: reduced fatty acid oxidation rates and increased glucose oxidation rates in the hearts of mice lacking PPARalpha are associated with higher concentrations of malonyl-CoA and reduced expression of malonyl-CoA decarboxylase. *J Biol Chem.* 2002 Feb 8;277(6):4098-103.

Chalfie M, Tu Y, Euskirchen G, Ward WW, Prasher DC. Green fluorescent protein as a marker for gene expression. *Science.* 1994 Feb 11;263(5148):802-5.

Chalfie M. Green fluorescent protein. *Photochem Photobiol.* 1995 Oct;62(4):651-6.

Cubitt AB, Heim R, Adams SR, Boyd AE, Gross LA, Tsien RY. Understanding, improving and using green fluorescent proteins. *Trends Biochem Sci.* 1995 Nov;20(11):448-55.

cvinfobase website: http://cvdinfobase.ic.gc.ca/GCVI/default.htm.

Davies SP, Helps NR, Cohen PT, Hardie DG. 5'-AMP inhibits dephosphorylation, as well as promoting phosphorylation, of the AMP-activated protein kinase. Studies using bacterially expressed human protein phosphatase-2C alpha and native bovine protein phosphatase-2AC. *FEBS Lett.* 1995 Dec 27;377(3):421-5.

Djouadi F, Brandt JM, Weinheimer CJ, Leone TC, Gonzalez FJ, Kelly DP. The role of the peroxisome proliferator-activated receptor alpha (PPAR alpha) in the control of cardiac lipid metabolism. *Prostaglandins Leukot Essent Fatty Acids.* 1999 May-Jun;60(5-6):339-43.

Donahue JK, Kikkawa K, Johns DC, Marban E, Lawrence JH. Ultrarapid, highly efficient viral gene transfer to the heart. *Proc Natl Acad Sci USA.* 1997 Apr 29;94(9):4664-8.

Dyck JR, Gao G, Widmer J, Stapleton D, Fernandez CS, Kemp BE, Witters LA. Regulation of 5'-AMP-activated protein kinase activity by the noncatalytic beta and gamma subunits. *J Biol Chem.* 1996 Jul 26;271(30):17798-803.

Dyck JR, Barr AJ, Barr RL, Kolattukudy PE, Lopaschuk GD. Characterization of cardiac malonyl-CoA decarboxylase and its putative role in regulating fatty acid oxidation. *Am J Physiol.* 1998 Dec; 275(6 Pt 2):H2122-9.

Dyck JR, Berthiaume LG, Thomas PD, Kantor PF, Barr AJ, Barr R, Singh D, Hopkins TA, Voilley N, Prentki M, Lopaschuk GD. Characterization of rat liver malonyl-CoA decarboxylase and the study of its role in regulating fatty acid metabolism. *Biochem J.* 2000 Sep 1;350 Pt 2:599-608.

Eckhart AD, Koch WJ. Beta-Adrenergic gene therapy for cardiovascular disease. *Curr Control Trials Cardiovasc Med.* 2000;1(3):131-134.

Escher P, Braissant O, Basu-Modak S, Michalik L, Wahli W, Desvergne B. Rat PPARs: quantitative analysis in adult rat tissues and regulation in fasting and refeeding. *Endocrinology.* 2001 Oct;142(10):4195-202.

French BA, Mazur W, Geske RS, Bolli. Direct *in vivo* gene transfer into porcine myocardium using replication-deficient adenoviral vectors. *Circulation.* 1994 Nov;90(5):2414-24.

Gao G, Widmer J, Stapleton D, Teh T, Cox T, Kemp BE, Witters LA. Catalytic subunits of the porcine and rat 5'-AMP-activated protein kinase are members of the SNF1 protein kinase family. *Biochim Biophys Acta.* 1995 Apr 6;1266(1):73-82.

Ginsberg HS. The ups and downs of adenovirus vectors. *Bull N Y Acad Med.* 1996 Summer;73(1):53-8.

Giordano FJ, Ping P, McKirnan MD, Nozaki S, DeMaria AN, Dillmann WH, Mathieu-Costello O, Hammond HK. Intracoronary gene transfer of fibroblast growth factor-5 increases blood flow and contractile function in an ischemic region of the heart. *Nature Med.* 1996 May;2(5):534-9.

Graham FL, Prevec L. Manipulation of Adenovirus Vectors. *Methods in Molecular Biology*, Vol. 7: Gene Transfer and Expression Protocols. Edited by: E.J. Murray © 1991 The Humana Press Inc., Clifton, NJ

Greelish JP, Su LT, Lankford EB, Burkman JM, Chen H, Konig SK, Mercier IM, Desjardins PR, Mitchell MA, Zheng XG, Leferovich J, Gao GP, Balice-Gordon RJ, Wilson JM, Stedman HH. Stable restoration of the sarcoglycan complex in dystrophic muscle perfused with histamine and a recombinant adeno-associated viral vector. *Nature Med.* 1999 Apr;5(4):439-43.

Gulick T, Cresci S, Caira T, Moore DD, Kelly DP. The peroxisome proliferator-activated receptor regulates mitochondrial fatty acid oxidative enzyme gene expression. *Proc Natl Acad Sci U S A.* 1994 Nov 8;91(23):11012-6.

Hajjar RJ, Schmidt U, Matsui T, Guerrero JL, Lee KH, Gwathmey JK, Dec GW, Semigran MJ, Rosenzweig A. Modulation of ventricular function through gene transfer in vivo. *Proc. Natl. Acad. Sci. USA*. 1998 Apr 28;95(9):5251-6.

Hammond HK, McKirnan MD. Angiogenic gene therapy for heart disease: a review of animal studies and clinical trials. *Cardiovasc Res.* 2001 Feb 16;49(3):561-7.

Hardie DG. Regulation of fatty acid and cholesterol metabolism by the AMP-activated protein kinase. *Biochim Biophys Acta.* 1992 Feb 12;1123(3):231-8.

Hardie DG, Carling D. The AMP-activated protein kinase--fuel gauge of the mammalian cell? *Eur J Biochem*. 1997 Jun 1;246(2):259-73.

Hardie DG, Corton J, Ching YP, Davies SP, Hawley S. Regulation of lipid metabolism by the AMP-activated protein kinase. *Biochem Soc Trans.* 1997 Nov;25(4):1229-31.

Hayashi T, Hirshman MF, Fujii N, Habinowski SA, Witters LA, Goodyear LJ. Metabolic stress and altered glucose transport: activation of AMP-activated protein kinase as a unifying coupling mechanism. *Diabetes*. 2000 Apr;49(4):527-31.

Heim R, Tsien RY. Engineering green fluorescent protein for improved brightness, longer wavelengths and fluorescence resonance energy transfer. *Curr Biol.* 1996 Feb 1;6(2):178-82.

Hierholzer JC, Wigand R, Anderson LJ, Adrian T, Gold JW. Adenoviruses from patients with AIDS: a plethora of serotypes and a description of five new serotypes of subgenus D (types 43-47). *J Infect Dis.* 1988 Oct;158(4):804-13.

Ilan Y, Droguett G, Chowdhury NR, Li Y, Sengupta K, Thummala NR, Davidson A, Chowdhury JR, Horwitz MS. Insertion of the adenoviral E3 region into a recombinant viral vector prevents antiviral humoral and cellular immune responses and permits long-term gene expression. *Proc Natl Acad Sci U S A.* 1997 Mar 18;94(6):2587-92.

Kannel WB, McGee D, Gordon T. A general cardiovascular risk profile: the Framingham Study. *Am J Cardiol.* 1976 Jul;38(1):46-51.

Kantor PF, Dyck JR, Lopaschuk GD. Fatty acid oxidation in the reperfused ischemic heart. *Am J Med Sci.* 1999 Jul;318(1):3-14.

Kantor P, Lopaschuk GD, Opie L. Myocardial Energy Metabolism. Heart Physiology and Pathophysiology. Fourth Edition. pg 543-569. Edited by Kurachi Y, Terzic A, Cohen M, and Sperelakis N. Copyright © 2001 by Academic Press.

Khurana R, Martin JF, Zachary I. Gene therapy for cardiovascular disease: a case for cautious optimism. *Hypertension.* 2001 Nov;38(5):1210-6.

Koch WJ. Gene transfer of beta-adrenergic signaling components for heart failure. *J Card Fail.* 2002 Dec;8(6 Suppl):S526-31.

Kolattukudy PE, Poulose AJ, Kim YS. Malonyl-CoA decarboxylase from avian, mammalian, and microbial sources. *Methods Enzymol.* 1981;71 Pt C:150-63.

Kornowski R, Fuchs S, Epstein SE, Branellec D, Schwartz B. Catheter-based plasmid-mediated transfer of genes into ischemic myocardium using the pCOR plasmid. *Coron Artery Dis.* 2000 Dec;11(8):615-9.

Kovesdi I, Brough DE, Bruder JT, Wickham TJ. Adenoviral vectors for gene transfer. *Curr Opin Biotechnol.* 1997 Oct;8(5):583-9.

Kudo N, Gillespie JG, Kung L, Witters LA, Schulz R, Clanachan AS, Lopaschuk GD. Characterization of 5'AMP-activated protein kinase activity in the heart and its role in inhibiting acetyl-CoA carboxylase during reperfusion following ischemia. *Biochim Biophys Acta.* 1996 May 31;1301(1-2):67-75.

Laham RJ, Simons M, Tofukuji M, Hung D, Sellke FW. Modulation of myocardial perfusion and vascular reactivity by pericardial basic fibroblast growth factor: insight into ischemia-induced reduction in endothelium-dependent vasodilatation. *J Thorac Cardiovasc Surg.* 1998 Dec;116(6):1022-8.

Laham RJ, Rezaee M, Post M, Sellke FW, Braeckman RA, Hung D, Simons M. Intracoronary and intravenous administration of basic fibroblast growth factor: myocardial and tissue distribution. *Drug Metab Dispos.* 1999 Jul;27(7):821-6.

Leone TC, Weinheimer CJ, Kelly DP. A critical role for the peroxisome proliferator-activated receptor alpha (PPARalpha) in the cellular fasting response: the PPARalpha-null mouse as a model of fatty acid oxidation disorders. *Proc Natl Acad Sci U S A.* 1999 Jun 22;96(13):7473-8.

Li X, Zhang G, Ngo N, Zhao X, Kain SR, Huang CC. Deletions of the Aequorea victoria green fluorescent protein define the minimal domain required for fluorescence. *J Biol Chem.* 1997 Nov 7;272(45):28545-9.

Marsin AS, Bertrand L, Rider MH, Deprez J, Beauloye C, Vincent MF, Van den Berghe G, Carling D, Hue L. Phosphorylation and activation of heart PFK-2 by AMPK has a role in the stimulation of glycolysis during ischaemia. *Curr Biol.* 2000 Oct 19;10(20):1247-55.

Maurice JP, Shah AS, Kypson AP, Hata JA, White DC, Glower DD, Koch WJ. Molecular beta-adrenergic signaling abnormalities in failing rabbit hearts after infarction. *Am J Physiol.* 1999 Jun;276(6 Pt 2):H1853-60.

McGarry JD, Woeltje KF, Kuwajima M, Foster DW. Regulation of ketogenesis and the renaissance of carnitine palmitoyltransferase. *Diabetes Metab Rev.* 1989 May;5(3):271-84.

Miao W, Luo Z, Kitsis RN, Walsh K. Intracoronary, adenovirus-mediated Akt gene transfer in heart limits infarct size following ischemia-reperfusion injury *in vivo*. *J Mol Cell Cardiol.* 2000 Dec;32(12):2397-402.

Morishita R. Recent progress in gene therapy for cardiovascular disease. *Circ J.* 2002 Dec;66(12):1077-86.

Motojima K, Passilly P, Peters JM, Gonzalez FJ, Latruffe N. Expression of putative fatty acid transporter genes are regulated by peroxisome proliferator-activated receptor alpha and gamma activators in a tissue- and inducer-specific manner. *J Biol Chem.* 1998 Jul 3;273(27):16710-4.

Neely JR, Rovetto MJ, Oram JF. Myocardial utilization of carbohydrate and lipids. *Prog Cardiovasc Dis.* 1972 Nov-Dec;15(3):289-329.

Neyroud N, Nuss HB, Leppo MK, Marban E, Donahue JK. Gene delivery to cardiac muscle. *Methods Enzymol.* 2002;346:323-34.

Ormo M, Cubitt AB, Kallio K, Gross LA, Tsien RY, Remington SJ. Crystal structure of the Aequorea victoria green fluorescent protein. *Science.* 1996 Sep 6;273(5280):1392-5.

Patel SR, Lee LY, Mack CA, Polce DR, El-Sawy T, Hackett NR, Ilercil A, Jones EC, Hahn RT, Isom OW, Rosengart TK, Crystal RG. Safety of direct myocardial administration of an adenovirus vector encoding vascular endothelial growth factor 121. *Hum Gene Ther.* 1999 May 20;10(8):1331-48.

Popesko P, Rajtova V, Horak J. A Color Atlas of the Anatomy of Small Laboratory Animals (2) Rat, Mouse and Golden Hamster. pg 43 & 45. Tanslated by Timcatkova I. © 1992 Wolfe Publishing Ltd. London, UK.

Prasher DC, Eckenrode VK, Ward WW, Prendergast FG, Cormier MJ. Primary structure of the Aequorea victoria green-fluorescent protein. *Gene.* 1992 Feb 15;111(2):229-33.

Prasher DC. Using GFP to see the light. *Trends Genet.* 1995 Aug;11(8):320-3.

Reid BG, Flynn GC. Chromophore formation in green fluorescent protein. *Biochemistry*. 1997 Jun 3;36(22):6786-91.

Rosenfeld MA, Yoshimura K, Trapnell BC, Yoneyama K, Rosenthal ER, Dalemans W, Fukayama M, Bargon J, Stier LE, Stratford-Perricaudet L, et al. *In vivo* transfer of the human cystic fibrosis transmembrane conductance regulator gene to the airway epithelium. *Cell.* 1992 Jan 10;68(1):143-55.

Rosenthal N, Musaro A. Gene therapy for cardiac cachexia? *Int J Cardiol.* 2002 Sep;85(1):185-91.

Rubanyi GM. The future of human gene therapy. *Mol Aspects Med.* 2001 Jun;22(3):113-42.

Russell RR 3rd, Bergeron R, Shulman GI, Young LH. Translocation of myocardial GLUT-4 and increased glucose uptake through activation of AMPK by AICAR. *Am J Physiol.* 1999 Aug;277(2 Pt 2):H643-9.

Russell WC. Update on adenovirus and its vectors. *J Gen Virol.* 2000 Nov;81(Pt 11):2573-604.

Saggerson D. Carnitine palmitoyltransferase in extrahepatic tissues. *Biochem Soc Trans.* 1986 Aug;14(4):679-81.

Shah AS, Lilly RE, Kypson AP, Tai O, Hata JA, Pippen A, Silvestry SC, Lefkowitz RJ, Glower DD, Koch WJ. Intracoronary adenovirus-mediated delivery and overexpression of the beta(2)-adrenergic receptor in the heart : prospects for molecular ventricular assistance. *Circulation.* 2000 Feb 1;101(4):408-14.

Sim AT, Hardie DG. The low activity of acetyl-CoA carboxylase in basal and glucagon-stimulated hepatocytes is due to phosphorylation by the AMP-activated protein kinase and not cyclic AMP-dependent protein kinase. *FEBS Lett.* 1988 Jun 20;233(2):294-8.

Stapleton D, Mitchelhill KI, Gao G, Widmer J, Michell BJ, Teh T, House CM, Fernandez CS, Cox T, Witters LA, Kemp BE. Mammalian AMP-activated protein kinase subfamily. *J Biol Chem.* 1996 Jan 12;271(2):611-4.

Stein SC, Woods A, Jones NA, Davison MD, Carling D. The regulation of AMP-activated protein kinase by phosphorylation. *Biochem J.* 2000 Feb 1;345 Pt 3:437-43.

Sullivan JE, Carey F, Carling D, Beri RK. Characterisation of 5'-AMP-activated protein kinase in human liver using specific peptide substrates and the effects of 5'-AMP analogues on enzyme activity. *Biochem Biophys Res Commun.* 1994 May 16;200(3):1551-6.

Suzuki J, Shen WJ, Nelson BD, Selwood SP, Murphy GM Jr, Kanehara H, Takahashi S, Oida K, Miyamori I, Kraemer FB, Kanefara H. Cardiac gene expression profile and lipid accumulation in response to starvation. *Am J Physiol Endocrinol Metab.* 2002 Jul;283(1):E94-E102.

Taniyama Y, Walsh K. Elevated myocardial Akt signaling ameliorates doxorubicin-induced congestive heart failure and promotes heart growth. *J Mol Cell Cardiol.* 2002 34:1241-7.

Tomko RP, Xu R, Philipson L. HCAR and MCAR: the human and mouse cellular receptors for subgroup C adenoviruses and group B coxsackieviruses. *Proc Natl Acad Sci U S A.* 1997 Apr 1;94(7):3352-6.

van Bilsen M, van der Vusse GJ, Reneman RS. Transcriptional regulation of metabolic processes: implications for cardiac metabolism. *Pflugers Arch.* 1998 Dec;437(1):2-14.

van der Lee KA, Vork MM, De Vries JE, Willemsen PH, Glatz JF, Reneman RS, Van der Vusse GJ, Van Bilsen M. Long-chain fatty acid-induced changes in gene expression in neonatal cardiac myocytes. *J Lipid Res*. 2000 Jan;41(1):41-7.

Van der Lee KA, Willemsen PH, Samec S, Seydoux J, Dulloo AG, Pelsers MM, Glatz JF, Van der Vusse GJ, Van Bilsen M. Fasting-induced changes in the expression of genes controlling substrate metabolism in the rat heart. *J Lipid Res*. 2001 Nov;42(11):1752-8.

Winder WW, Wilson HA, Hardie DG, Rasmussen BB, Hutber CA, Call GB, Clayton RD, Conley LM, Yoon S, Zhou B. Phosphorylation of rat muscle acetyl-CoA carboxylase by AMP-activated protein kinase and protein kinase A. *J Appl Physiol.* 1997 Jan;82(1):219-25.

Wright MJ, Wightman LM, Latchman DS, Marber MS. *In vivo* myocardial gene transfer: optimization and evaluation of intracoronary gene delivery *in vivo*. *Gene Ther*. 2001 Dec;8(24):1833-9.

Wright MJ, Wightman LM, Lilley C, de Alwis M, Hart SL, Miller A, Coffin RS, Thrasher A, Latchman DS, Marber MS. *In vivo* myocardial gene transfer: optimization, evaluation and direct comparison of gene transfer vectors. *Basic Res Cardiol.* 2001 May-Jun;96(3):227-36.

Wu P, Inskeep K, Bowker-Kinley MM, Popov KM, Harris RA. Mechanism responsible for inactivation of skeletal muscle pyruvate dehydrogenase complex in starvation and diabetes. *Diabetes*. 1999 Aug;48(8):1593-9.

Yla-Herttuala S, Martin JF. Cardiovascular gene therapy. *Lancet*. 2000 Jan 15;355(9199):213-222.

Young ME, Goodwin GW, Ying J, Guthrie P, Wilson CR, Laws FA, Taegtmeyer H. Regulation of cardiac and skeletal muscle malonyl-CoA decarboxylase by fatty acids. *Am J Physiol Endocrinol Metab*. 2001 Mar;280(3):E471-9.

Youvan DC, Michel-Beyerle ME. Structure and fluorescence mechanism of GFP. *Nat Biotechnol.* 1996 Oct;14(10):1219-20.

CHAPTER 2. METHODS AND MATERIALS

CHAPTER 2 – MATERIALS AND METHODS

Materials

[U-^{14}C]glucose and [9, 10-^{3}H] palmitic acid were purchased from Amersham Canada Ltd (Oakville, Ontario) and NEN (Boston, MA), respectively. Bovine serum albumin (BSA fraction V, fatty acid free) was obtained from Boehringer Mannheim (Indianapolis, IN). Hyamine hydroxide (1M in methanol solution) was obtained from NEN Research Products (Boston, MA). All needles were obtained from Becton Dickinson (Franklin Lake, NJ). Sutures were purchased from Ethicon Inc. (Somerville, NJ). Aqueous counting scintillant was obtained from Amersham (Arlington Heights, IL). Ecolite scintillant was purchased from ICN (Costa Mesa, CA). Triacylglycerol assay kits were obtained from Sigma Diagnostics (St. Louis, MO). For HPLC analysis of the CoA esters, a Nova-Pac 4 μm, 60A°, C18 precolumn cartridge was obtained from Waters Company (Milford, MA). Additionally, C18, 3 μm, 150 mm X 4.6 mm column was obtained from Alltech Associates/Mandel Scientific (Guelph, Ontario). ECL Western blotting detection reagents were obtained from Amersham International (Amersham, UK). GFP primary antibody was kindly provided as a gift from Dr. Berthiaume (Department of Biochemistry, University of Alberta). Akt primary antibody was purchased from NEB (Beverly, MA). MCD antibody was prepared by Dr. Dyck and A. Barr (Dr. Lopaschuk Lab. Cardiovascular

Research Group, University of Alberta). Primary antibodies to phosho-ACC were purchased from Upstate Biotech (Lake Placid, NY). Primary antibodies to total and phosho-AMPK were purchased from Cell Signalling Technology (Beverly, MA). PPARα primary antibody was purchased from ABR (Golden, CO). The agent used to detect ACC, peroxidase labeled streptavidin, was purchased from Mandel Scientific from Kirkegaard & Perry Laboratories Inc. (Gaithersburg, MD). All other primary antibodies were purchased from Santa Cruz (Santa Cruz, CA). Secondary antibodies (peroxidase conjugated affinipore goat-anti-mouse IgG and peroxidase conjugated affinipore goat-anti-rabbit IgG) were purchased from Santa Cruz (Santa Cruz, CA). Trans-blot transfer medium (nitrocellulose membrane) was obtained from BioRad (Richmond, CA). Kodac Biomax MR x-ray film was purchased from Eastman Kodac Company (Rochester, NY). Tissue homogenizer (model: PowerGlen 125) was purchased from Fisher Scientific (Edmonton, AB). HEK 293 cells were obtained from Micobix Biosystems (Toronto, Canada). All other chemicals were purchased from the Sigma Chemical Company (St. Louis, MO).

METHODS

Animals

All experiments were performed with accordance with the guidelines of the Canadian Council of Animal Care and were approved locally by the Health Sciences Laboratory Animal Welfare Committee of the University of Alberta. Following acclimatization

for one week, pathogen-free male Sprague-Dawly obtained from the University of Alberta Biosciences (250-300 g) were randomly assigned to either the control or fasted group. The control group was allowed to eat *ad libitum* and the fasted group had food removed and were fasted for 72 hours prior to perfusion. All animals were placed in individual cages and monitored during the fasting period. The rats were weighed and anaesthetized with Euthanyl® (sodium pentobarbital 1 ml/kg of 240 mg/ml Biomeda-MTC Cambridge, ON) administered i.p. at a dose of 1ml/kg. Following conformation of sensory loss (as judged by lack of pedal response), the chest cavity was entered laterally to the sternum and the heart was removed for examination via the working heart model. For hearts undergoing *in vivo* gene therapy, rats were weighed and anaesthetized with Somnotol (sodium pentobarbital 50 mg/ml) administered i.p. at a dose of 1ml/kg.

Preparation of Hearts for Perfusion

The technique of perfusion was adapted from Lopaschuk et al. (1997). In this set-up, hearts were mounted and tied to the perfusion apparatus in a Langendorff, non-re-circulating mode at a constant pressure of 60 mmHg. A modified Krebs–Henseleit (KH) solution that contained, in mM: NaCl 118, $NaHCO_3$ 25, KCl 4.7, KH_2PO_4 1.2, $MgSO_4$ 1.66, $CaCl_2$ 2.5 and glucose 5. This solution was gassed continuously with a mixture of 95% O_2 / 5% CO_2 (carbogen).

Preparation of Working Heart Solution.

The previously mentioned KH solution was taken and to it, 3% BSA was added. To this slurry, 0.4 mM of palmitate and 2µl of ^{3}H-palmitate per 100 ml of final buffer volume, dissolved in ethanol and $NaCO_3$ was added so that the palmitate would bind to the albumin. This solution was then dialysed for 8 hours in Spectra/Por® dialysis tubing (6000-8000 MW). The buffer was then vacuum filtered through Whatman #1 filter paper and 100µU of insulin per 1 L of buffer was added. 5 mM of glucose was then added to the buffer as was 50µl of ^{14}C-glucose per 100 ml of buffer. 100 ml of prepared buffer was then added to the reservoir of the working heart perfusion system.

Preparation of Hearts for Working Mode Perfusion

Rats were injected intraperitoneal (i.p.) with Euthanyl (1 ml/kg of 240 g/l as described above in Animal section) and, following confirmation of sensory loss, the chest cavity was opened and the heart was removed and quickly placed into ice-cold KH solution. The aorta was cannulated and Langendorff perfusion was initiated and performed for 15 minutes at a hydostatic pressure of 60 mmHg with a modified Krebs–Henseleit (KH) solution that contained, in mM: NaCl 118, $NaHCO_3$ 25, KCl 4.7, KH_2PO_4 1.2 $MgSO_4$ 1.66, $CaCl_2$ 2.5, EDTA 0.5 and glucose 5. The heart was initially perfused in Langendorff mode during which time extraneous tissue such as lungs, thymus and pericardial connective tissue were excised. The left atrium was then cannulated and

the perfusion mode was switched from Langendorff to working as previously described (Lopaschuk et al. 1997). In working mode, the spontaneously beating hearts were perfused aerobically with the working heart perfusion solution. Heart perfusion was performed in a closed re-circulating system in contact with carbogen and was maintained at a constant temperature of 37 °C. Every 10 minutes the following samples were taken as previously described by Lopaschuk et al. (1997) to determine levels of glucose and palmitate oxidation. Briefly, samples of the buffer were taken and stored for further analysis of $^{3}H_2O$ (as would indicated the oxidation of the radiolabelled palmitate). Additionally, buffer samples were added to 9N H_2SO_4 and CO_2 released from this reaction was captured by a hyamine trap, to which ACS scintillant was added and the radiolabel content was counted for presence of $^{14}CO_2$ levels (as would indicate the amount of glucose oxidation occurring during cardiac perfusion). Finally, 300 µl of hyamine hydroxide, through which CO_2 bubbled during the perfusion, was pipetted into ACS for counting of the radiolabel to determine the amount of glucose oxidation, as shown by $^{14}CO_2$ levels in the carbogen of the closed working system. The perfusion solution entered the left atrium at a pressure of 11.5 mmHg and was pumped out of the heart against a column height corresponding to 80 mmHg. Hearts were perfused aerobically for 60 minutes. Following the perfusion, heart ventricles were freeze-clamped using Wollenberger clamps, placed in liquid nitrogen, pulverized and stored at –80 °C for further analysis. Heart atria were removed from the perfusion cannula, dried and weighed to determine atrial dry weight of each heart.

Assessment of Mechanical Function of the Isolated Working Rat Heart

Heart rate and diastolic and systolic aortic pressure were measured and calculated using a Data Acquisition System (PowerLab ADI Instruments). Aortic flow and cardiac output were measured using flow probes (Transonic Systems Inc. Ithica NY), which were placed in the aortic preload line (aortic flow) and the column outflow (cardiac output) lines. Coronary flow (ml/min) was determined by calculating the difference between the cardiac output and the aortic flow.

Assessment of Fatty Acid Oxidation in the Isolated Working Heart

Buffer samples were taken every 10 minutes and stored in a glass vial, under mineral oil (to not allow loss of CO_2). Vials were prepared (Fisherbrand, USA) that contained 500 µl of ddH_2O. Capless microfuge tubes were then placed into each vial and into the microfuge tubes, 200 µl of the collected buffer was added. The vials were then capped and incubated for 24 hours at 50 °C. Following the 24 hour incubation, vials were then placed at 4°C for 6 hours. Following the 6 hour cooling, the vials were uncapped and the microfuge tubes were removed and all condensation from the outer walls of the microfuge tubes was scraped off and added back to the water in the vial. To the vials, Ecolite scintillant was added and the vials were counted for ^3H_2O levels.

Wet to Dry Weight Determination of the Perfused Hearts

Following perfusion, the hearts were frozen in liquid nitrogen. The hearts were then weighed and masses were recorded for the total ventricular weight of the heart. Hearts were then taken and pulverized in liquid nitrogen to form a fine powder. A small amount of the powder was taken and the mass was recoded for wet weight of the given sample. This sample was then oven-dried and the dry weight was recorded. This process allowed for a total wet weight and dry weight of the each perfused heart. This measurement was later used to determine the fuel metabolism in each heart based on the gram dry mass of the heart. The remaining crushed tissue from each pulverized heart was placed in cryogenic vials and stored at -80 °C for further analysis.

Malonyl CoA Decarboxylase Activity Assay

10-15 mg (exact amount recorded) of the crushed tissue was taken from the control and fasting heart group and homogenized (PowerGen 125. Fisher Scientific) in 370 µl of homogenization buffer (in mM: 75 KCl, 20 sucrose, 10 HEPES, 1 EGTA, 50/5 NaF / NaPPi). A standard acetyl CoA curve was made by dissolving acetyl CoA in homogenization buffer to render to following final concentrations: 0 nM, 1 nM, 2 nM, 5 nM, 10 nM and 20 nM. 50 µl of tissue homogenate or sample curve was pipetted into glass culture tubes (Fisherbrand 12 x 75) and to all tubes, 105 µl of incubation buffer was added (in mM: 100 Tris base (pH 8), 1 DTT, 50 / 5 NaF / NaPPi). Following the addition of the incubation buffer, 35 µl of ddH_2O was added to each tube, and the tubes were incubated at 37 °C for 30 minutes. 20 µl of malonyl CoA

(10.5 mM) was added to each tube and to samples were vortexed and incubated at 37°C for 10 minutes. The reaction was then stopped after exactly 10 minutes with 40 µl of PCA (0.5 M) and the samples were again vortexed and neutralized by the addition of 10 µl $KHCO_3$ (2.2 M pH 10). Samples were then centrifuged at 1500 X g for 5 minutes. Following centrifugation of the samples, 100 µl of the supernatant was removed and combined with 80 µl of ddH_2O in a separate glass culture tube. 20 µl of DTT (0.01 M) and 20 µl of CuSO4 / K+ Acetate solution (1 / 400 mM) was added to each and samples were then incubated at room temperature for 30 minutes. 20 µl of EDTA (60 mM) was added to the samples and they were incubated at room temperature for 5 minutes. 30 µl of NEM (30 mM) was added and the samples were incubated for 5 minutes at room temperature. 20 µl of ^{14}C oxaloacetate solution was then added to each sample (total volume of ^{14}C oxaloacetate solution to be produced = 2400 µl. Made by combining 240 µl of 500 mM Hepes, 80 µl of 60 mM EDTA, 240 µl of 20 mM α-ketoglutarate, 42 µl of glutamic oxoacetic transaminase (GOT), 12 µl of ^{14}C aspartate (Amersham UK) and 1672 µl of ddH_2O). 10 µl of citrate synthase was added to each tube and all tubes were incubated at room temperature for 20 minutes. 20 µl of PCA (1 mM) was added to the tubes following the incubation and tubes were vortexed and then 43 µl of KOH (0.6 M) was added and neutralization was confirmed by pH testing. 30 µl of Na^+ glutamate / GOT solution was added (200 mM / 20 mM) and tubes were incubated at room temperature for 20 minutes. 1 ml of Dowex slurry (1g Dowex / 2 ml dd water) was added to each tube and tubes were vortexed every 10 minutes for 60 minutes. Following the 60 minutes, tubes were

centrifuged for 5 minutes at 1500 X g. 0.5 ml of supernatant was removed and added to Ecolite in scintillant tubes (Fisherbrand) and counted for radioactivity. Radioactive readings were standardized to the results from the standard curve and activity results were calculated.

Tissue Triacylglycerol Determination

20 mg of pulverized tissue was taken and placed in a microcentrifuge tube. To the tissue sample, 400 µl of chloroform : methanol solution (2:1) was added and homogenized for 45 seconds. To each sample, 80 µl of methanol was then added and samples were vortexed well and centrifuged for 10 minutes at 1100 x g. Supernatant was removed, placed into a separate microfuge tube, and the volume was recorded. 0.2 volume of 0.04% $CaCl_2$ was added (based on collected supernatant volume) and solution was centrifuged at 550 x g for 20 minutes. The upper phase of each sample was removed and the interface between phases was rinsed 3 times with 150 µl of pure solvent upper phase (for making 49 ml, 1.5 ml of chloroform, 24 ml of methanol and 23.5 ml of water). Following the removal of the upper phase of the last wash, 50 µl of methanol was added to each sample (creates one phase). Samples were then dried using dry nitrogen at 60 °C. Following the drying, samples were re-dissolved in 50 µl in re-suspension buffer (tert-butyl alcohol : triton X-100 : methanol, 3:1:1). A standard curve was made by using glycerol standards (Sigma Diagnostics) dissolved in the re-suspension buffer and pipetted into a standard 96 well plate. 4 µl of the re-suspended tissue samples was added to the plates and 200 µl of color reagent (Sigma

Diagnostics) was added to each well of the plate. Plates were colorimetrically examined at 600nm and tissue TG levels were determined by comparing read-out values to the known standards.

[^{3}H] Palmitate Incorporation into Triacylglycerol Stores

Palmitate incorporation into endogenous TG stores was determined using an aliquot from the total TG isolated as described above. Total cardiac TG was re-suspended in 4 ml organic scintillant fluid (Ecolite) and counted for the presence of [^{3}H]palmitate. (Standard curve created by using [^{3}H]palmitate known amounts).

Fatty Acid Uptake Into the Heart

In order to determine the level of fatty acid uptake into the heart during the 60 minute perfusion period, the following equation was used: [total ^{3}H-palmitate oxidized during the perfusion period] + [^{3}H Palmitate incorporation into triacylglycerol stores]. This formula has its limitations since it does not recognize fatty acids that could be incorporated into phospholipids or other neutral lipids other than TG such as cholesterol esters, monoacyl and diacyl glycerol. However, it has been shown that during a 60 minute working heart perfusion, only a small percentage of fatty acids taken into the myocytes are incorporated into neutral myocardial lipids other than TG (Saddik et al. 1991). Therefore, it can be assumed that this formula can be loosely used to demonstrate the concentration of free fatty acids that are taken up into the myocytes during the perfusion period.

Additionally, from the percentage of free fatty acids that are incorporated into the TG stores, uptake can be determined by the following equation. ([free fatty acid uptake during 60 minutes] + [^{3}H Palmitate incorporation into triacylglycerol stores]) x 100. This equation can be used to demonstrate the % of fatty acids that are incorporated into TG stores, rather than oxidized during the perfusion period.

Plasma Triacylglycerol and Free Fatty Acid Levels

Prior to the removal of the hearts before perfusion, blood was taken from control and fasted rats from the mesenteric artery. Blood was placed on ice for approximately 15 minutes and centrifuged at 1500 X g for 15 minutes. Following centrifugation, the plasma (top layer) was removed and examined for TG levels by pipetting 4 µl of plasma into wells of a 96 well plate. The standard curve was created in the same way as the standard curve for the tissue TG examination (see above section) and to each well, and 200 µl of color reagent (Sigma Diagnostics) was added. Plates were colorimetrically examined at 600nm and plasma TG concentrations were determined by comparing read-out values to the known standards.

Plasma free fatty acid levels were measured by using a enzymatic colorimetric assay (Waco® Pure Chemical Industries, Osaka, Japan). Plasma samples were loaded onto a 96 well plate as were known standards and the plate was read at 550nm for quantification.

Tissue CoA Extraction

80 mg of pulverized tissue from the control and fasted rat hearts was taken and placed into 2 ml microcentrifuge tubes. To each sample, 600 µl of homogenization buffer (6% PCA and 1 mM DTT) was added and samples were homogenized (PowerGen 125. Fisher Scientific). Samples were incubated on ice for 10 minutes, centrifuged at 13,400 X g for 5 minutes and the supernatant was removed and the volume was recorded. 400 µl of the supernatant was placed into high performance liquid chromatography (HPLC) tubes and underwent HPLC for determination of tissue malonyl CoA and acetyl CoA levels as previously described by Saddik et al. 1993).

Recombinant Adenoviral Formation

This method of adenoviral formation is taken from He et al. (1998). It was used to make the adenovirus containing GFP and caAMPK-GFP. The Ad-Akt1 (myristolated) was a gift provided by Ken Walsh's lab at Boston University Medical Center. Their technique for making the virus was similar to ours.

Sub-cloning cDNA into Shuttle Vector

The cDNA of interest, GFP and caAMPK-GFP, was made by Amy Barr and Judith Altarejos, respectively as previously described (Woods et al. 2000). The method of producing the caAMPK was originally documented by Stein et al. 2000. Briefly, cDNA encoding residues 1 to 312 of the α1 catalytic subunit contained a mutation that altered threonine at position 172 to an aspartic acid in that position (Stein et al.

2000 and Woods et al. 2000). This mutation rendered AMPK constitutively active since phosphorylation at the The-172 site was not necessary for activity (Stein et al. 2000).

The cDNA was sub-cloned into the shuttle vector pAdTrack-CMV. This new construct, containing the Pme 1 restriction site insert, was then cut. This linearized construct was then cleaned in phenol/chloroform and then precipitated with sodium acetate and ethanol. Following the precipitation, the DNA was re-suspended in sterile water and quantified.

Generation of Recombinant Adenoviral Plasmids by Homologous Recombination

100 ng of the adenoviral backbone vector, pAdEasy1, with 100 ng Pme 1 cut construct. 20 µl of BJ5183 electroporation competent cells (as described in He et al. 1998) was then added and placed in a pre-chilled electroporation cuvette. BioRad MicroPulser was set to program Ec2. 500 µl of LB was directly added to the electroporation cuvette and everything was transferred to a 14 ml Falcon 2059 tube and the kV and ms was recorded. The Falcon tube was placed in a 37°C gyratory water bath at 150 rpm for a duration of 1 hour. The contents of the tube were then plated onto LB agar kanamycin (50 µg/ml) plates with 50 µl, 100 µl, 150 µl and 200 µl and incubated overnight at 37°C.

Screening for Recombinants

10 small colonies were grown in 3 ml of LB kanamycin (25 µg/ml) and shaken at 37°C overnight. 1.7 ml of culture was miniprepped (Sigma GenElute Plasmid Miniprep Kit. St. Louis, USA). 10 µl of the miniprep was then digested using Pac 1 and pAdEasy1 was used as a control. The digested DNA and uncut DNA was then run side-by-side on a 1% agarose gel. Proper recombination can be confirmed if the cut DNA bands line up with control pAdEasy band and a 4.5 or 3 kb band. The correct DNA was then transformed into XL1 Blue cells for large scale prep. Following the transformation, rescreening via miniprep as mentioned above was performed. A maxiprep using one colony was then performed under sterile conditions. 8 µg of the recombinant was digested using Pac 1. The digest was then inactivated by heating sample at 65°C for 20 minutes.

Production of Adenovirus in Mammalian Cells

HEK 293 cells were grown to 70-80% confluency. The HEK 293 cells were split the day prior to transfection (cells were not used past passage 40). Two solutions were then prepared. Solution A contained 8 µg of heat inactivated Pac 1 digested recombinant (max. 40 µl) into 200 µl of serum free OPTI-MEM. Solution B contained 40 µl of LipofectAMINE in 200 µl serum free OPTI-MEM. Both solution A and B were mixed gently and incubated separately for 30 minutes at room temperature. Solutions A and B were combined and incubated at room temperature for 15 minutes. The cells were rinsed with 4 ml serum free OPTI-MEM and the media

was removed. 2.5 ml of serum free OPTI-MEM was added and the cells were incubated in the CO_2 incubator for 10 minutes. Following the 15 minute incubation, 1.6 ml of serum free OPTI-MEM was added to the A and B solution combination and this solution was gently mixed. 1 ml of A and B combo was removed and added into a T25 flask containing 2.5 ml of serum free OPTI-MEM. The flask was incubated for 4 hours in the CO_2 incubator. The media was then removed and 6 ml of MEM alpha, 5 % horse serum and 10 µg/ml gentamycin was added. The lysis occurs in approximately 7 days and once 70% of lysis occurred, the cells and media were removed and stored at 4°C.

Testing of Virus

The media from the lysate was used to infect cells (H9c2 cells). The cells were incubated with media (MEM (15 to 20 ml), 5% horse serum and 10 µg/ml of gentamycin) and virus for 24 hours. The media and virus was then removed and fresh medium and serum was added and then incubated for 48 hours in a CO_2 incubator. The cells were then washed in PBS, scraped and transferred to a microfuge tube. The sample was then sonicated and centrifuged for 10 minutes at 400 x g. the supernatant was removed and a Bradford protein assay was performed. Immunoblotting was then performed for identification of the protein of interest (as described later in the chapter).

Large Scale Adenovirus Production

Firstly, 1 ml of the media from the original lysate was taken to infect one 150 mm dish of HEK 293 cells with MEM (20 ml), 5% horse serum and 10 µg/ml of gentamycin. When approximately 80% of the cells had lysed, the lysate was stored in the fridge. Secondly, 20 150 mm dishes of HEK 293 cells were grown to approximately 90% confluency. The lysate was divided evenly into 8 50 ml blue max tubes and the final volume was brought up to 50 ml using MEM, 5% horse serum and 10 µg/ml of gentamycin. The media was removed and 20 ml of diluted adenovirus was added to each. The dishes were then incubated in the CO_2 incubator. Cells were then left and observed until approximately 90% lysis had occurred (generally 2-3 days). Once the lysis the cells and media were removed and up to 40 ml was transferred into 50 ml blue max tube. This was then frozen in liquid nitrogen. Lysate was then thawed at 37 °C and refrozen in liquid nitrogen. This was repeated 3 times and the final thaw was centrifuged at 1000 x g for 5 minutes. The lysate was then removed and transferred into a sterile 600 ml beaker and the volume was recorded. 242.3 g/l of powdered ammonium sulphate was added to the lysate and was stirred for 2 hours at room temperature. The precipitate was centrifuged for 15 minutes at 1620 x g at room temperature. Pellet was dissolved in sterile 1 x PBS at a ratio of 1/40 to 1/20 (Schagen et al. 2000). The dissolved precipitate was then pooled into 1 tube and centrifuged at 1620 x g for 5 minutes to remove debris. The supernatant was then used in the cesium chloride gradient.

Cesium Chloride Gradient

The cesium chloride was prepared in dd water and 1 ml weighed grams shown (eg. 1.5 g/ml cesium chloride, 1 ml weighs 1.5 g). 3 concentrations were made which included 1.5, 1.35 and 1.25 g/ml of cesium chloride. These solutions were filter sterilized through a 0.2 μm filter. 1.25 g/ml = 14 g cesium chloride with 40 ml ddH_2O. 1.5 g/ml = 15 g cesium chloride with 21.7 ml ddH_2O. To the bottom of the sterile Nalgene centrifuge tube, 1 ml of the 1.5 g/ml cesium chloride was added. Then, 6 ml of the 1.35 g/ml cesium chloride was added above the last layer and finally, 6 ml of 1.25 g/ml of cesium chloride was added above the last layer. The dissolved viral precipitate was then layered on the cesium chloride gradient. The ultrabottle assembly centrifuge tubes (25 x 89 mm Nalge Nunc International. Rochester, NY) were balanced and centrifuged at 150,000 x g for 22 hours at 10°C in the 60Ti rotor Beckman).

Dialysis

Using a sterile Pasteur pipette, the gray adenoviral band, found at approximately 3/4 down from the top of the tube, was removed and placed into a sterile blue max tube. 2 liters of 1 x PBS and 10% glycerol was filter sterilized and 1 liter was placed into a 1 liter sterile glass beaker. A Pierce Slide-A-Lyzer dialysis cassette (10000MWCO, 3-15 ml sample, No. 66451) was wet for 1 minute in the sterile 1 x PBS 10 % glycerol. Using a 10 cc syringe with an 18 G needle, the adenovirus was drawn-up into the syringe and the tube was rinsed with 1 ml of the sterilized PBS glycerol solution. The

sample was injected into port 1 and the excess air was removed from port 2. The solution was dialyzed for 3 hours at 4°C while slowly mixing in sterile 1 x PBS, 10% glycerol. The dialysis sample was then changed with 1 liter of buffer and left stirring overnight at 4°C.

Adenovirus Storage

The adenovirus was removed from the Slide-A-Lyzer. A 10 cc syringe with an 18 G needle was used to inject air into port 3 and the virus was removed through port 4 and placed into 50 ml sterile blue max tubes. Debris was removed by spinning the sample for 5 minutes at 1620 x g. The virus was aliquotted into sterile microcentrifuge tubes and stored at 4°C.

Titering of Virus

HEK 293 cells were plated and grown to approximately 50-60% confluency in 35 mm dishes. In a final volume of 1 ml MEM alpha, 5% horse serum and 10 μg/ml of gentamycin, the adenovirus was diluted (generally to 10^7 to 10^{11}) while one plate was kept with just the media as a control. The media was removed from each plate and the diluted adenovirus was added to each plate and the plates were incubated in the CO_2 incubator for 4 hours. While the virus was incubating, sterile 1% agar (Difco 214530 (0145-17)) was heated in the microwave (to increase solubility of the agar) and placed at 42°C. From a powder, 3 x MEM alpha (Gibco) with bicarbonate (filter sterilized)

was prepared. At 40°C in the hood, 1 X MEM alpha with bicarbonate, 5% horse serum and 0.5% agar was made. The adenovirus was removed from the plates and 2 ml of 1 X MEM alpha with bicarbonate, 5% horse serum and 0.5% agar was added to the plates. The plates were allowed to solidify in the hood and then were placed in a CO_2 incubator. Every 4-5 days, 1.5 ml of 1 X MEM alpha with bicarbonate, 5% horse serum and 0.5% agar was added on top of the existing agar. The plaques were then counted after 4 days to determine the fluorescence titer. Plaque formation was monitored over next 2 weeks to determine the number of plaque forming units generated from each adenoviral dilution.

Preparation of Rats for Surgery

Following anesthesia, rats were placed and secured on their back by loosely taping their 4 limbs to the surgical surface. Using a razor blade, the area of flesh covering the heart was shaved and topically sterilized using an ethanol wipe.

Intubation and Ventilation of Rats

The front two teeth upper teeth of the rat were pulled back with string. A surgical microscope light (Reichert Scientific Instruments Buffalo, NY) was then directed onto the neck so that the path down the trachea, through the vocal chords, could be visualized. A two inch, 16 gauge catheter, whose needle shaft was filed-down and

shortened so that the plastic coating maintained structural integrity while not damaging the trachea, was advanced down the trachea. The metal shaft was then retracted leaving the plastic catheter in the trachea. The catheter was then connected to the ventilator (Harvard Apparatus South Natick MA) and proper intubation was confirmed by observing the rise and fall of the chest cavity corresponding to the rate of the ventilator. The volume of air delivered per breath was approximately 3.5 cm^3 at a rate of 85 breaths per minute.

Thoracotomy

The chest cavity of the rat was opened via an incision left medial to the sternum. The length of the incision covered approximately the distance from the clavicle to the bottom of the 7^{th} rib. The descending and transverse pectoralis major muscle was then cut in line with the cutaneous incision and the ascending pectoralis muscle was partially cut in line with its superior counterpart, up to the tendon for the rhomboid muscle of the thorax. The lower uncut area of the ascending pectoralis muscle was dissected from the connective tissue and pushed to the distal side of the cut (Figure 2-1). The dorsal scalanus muscle was then identified and dissected medially and pushed laterally to the sternum without cutting or affecting the structural integrity of the muscle. The thoracic ventral serratus muscle was then scored at all areas which it covered the ribs 3 through 6 (Figure 2-2). These ribs were then each squeezed slightly using dissecting forceps so that blood flow through the intercostal arteries and

veins could be clotted to decrease bleeding following cutting. The ribs were then individually cut through the cartilage connecting the ribs to the sternum and retracted to reveal the heart. Special attention was paid during retraction so that the lungs were not damaged. (Note: If there is any damaging contact the lungs will collapse and the chance of the rats surviving post-surgery will be minimal.)

Preparation of the Heart for Viral Gene Delivery

Firstly, the pericardium was gently cut and dissected away from the surface of the heart. The thymus was then retracted and clamped to the superficial cut pectoralis major muscle using hemostats to reveal the aorta and the pulmonary arteries. The apex of the heart was then identified and sutured using a 7-gauge silk suture. The suture was used to allow for manipulation and steadying of the heart during viral delivery.

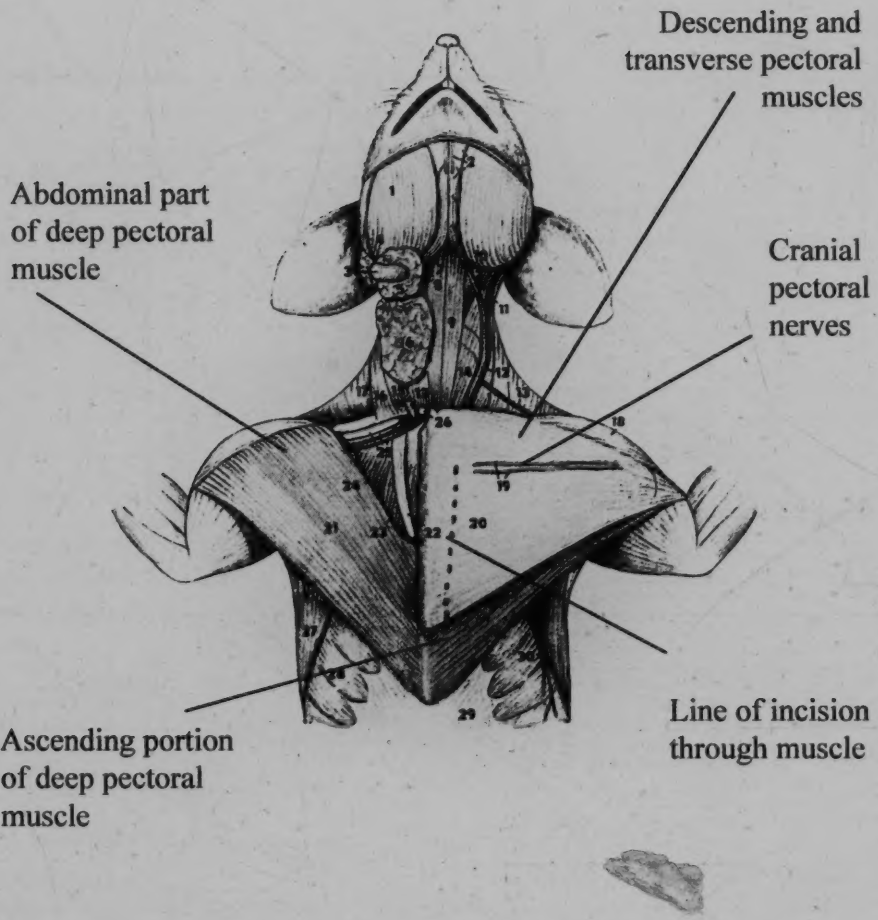
Descending and transverse pectoral muscles
Abdominal part of deep pectoral muscle
Cranial pectoral nerves
Ascending portion of deep pectoral muscle
Line of incision through muscle

Figure 2-1. Rat anatomy 1. For both the intracoronary and direct myocardial injection gene delivery techniques, the chest cavity was opened through the following muscles. Firstly the descending and transverse pectoral muscles were cut while avoiding the cranial pectoral nerves. In line with the ascending portion, the abdominal part of the deep pectoral muscle was then cut to the tendon for the rhomboid muscle of the thorax. (Popesko et al. 1992)

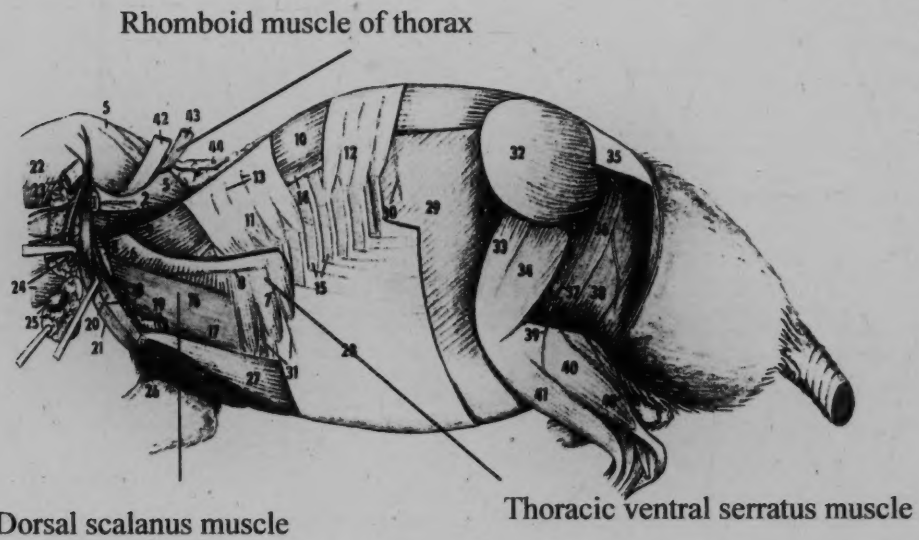

Figure 2-2. Rat anatomy 2. The rhomboid muscle of the thorax was not cut, but rather dissected proximal to the incision. The dorsal scalanus muscle was then dissected and pushed lateral to the incision. Finally, the thoracic ventral serratus muscle was scored so that the ribs could be directly accessed for squeezing by forceps. (Popesko et al. 1992)

Intracoronary Viral Gene Delivery

The intracoronary technique was originally documented by Barr et al. (1994) and was modified by Hajjar et al. (1998) to the following method.

The aorta and pulmonary arteries were clamped using a vascular clamp (Fine Scientific Tools Vancouver, BC). The apex of the heart was then slightly pulled out of the thoracic cavity and a 22 gauge, one and a half inch catheter was advanced through the apex, up through the left ventricle. The center metal shaft of the catheter was then retracted and a syringe containing the viral solution was attached to the plastic shaft of the cannula. The tip of the catheter was then advanced through the aortic valve of the heart so that the viral solution had direct access to the coronary arteries (Figure 2-3). Over a timeframe of approximately 1 minute, 200µl (3.85×10^{10} pfu/ml of Ad-GFP and Ad-caAMPK-GFP or 2.5×10^{10} pfu/ml of Ad-Akt1) of viral solution was infused through the catheter, into the heart. Following the delivery, the clamp was removed from the pulmonary artery and aorta and the thymus was unclamped from the pectoralis major muscle.

Intracoronary Delivery with Histamine

The intracoronary delivery in the presence of histamine was performed in the following way. Following cross-clamping, 200 µl of calcium-free, histamine-containing Krebs solution (in mM: NaCl 118, $NaHCO_3$ 25, KCl 4.7, KH_2PO_4 1.2 $MgSO_4$ 1.66, histamine 20 mM and glucose 5) was perfused through the coronaries in the exact same way as the viral solution in the above intracoronary viral delivery.

Following a 1 minute delivery time, the clamp was removed and the heart was allowed a 3 minute recovery time for the histamine to have its endothelial permeabilizing effects (Svensson et al. 1999). The viral delivery was then performed in the exactly same way as the intracoronary delivery without histamine (above in the method section).

Direct Myocardial Gene Delivery

This technique of direct injection is based on the technique published by Acsadi et al. (1991).

A 25 gauge, half-inch needle was prepared by using parafilm to control the depth of viral administration into the myocardium. Parafilm was wrapped around the end of the needle so that the needle could only penetrate to a depth of 1.75mm into the ventricular myocardium (Figure 2-4). The needle was attached to a syringe containing the viral solution and ten sites on the lower half of the left ventricle and demonstrating few blood vessels, were identified. Into each of these ten sites, 10μl of the viral solution was injected and following each injection, the needle was maintained in the myocardium for approximately ten seconds to allow for some absorbance and the minimizing of leaking when the needle was removed from the infection site.

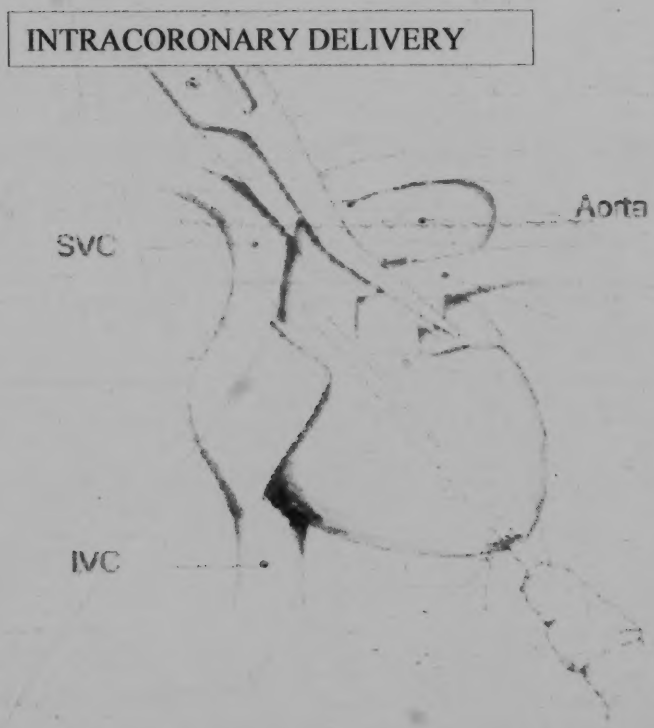

Figure 2-3. Method of intracoronary gene delivery. Following thoracotomy, the exposed heart was apically sutured to allow for manipulation during viral delivery. The pulmonary artery and aorta were cross-clamped. A catheter was advanced from the apex of the heart, through the left ventricle, past the aortic valve to the level of the coronary arteries and the viral solution was administered. 200 µl of adenovirus solution (3.85 x 10^{10} pfu/ml of Ad-GFP and Ad-caAMPK-GFP. 2.5 x 10^{10} pfu/ml of Ad-Akt) was delivered over the course of approximately 1 minute. (Figure taken from Hajjar et al. 2000)

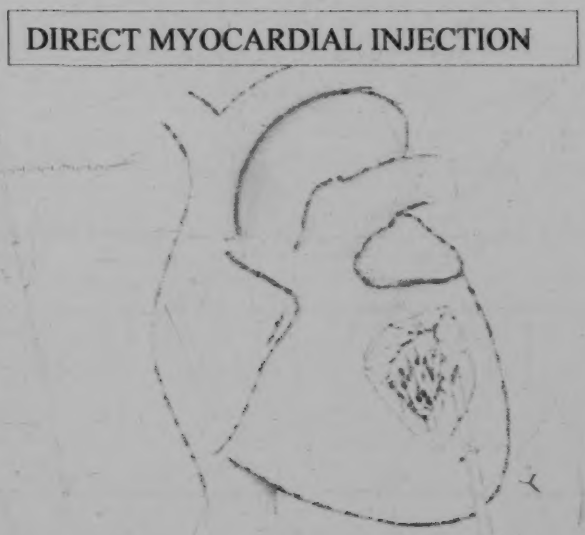

Figure 2-4. Method of direct myocardial gene delivery (direct injection technique). Following thoracotomy, the heart was exposed. 10 sites on the left ventricle were identified and into each site 10µl of virus was injected (3.85×10^{10} pfu/ml of Ad-GFP). (Figure taken from Hajjar et al. 2000)

Suturing and Post-surgical Care

Following gene delivery, the ribs were sutured together via the intercostal muscles and a small catheter was placed in the cavity for blood and air extraction from the cavity. The dissected dorsal scalanus muscle was returned to its original location and the pectoralis muscles were sutured. Finally, the cutaneous layer was sutured and the rats were warmed as they regained consciousness. The intubation tube was removed after it was determined that the rats could breath without artificial aid. This was determined by removing the breathing tube from the catheter and confirming that the rats' breath was constant, rhythmic and unstrained. After this was confirmed, the rats were extubated and placed individually in their own cages. They were observed carefully and Buprenex (buprenorphine hydrochloride 0.3 g/l. Reckitt & Coleman. Richmond, VA) was administered as needed (typically, a 50 µl bolus (0.015 g) was administered during waking and an additional 30 µl (0.009 g) was administered the day following the surgery if needed). The rats were then returned to the general population of rats and observed to ensure maximal comfort and optimal recovery. Rats were allowed 5 days to recover prior to further experimentation except for the Ad-Akt1 delivery group. These animals were left for 3 days and then were sacrificed for immunoblot analysis.

Assessment of Cardiac Protein Expression

Immunoblot Analysis

Frozen left ventricle samples (200 mg) of the hearts were pulverized, weighed and homogenized (PowerGen 125. Fisher Scientific) at 4 °C in 200 µl homogenization buffer (50mM Tris-HCl, 50mM NaF, 5mM NaPi, 1mM EDTA, 1mM EGTA, 250mM mannitol, 10% wt/vol glycerol, 1 µl/ml protease inhibitor cocktail and 10 µl/ml 100mM DTT (to prevent oxidation during homogenization)) using a PowerGen 125 (Fisher Scientific) homogenizer. The samples were tested for the amount of protein present by the Bradford Protein assay and were subsequently normalized. After normalization, the samples were treated with protein sample buffer (30% glycerol, 3% ß-mercaptoethanol, 6% SDS, 10 mg/ml Bromophemol blue and 1.13 M Tris. Solution was brought to pH 6.8) and boiled at 100 °C for 10 minutes. Samples were loaded (50 µg/ well of Ad-GFP and Ad-cAMPK-GFP hearts, 100µg/well of Ad-Akt1 hearts. 50 µg/ well of all other tissue samples) in wells of 5%, 9% or 12% (depending on size of protein being detected) SDS polyacrylamide gel with molecular markers loaded for comparison of molecular weights. The gels were subjected to electrophoresis (SDS-PAGE) using a Mini Trans-Blot Cell (BioRad® Hercules, CA, USA) in protein reservoir buffer containing 25 mM Tris (pH 8.3), 0.192 M glycine, and 0.1% sodium dodecylsulphate. Proteins were then transferred to nitrocellulose membranes at 4°C in Towbin's transfer buffer containing 25 mM Tris (pH 8.3), 192 mM glycine and 20% methanol. Nitrocellulose membranes were then blocked from non-specific protein

binding using tris-buffered saline (TBS) supplemented with 0.05% (vol/vol) of Tween 20 (TBS-T) and 5% (wt/vol) of skimmed milk at room temperature for 1 hour.

Determination of Protein Contents

The following table demonstrates the primary and secondary antibodies used for detection of specific proteins and the time the membranes were incubated in the antibodies.

All antibody incubations were performed in 5% skim milk in TBS-T. Following the incubation of the membranes in primary and secondary antibodies, the membranes were washed in TBS-T three times for 5 minutes, then washed for a final time in TBS (refer to Table 2.1 for concentrations of antibodies and incubation times). Membranes were then visualized using enhanced chemiluminescence detection (Amersham).

Densitometric Analysis

X-Ray films were scanned using a GS-800 Calibrated Denistometer and analyzed using Quantity One® software. The densities of the detected bands were expressed as arbitrary units. All bands detected for each individual protein were directly compared to each other to determine expressional differences in cellular protein content.

Table 2.1

Immunoblotting Protocol.

Protein	[1° Ab]	Incubation in 1° Ab (at 4 ° C)	[2° Ab]	Incubation in 2° Ab
GFP	1:3000	Overnight	GAR 1:3000	1 hour
caAMPK (c-myc)	1:250	Overnight	GAM 1:7500	1 hour
Akt	1:1000	Overnight	GAR 1:3000	1 hour
MCD	1:500	Overnight	GAR 1:2000	1 hour
ACC-1	1:500	45 minutes	Not Required	Not Required
ACC-2	1:500	45 minutes	Not Required	Not Required
P-ACC-1	1:1000	Overnight	GAR 1:2000	1 hour
P-ACC-2	1:1000	Overnight	GAR 1:2000	1 hour
t-AMPK	1:1000	Overnight	GAR 1:3000	1 hour
P-AMPK	1:1000	Overnight	GAR 1:3000	1 hour
PPARα	1:3500	Overnight	GAM 1:5000	1 hour

Cardiac Myocyte Isolation

The method of cardiac myocyte isolation is based on the technique as described by Shimoni et al. 1998.

Solution Preparation

A total of 500 ml of myocyte isolation buffer (in mM: 140 NaCl, 5 KCl, 1 $MgCl_2$, 10 glucose: pH 7.4) was taken and separated into four flasks in the following volumes: Into flask A 100 ml; flask B 100 ml; flask C 200 ml; and flask D 100ml. To these solutions, calcium chloride was added to render the final concentrations: flask A and D 1mM; flask B 5 μM; flask C 8 μM. Solutions A, B and C were then placed in a water bath at a temperature of 39°C. Flasks A, B and C were then individually oxygenated with carbogen (95%O_2 / 5% CO_2) while in the water bath. Solution D was also oxygenated with carbogen briefly and then incubated at 4°C. 50 ml of the solution from flask C was then taken from the water bath and placed in a smaller flask (flask F). Chemicals were then added to the flasks to render the following concentrations: To flask C, 0.12 mg/ml of collagenase (Worthington Biochemical) and 0.013 mg/ml of protease; (Sigma product #P-5147); To flask F, 3 mg/ml of bovine serum albumin (Sigma product #T-0625) and calcium chloride 3 μM was added. Finally, from Flask F, 13 ml of prepared solution was removed and put into a separate falcon tube and 0.23mg/ml of collagenase (Yakult Honsha product #Yk-101) and 0.077 mg/ml of protease (Sigma product Type XIV #P-5147) was added.

Equipment Preparation

An extraction tube, connected to a peristaltic mini pump, was put into solution A and the tube was purged with this solution. The end of the tube was connected to a 5ml syringe and the solution from flask A was pumped while the syringe was inverted to purge air from the syringe. The syringe was then inverted back and clamped. The end of the syringe was connected to a small tube with a thin catheter at the distal end. The pump's rate was adjusted to approximately 10-12 ml/min and the pump was then turned off in preparation for the heart to be hung for collagenase digestion.

Rat Preparation

The rats (gene delivery group) were aneathetized with Euthanyl® (1 ml/kg of 240 g/l) and heparin (2ml/kg of 100 units heparin sulphate (in 1% benzyl alcohol solution) Organon Canada Ltd.). As always, loss of sensation was confirmed by using the toe-pinch method. The chest cavity was then entered via the cutting through the chest cavity on the left-lateral side of the sternum. The heart was then identified and removed from the chest cavity and placed immediately into Flask D. The aorta was identified and mounted onto the catheter attached to the syringe. The aorta was tied to the catheter and the extra-cardiac tissue such as the thymus and esophagus was trimmed from the heart. The pump was turned on and confirmation of coronary perfusion was performed. This set-up allowed for Langendorff perfusion of the heart with the desired solutions.

Cardiac Myocyte Isolation

The solution from Flask A was perfused through the heart. The extraction tube was then switched to Flask B. The heart gradually stopped beating at this point due to the low amounts of calcium in this solution. After all of this solution was perfused through the heart, the extraction tube was then placed into Flask C and this solution was allowed to perfuse the heart for 15 minutes. As this collagenase solution perfused the heart, the heart's color changed to a milky white and the size of the heart increased, demonstrating and confirming the collagenase digestion of the connective tissues binding together the cardiac myocytes.

Following this initial collagenase digestion (primary collagenase) of the heart, the hearts were then cut-down from the Langendorff perfusion, and subjected further to collagenase digestion (secondary collagenase). The left ventricles of the hearts from all surgical groups (both histamine and non-histamine intracoronary deliveries and direct myocardial injection delivery) were cut from the whole heart and placed in a flask containing some of the solution from the falcon tube containing the Yakult collagenase. The flask was incubated (in shaker bath at 37°C). Aliquots of cells were removed over the next 30-60 minutes and stored in an enzyme-free solution in 0.1mM $CaCl_2$ and 3 mg/ml albumin. Visualization of cell aliquots was then performed under a fluorescence microscope to determine and quantify percentage of cells that were infected via the different gene delivery techniques.

Additional Examination of Direct Myocardial Injection Hearts

Prior to the secondary collagenase of the direct myocardial injection delivery hearts, following the removal of a portion of the left ventricle, the remaining portion of the heart was visualized *in situ* to determine whether there were any additional injection sites. Areas that fluoresced were dissected from the heart (area around the injection site also cut was approximately 3 mm) and further digested with collagenase in Yakult solution separately so that quantification of myocytes in the injection area could be determined.

Preparation of Heart Slices for GFP Fluorescence Analysis.

Histological analysis of GFP location

Animals from the intracoronary (with histamine), direct injection and control (uninfected) group were anaesthetized using Euthanyl (1ml/kg of 240 g/l). Following confirmation of sensory loss, hearts were removed and rinsed in cold Krebs solution (in mM: NaCl 118, $NaHCO_3$ 25, KCl 4.7, KH_2PO_4 1.2 $MgSO_4$ 1.66, $CaCl_2$ 2.5, EDTA 0.5 and glucose 5). Hearts were then fixed and incubated overnight in 10% formalin. Following fixation, hearts were then embedded in paraffin and 10 µm sections were sliced using a microtome. Slices were mounted on glass slides for fluorescence visualization (slices were not stained to avoid any kind of interaction the stain may have with the fluorescence). Slides were visualized using a Zeiss microscope attached to a Leistungselektzonit fluorescent pac (JENA GmbH Goschwistar Strabe, Germany)

to determine the location of GFP fluorescence in the infected and control (uninfected) tissue.

Statistics

Data was analyzed using either the Student-Neumman-Keuls test for groups where there was no significant difference between standard deviations or the Welch's Test for unequal variance for groups where there was significant difference between standard deviations. Values are shown as mean ± the standard error of the mean (SEM). The data were analyzed using the statistical program Instat 2.01. Two-tailed values were deemed significant when $p<0.05$.

REFERENCES

Acsadi G, Jiao SS, Jani A, Duke D, Williams P, Chong W, Wolff JA. Direct gene transfer and expression into rat heart in vivo. *New Biol.* 1991 Jan;3(1):71-81.

Barr E, Carroll J, Kalynych AM, Tripathy SK, Kozarsky K, Wilson JM, Leiden JM. Efficient catheter-mediated gene transfer into the heart using replication-defective adenovirus. *Gene Ther.* 1994 Jan;1(1):51-8.

Hajjar RJ, Schmidt U, Matsui T, Guerrero JL, Lee KH, Gwathmey JK, Dec GW, Semigran MJ, Rosenzweig A. Modulation of ventricular function through gene transfer in vivo. *Proc. Natl. Acad. Sci. USA*. 1998 Apr 28;95(9):5251-6.

He TC, Zhou S, da Costa LT, Yu J, Kinzler KW, Vogelstein B. A simplified system for generating recombinant adenoviruses. *Proc Natl Acad Sci USA*.. 1998 Mar 3;95(5):2509-14.

Lopaschuk GD, Barr RL. Measurements of fatty acid and carbohydrate metabolism in the isolated working rat heart. *Mol Cell Biochem.* 1997 Jul;172(1-2):137-47.

Saddik M, Lopaschuk GD. Myocardial triglyceride turnover and contribution to energy substrate utilization in isolated working rat hearts. *J Biol Chem*. 1991 May 5;266(13):8162-70.

Saddik M, Gamble J, Witters LA, Lopaschuk GD. Acetyl-CoA carboxylase regulation of fatty acid oxidation in the heart. *J Biol Chem*. 1993 Dec 5;268(34):25836-45.

Shimoni Y, Light PE, French RJ. Altered ATP sensitivity of ATP-dependent K+ channels in diabetic rat hearts. *Am J Physiol*. 1998 Oct;275(4 Pt 1):E568-76.

Stein SC, Woods A, Jones NA, Davison MD, Carling D. The regulation of AMP-activated protein kinase by phosphorylation. *Biochem J*. 2000 Feb 1;345 Pt 3:437-43.

Svensson EC, Marshall DJ, Woodard K, Lin H, Jiang F, Chu L, Leiden JM. Efficient and stable transduction of cardiomyocytes after intramyocardial injection or intracoronary perfusion with recombinant adeno-associated virus vectors. *Circulation*. 1999 Jan 19;99(2):201-5.

Woods A, Azzout-Marniche D, Foretz M, Stein SC, Lemarchand P, Ferre P, Foufelle F, Carling D. Characterization of the role of AMP-activated protein kinase in the

regulation of glucose-activated gene expression using constitutively active and dominant negative forms of the kinase. *Mol Cell Biol.* 2000 Sep;20(18):6704-11.

CHAPTER 3.

The Fasting-Induced Increase of PPARα Expression and Fatty Acid Oxidation Does Not Occur in Conjunction with Altered Expression of Malonyl CoA Decarboxylase, Acetyl CoA Carboxylase or 5' AMP-Activated Protein Kinase.

My role in this work involved performing all perfusions and biochemical experiments with the exception of the HPLC analysis of CoA esters, which was performed by Ken Strynadka.

CHAPTER 3

The Fasting-Induced Increase of PPARα Expression and Fatty Acid Oxidation Does Not Occur in Conjunction with Altered Expression of Malonyl CoA Decarboxylase, Acetyl CoA Carboxylase or 5' AMP-Activated Protein Kinase.

Abstract

During periods of nutritional deficiency, the energy derived from fatty acid oxidation in the heart increases to up to 90%. Although the mechanism by which this increase occurs is not fully understood, fasted rats demonstrate an increase in the myocardial expression level of PPARα, a ligand-activated transcription factor suggested to play a role in controlling the expression in genes involved in fatty acid uptake and oxidation in the heart. We determined whether the regulation of fatty acid oxidation is altered through PPARα-mediated changes in the expression and activity of MCD, ACC and AMPK. Isolated working rat hearts demonstrated a significant increased in fatty acid oxidation following a 72 hour fasting period, while glucose oxidation significantly decreased. PPARα expression was also significantly increased in the fasted rats

relative to control. However, there was no significant difference in expression levels of enzymes involved in cardiac metabolism, including AMPK, MCD and ACC (both the 265 and 280 kDa isomers). Additionally, no change in activity of AMPK or ACC was noted (as determined through examining the phosphorylation status of the enzyme). Significant increase in MCD activity was noted in the fasted rats relative to control. When the levels CoA esters was determined, no significant change in acetyl CoA or malonyl CoA levels was noted in the fasted hearts relative to controls. Finally, fatty acid uptake levels were examined and fasted hearts demonstrated an increase in fatty acid uptake; however, no change in ^{3}H-palmitate incorporation into endogenous TG stores was noted between groups. Taken together, we show that the increase in cardiac fatty acid oxidation during fasting is associated with an increase in PPARα expression. However, our data also suggest that the increase associated with PPARα is not due to increased expression of MCD, ACC or AMPK.

Nutritional deficiency results in a shift of energy use by the heart from glucose to fatty acids (Van der Lee et al. 2001 and Suzuki et al. 2002). During fasting, fatty acid oxidation can account for up to 90% of cardiac energy production (see Kantor et al. 2001 for review) although the mechanism by which this increase occurs has not been fully elucidated.

A prime candidate for the increase in fatty acid oxidation noted during fasting is PPARα, a lipid-activated nuclear receptor that has been shown to regulate the transcription of a number of genes involved in cardiac lipid metabolism (Gulick et al. 1994, Brandt et al. 1998, Van der Lee et al. 2000, Escher et al. 2001 and Campbell et al. 2002). PPARα induces the transcription of genes such as the fatty acid transporter CD36, fatty acid binding proteins and muscle-specific CPT-1 (Brandt et al. 1998, Gulick et al. 1994, Van der Lee et al. 2000 and Campbell et al. 2002). Additionally, PPARα has been shown to regulate the expression of genes involved in the regulation of mitochondrial oxidation such as medium, long and very long chain acyl dehydrogenases (MCAD, LCAD, VLAD) and 3-ketoacyl-CoA thiolase (KAT) (Djouadi et al. 1999, Gulick et al. 1994 and Van Der Lee et al. 2000).

PPARα also regulates the expression of MCD, an enzyme involved in the regulation of fatty acid transport into the mitochondria (Young et al. 2001 and

Campbell et al. 2002). However, studies performed previously in our laboratory using PPARα over-expressing mice showed no change malonyl CoA levels or MCD expression in the transgenic mice relative to controls (unpublished data). Therefore, the question as to whether PPARα regulates the expression of MCD is still unanswered. A PPARα induced increase in MCD activity would help explain the increase in fatty acid oxidation noted during fasting; however, it is possible that the alternation in metabolism is due to the regulation of expression of other enzymes involved in cellular lipid metabolism other than MCD.

In this study we determined whether the fasting induced increase in fatty acid oxidation was associated with an increase in the expression of specific enzymes involved in the regulation of fatty acid oxidation. Using a 72 hour fasted rat model, we performed *ex vivo* working heart experiments to examine the control of cardiac metabolism induced by the nutritional deficiency. In addition to directly measuring fatty acid oxidation, we also examined whether there were alterations in expression of PPARα, MCD, ACC and AMPK, all of whose activities have been related to alterations in fatty acid oxidation.

METHODS

Fasting Protocol

Male Spague-Dawly were separated randomly into two groups. The control group was allowed to eat *ad libitum* for 72 hours whereas the fasted group was deprived of food for a 72 hour period.

Heart Perfusion Protocol

Hearts were removed from the control and fasted group and subjected to isolated working heart perfusions. Perfusion protocol and measurement of functional parameters were performed as described in Chapter 2.

Plasma Measurements

Following anesthesia but before the heart was removed, blood was collected from the mesenteric artery and plasma was extracted and examined for plasma triacylglycerol (TG) and fatty acid content as described in Chapter 2.

Tissue Extractions

Tissue TG levels and ^{3}H-palmitate incorporation into TG stores were determined using the silicic acid separation as described in Chapter 2. MCD activity was determined as described in Chapter 2. CoA ester levels were extracted and subjected to HPLC analysis as described in Chapter 2.

Immunoblotting

Pulverized tissue was homogenized as described in Chapter 2. Samples were standardized via Bradford Protein assay and examined for expression levels of PPARα, MCD, AMPK (total and phosphorylated) and ACC (total and phosphorylated) via immunoblotting techniques as described in Chapter 2.

MCD Activity

Pulverized heart tissues was taken analyzed for MCD activity as described in Chapter 2.

Statistics

Data was analyzed using either Student-Neumman-Keuls test for groups where there was no significant difference between standard deviations or the Welch's Test for unequal variance for groups where there was significant difference between standard deviations. Values are shown as mean ± the standard error of the mean (SEM). The data were analyzed using the statistical program Instat 2.01. Two-tailed values were deemed significant when $p<0.05$.

Perfusion Data from Control vs. Fasting Rats

Hearts from the control (n=10) and fasted groups (n=12) were perfused and metabolic changes in fuel usage were compared. No significant change in heart rate, peak systolic pressure, developed pressure or cardiac output was noted between the fasted and control group. (Table 3.1 shows all functional parameters of perfusion). Glucose oxidation rates in the isolated working heart were significantly decreased following fasting relative to control from 1236 ± 200 vs. 500 ± 104 nmol ^{14}C glucose oxidized / g dry / minute, respectively. Palmitate oxidation rats were significantly increased following fasting relative to control from 285 ± 33 vs. 369 ± 35 nmol ^{3}H palmitate oxidized / gram dry / minute, relative to control (Figure 3-1).

Contribution of Acetyl CoA to TCA Cycle Acetyl CoA

The contribution to the TCA cycle of acetyl CoA derived from the oxidation of glucose and palmitate was determined from the metabolic results. Since 2 moles of acetyl CoA is derived from each mole of glucose oxidized and 8 moles of acetyl CoA is derived from each mole of palmitate oxidized, the total acetyl CoA contribution to the TCA cycle can be determined by calculating from the rates of glucose and palmitate oxidation. Fasted hearts demonstrated a significant increase in the contribution of acetyl CoA from palmitate oxidation relative to the control (75 ± 6%

vs. 48 ± 5%). Acetyl CoA contribution from glucose oxidation in the fasted hearts was significantly decreased relative to control hearts (25 ± 3% vs. 52 ± 6%). (Figure 3-2).

Malonyl CoA Decarboxylase Activity Level of Perfused Hearts

Tissues taken from control and fasted hearts from the end of perfusion were pulverized, homogenized and examined for MCD activity. The activity of MCD significantly increased in the fasted hearts relative to control from 1858 ± 102 to 2308 ± 66 n mol MCD activity / g dry / minute, respectively (Figure 3-3).

PPARα Expression Level

Tissues from fasted and control hearts were examined by immunoblot analysis and compared for PPARα protein levels. There was a significant increase in PPARα expression levels in fasted hearts relative to control as shown by arbitrary units following densitomeric analysis following immunoblotting (0.25 ± 0.03 to 0.14 ± 0.02, respectively) (Figure 3-4).

Triacylglycerol Tissue Levels of Perfused Hearts

Tissues taken from control and fasted hearts were pulverized, homogenized and examined for TG levels. TG levels in fasted hearts were significantly decreased compared to control 4.22 ± 0.78 vs. 2.08 ± 0.21 μmol triacylglycerol / g dry tissue

weight, respectively. However, the concentration of ^{3}H-palmitate incorporated into endogenous TG was not different between fasted and control hearts 1.3 ± 0.2 vs. 1.6 ± 0.3 μmol triacylglycerol / g dry tissue weight, respectively.

Levels of fatty acid uptake was determined as described in Chapter 2. Levels of fatty acid uptake in the fasted hearts was significantly higher (26.62 ± 2.47 mmol/l) than that of the control group (17.49 ± 2.00 mmol/l). The percent of fatty acids incorporated into endogenous TG stores was also calculated (as per Chapter 2). There was a significant decrease in the percentage of fatty acids incorporated into TG stores during the 60 minute perfusion period in the fasted hearts (4.5 ± 0.7%) relative to control hearts (10.6 ± 1.4%) (Table 3.2) while a significant increase in the up-taken fatty acids being oxidized was recorded (89.4 ± 1.5% control vs. 95.5 ± 1.2%).

Plasma TG and Free Fatty Acid Levels.

Plasma isolated from the blood taken from control and fasted rats prior to perfusion was analyzed for TG levels. Plasma TG levels in fasted hearts was significantly decreased relative to control hearts (1.70 ± 0.32 vs. 0.30 ± 0.04 mmol/l TG, respectively). Plasma was also analyzed for levels of free fatty acid. The levels of free fatty acids extracted from the plasma of the fasted rats (0.26 ± 0.02 mmol/l) was significantly higher than that in the control group (0.12 ± 0.03 mmol/l) (Table 3.3).

CoA Tissue Levels

Tissues from fasted and control hearts were examined for levels of malonyl CoA. No significant change was noted between the control and fasted group (1.8 ± 0.3 and 1.2 ± 0.2 nmol / g dry, respectively) (Table 3.4).

Tissues from fasted and control hearts were also examined for levels of acetyl CoA. No significant change was noted between the control and fasted group (45.2 ± 4.7 and 36.4 ± 3.1 nmol / g dry, respectively) (Table 3.4).

Protein Expression Levels

Tissues from fasted and control hearts were examined for MCD protein levels. There was no significant change in MCD expression levels between the control and fasted group. Control MCD expression levels was 0.41 ± 0.02 arbitrary units while fasted MCD expression levels was 0.42 ± 0.04 arbitrary units (Figure 3-3).

Tissues from fasted and control hearts were examined for ACC1 (265 kDa isoform) and ACC2 (280 kDa isoform) protein levels. There was no change in ACC1 levels in fasted hearts relative to control (0.17 ± 0.02 vs. 0.181 ± 0.03 arbitrary units, respectively) (Figure 3-5). There was also no change in ACC2 levels between fasted and control groups (0.93 ± 0.05 to 0.922 ± 0.07 arbitrary units, respectively) (Figure 3-5).

Tissues from fasted and control hearts were also examined for phospho-ACC1 and phospho-ACC2 protein levels. There was no change in phospho-ACC1 levels in

fasted hearts relative to control (0.65 ± 0.05 vs. 0.50 ± 0.06 arbitrary units, respectively) (Figure 3-6). There was also no change in phospho-ACC2 levels between fasted and control groups (1.4 ± 0.02 to 1.277 ± 0.07 arbitrary units, respectively) (Figure 3-6).

Tissues from fasted and control hearts were also examined for AMPK protein levels. There was no change in AMPK levels in fasted hearts relative to control (1.83 ± 0.09 vs. 2.0 ± 0.04 arbitrary units, respectively) (Figure 3-7).

Finally, tissues from fasted and control hearts were examined for phospho-AMPK protein levels. There was no change in phospho-AMPK levels in fasted hearts relative to control (0.66 ± 0.11 vs. 0.85 ± 0.16 arbitrary units, respectively) (Figure 3-7).

Table 3.1

Perfusion Functional Parameters of Control and Fasted Rats

	Control (n=10)	fasted (n=12)
Heart Rate (bpm)	275 ± 16	298 ± 33
Peak Systolic Pressure (mmHg)	128 ± 7	123 ± 4
Developed Pressure (mmHg)	63 ± 9	51 ± 4
Cardiac Output (ml/min)	45 ± 3	47 ± 2

Values are mean ± SE (n=10 control and n=12 fasted).

No significant differences were noted between control and 72 hr fasted group.

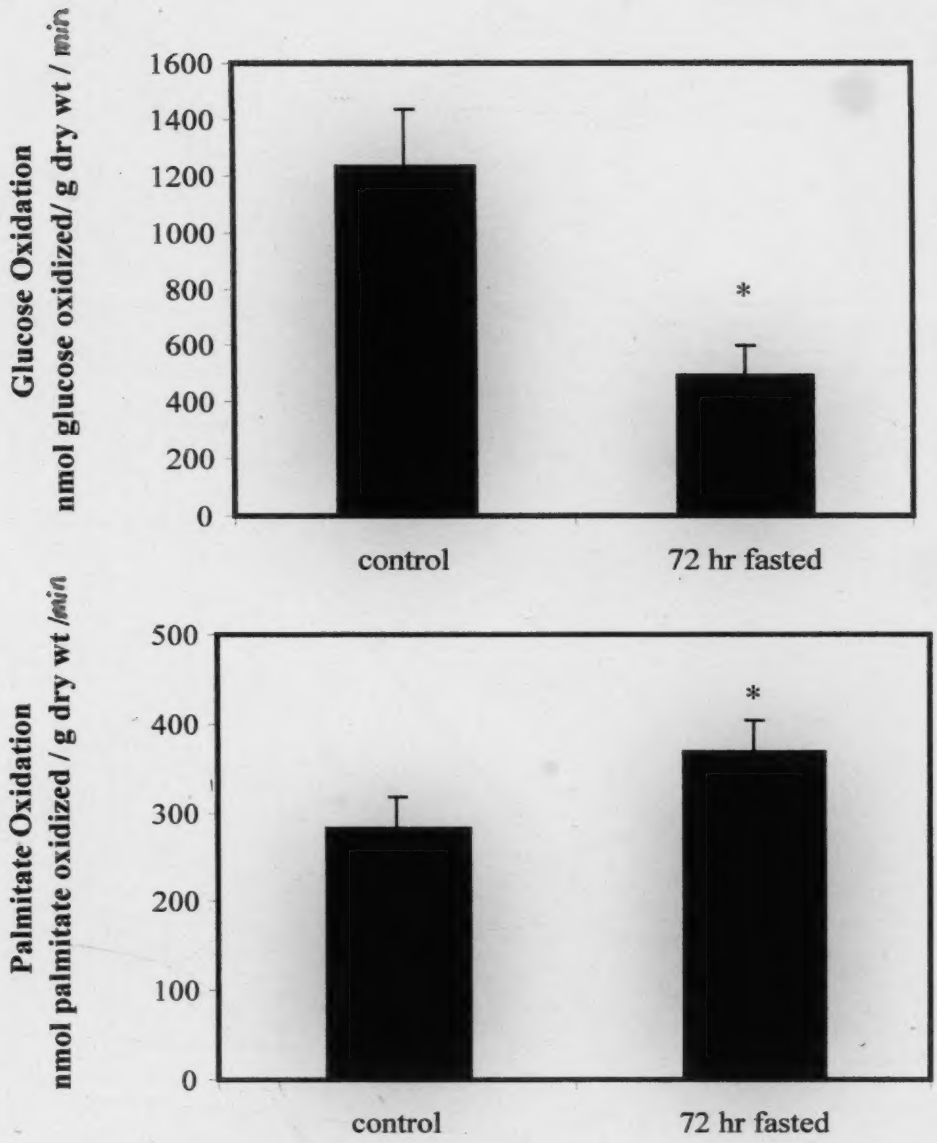

Figure 3-1. Glucose and palmitate oxidation rates in isolated working hearts from control and 72 hr fasted rats. Values are means ± SE (n=10 control and n=12 fasted, respectively). * Significant difference in fasted group relative to control group.

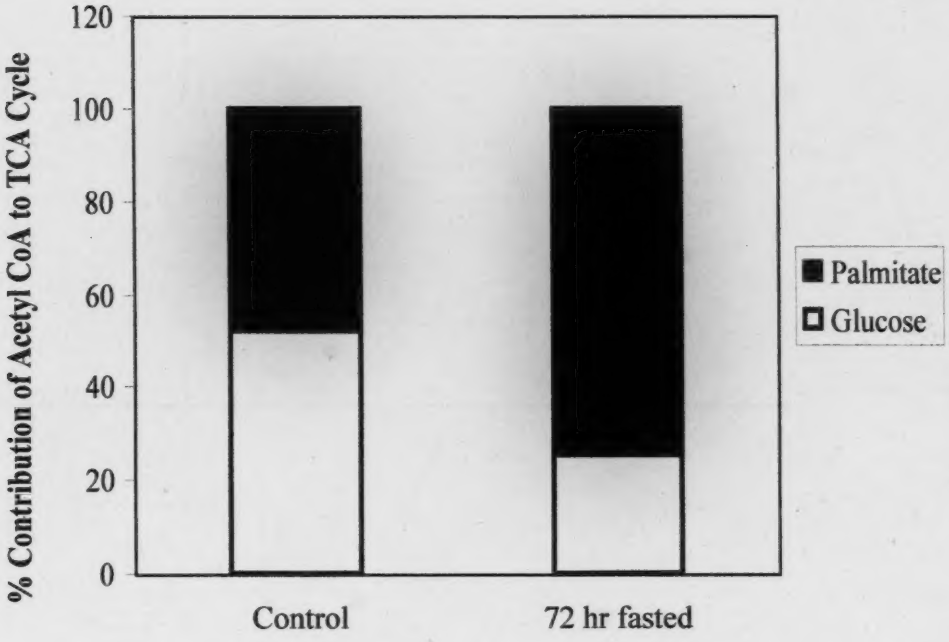

Figure 3-2. Acetyl CoA contribution to tricarboxylic acid (TCA) cycle from glucose and palmitate oxidation. Values are mean ±SE (n=10 control and n=12 fasted).

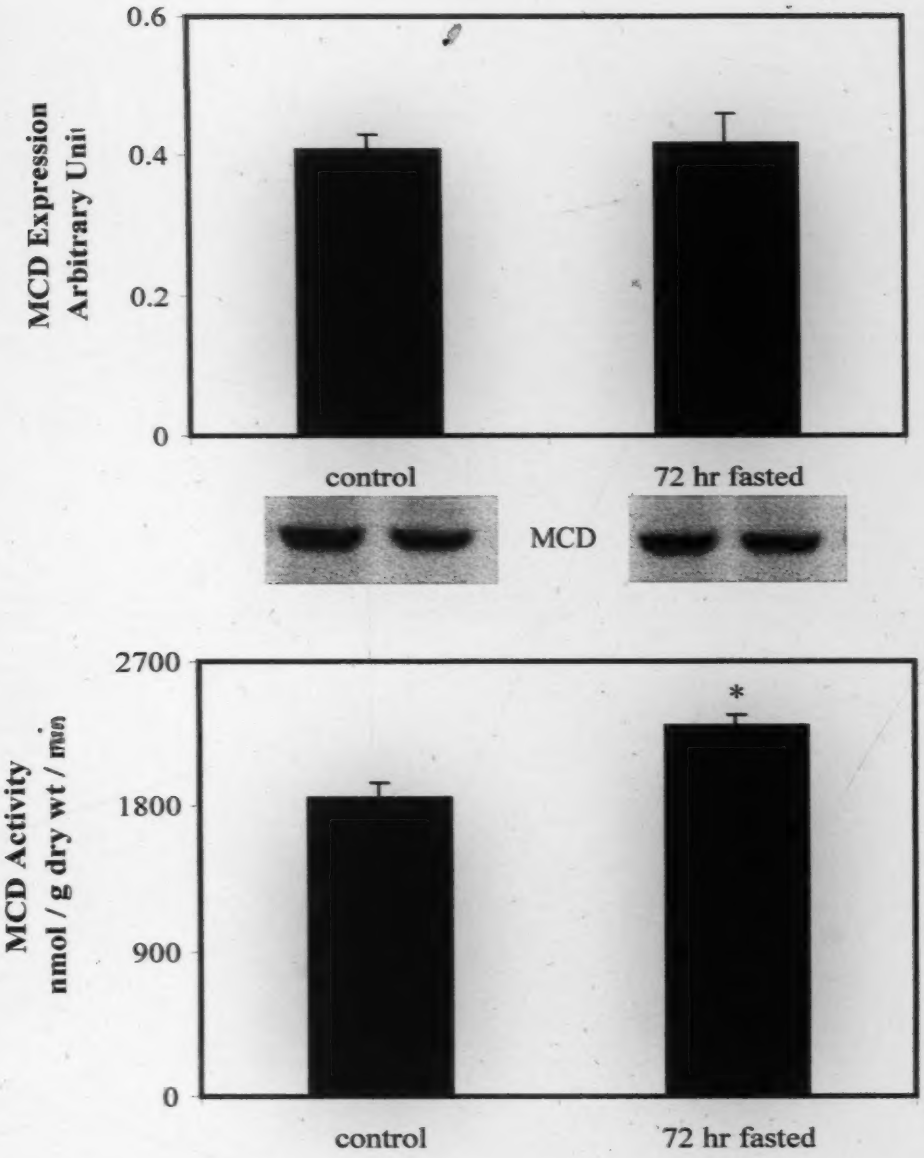

Figure 3-3. MCD expression and activity levels in hearts from control and fasted hearts. The top graph shows the expression level MCD in control and fasted hears. The bottom graph shows the MCD activity in hearts from control and fasted rats. Values are mean ± SE (n=10 control and n=12 fasted). * Significant difference in fasted group relative to control group.

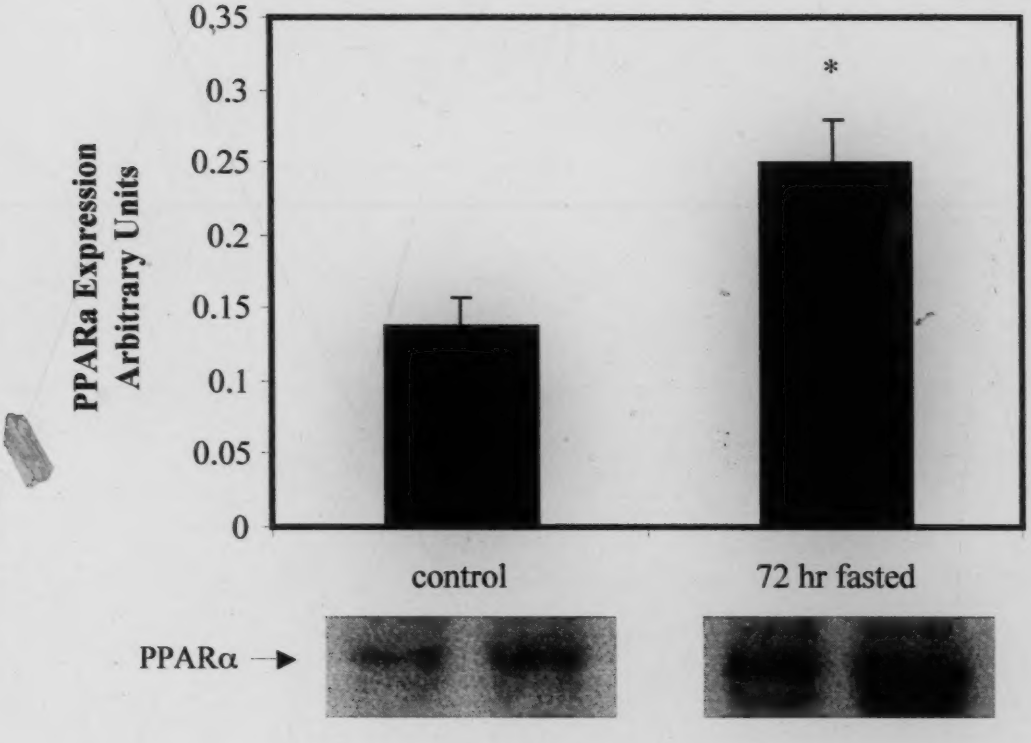

Figure 3-4. PPARα expression in hearts from control and fasted hearts. Values are mean ± SE (n=10 control and n=12 fasted). * Significant difference in fasted group relative to control group.

Table 3.2

Tissue TG, Fatty Acid Uptake and ^{3}H-Palmitate Incorporation into Endogenous TG Stores in Control and Fasted Rats

	Control (n=10)	fasted (n=12)
TG Levels of Perfused Hearts (µmol / g dry wt)	4.2 ± 0.8	2.1 ± 0.2 *
^{3}H-Palmitate Levels in TG Stores (µmol / g dry wt)	1.7 ± 0.3	1.3 ± 0.2
FA Uptake (µmol / g dry wt)	17.5 ± 2.0	26.6 ± 2.5 *
% of FA Uptake Stored as TG	10.6 ± 1.4	4.5 ± 0.7 *
% of FA Uptake Oxidized	89.4 ± 1.2	95.5 ± 1.2 *

Values are mean ± SE (n=10 control and n=12 fasted).

* Significantly different from control hearts.

Table 3.3

Plasma TG and Fatty Acid Levels in Control and Fasted Hearts.

	Control (n=10)	fasted (n=12)
Plasma TG Levels (mmol/l)	1.71 ± 0.32	0.31 ± 0.04 *
Plasma FA (mmol/l)	0.12 ± 0.03	0.26 ± 0.02 *

Values are mean ± SE (n=10 control and n=12 fasted).

* Significantly different from control hearts.

Table 3.4

Malonyl CoA and Acetyl CoA Measurements in Control and Fasted Rats

	Control (n=10)	fasted (n=12)
Malonyl CoA Levels (nmol / g dry wt)	1.79 ± 0.28	1.19 ± 0.25
Acetyl CoA Levels (nmol / g dry wt)	45.23 ± 4.70	36.39 ± 3.13

Values are mean ± SE (n=10 control and n=12 fasted).

No significant differences were noted between control and 72 hr fasted group.

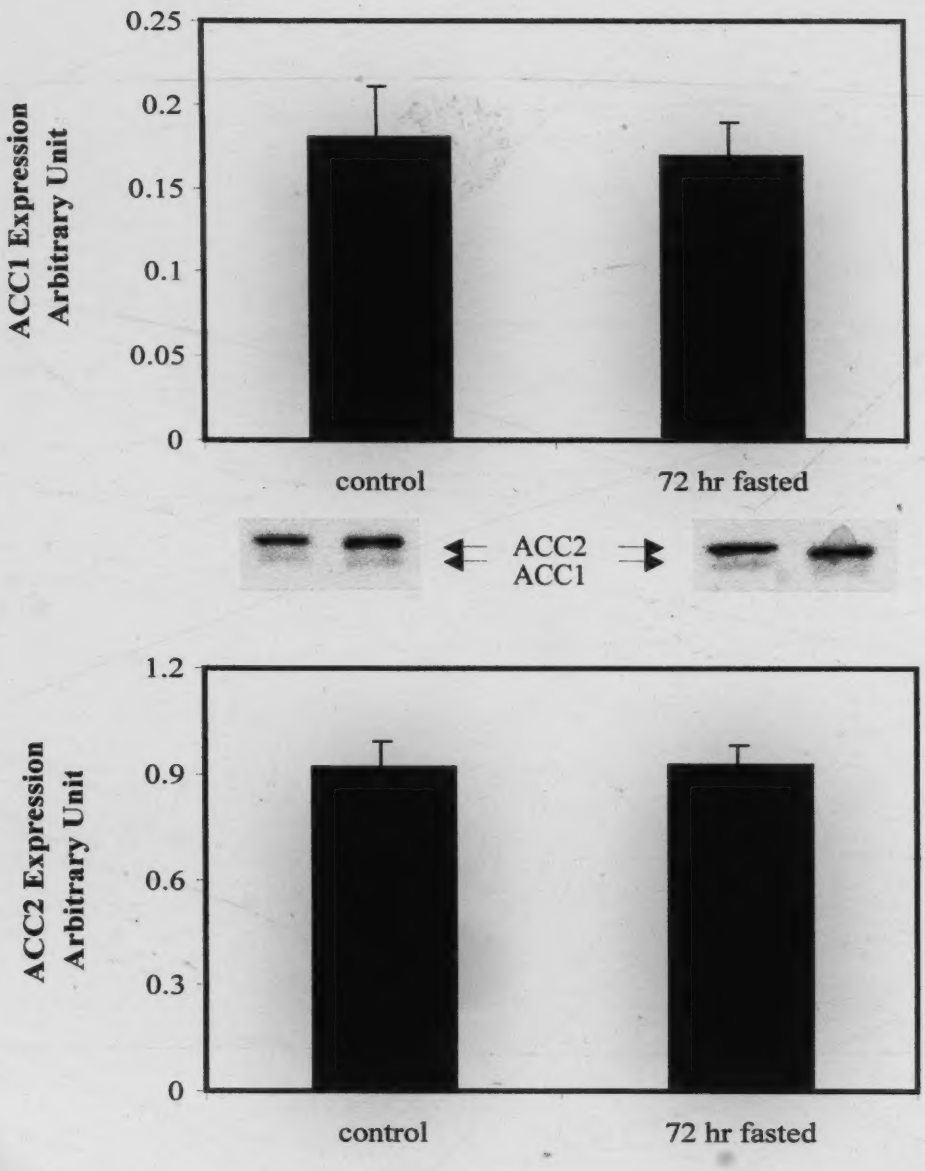

Figure 3-5. ACC1 (265 kDa isoform) and ACC2 (280 kDa isoform) expression in hearts from control and fasted hearts. Values are ± SE (n=10 control and n=12 fasted).

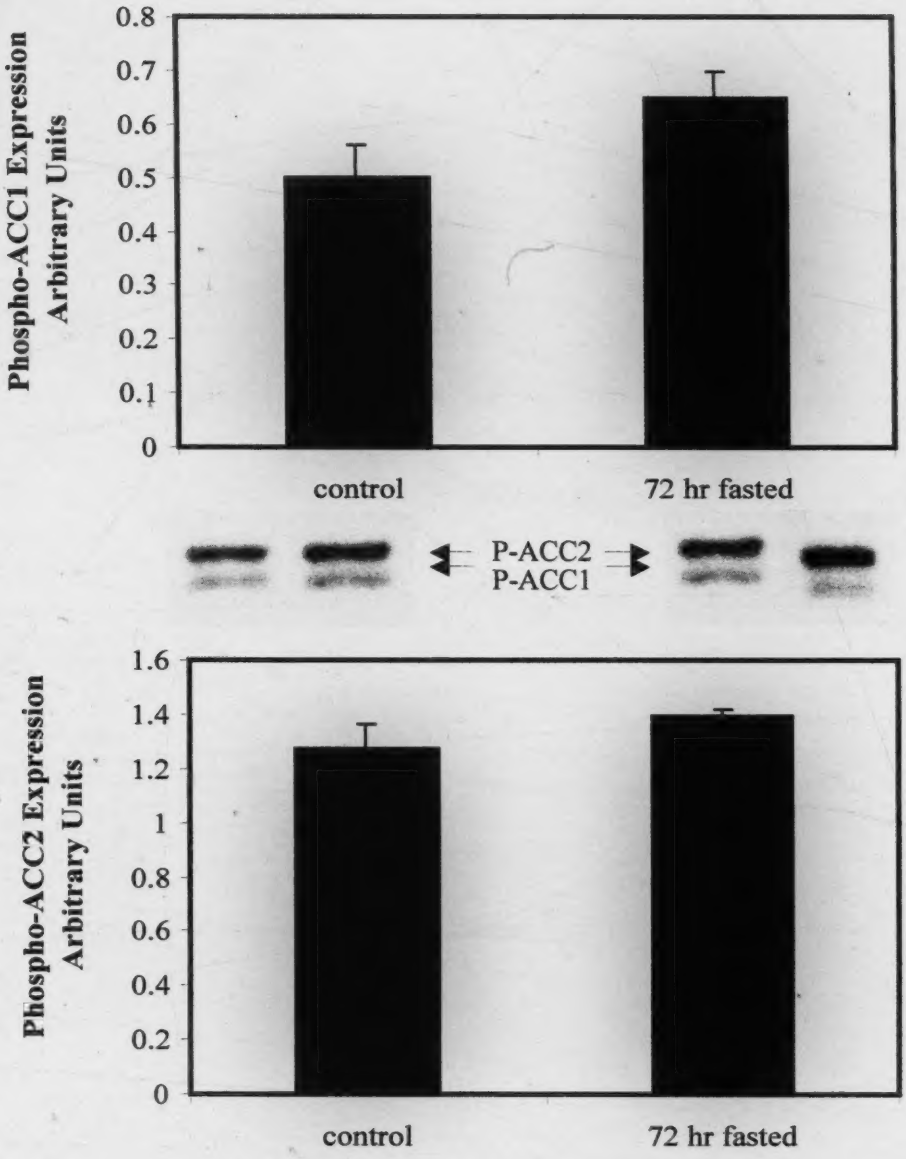

Figure 3-6. Phospho-ACC1 (265 kDa isoform) and Phospho-ACC2 (280kDa isoform) expression in hearts from control and fasted rats. Values are mean ± SE (n=10 control and n=12 fasted).

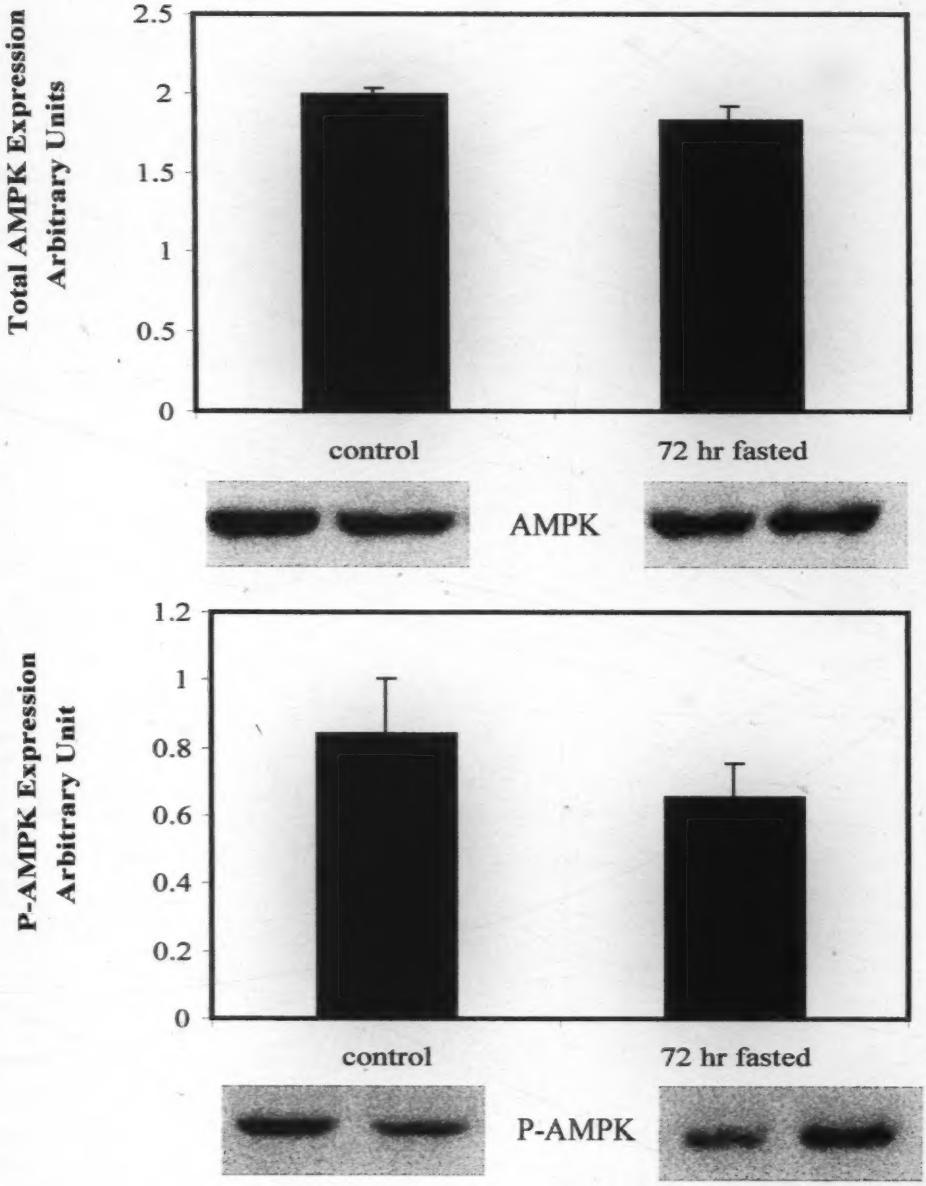

Figure 3-7. AMPK and Phospho-AMPK expression in hearts from control and fasted rats. Values are mean ± SE (n=10 control and n=12 fasted).

DISCUSSION

In this study, we demonstrated an increase in cardiac fatty acid oxidation in fasted rats relative to control rats. The purpose of the study was to examine whether the increase in fatty acid oxidation was due to an increase in the expression of enzymes involved in the regulation of malonyl CoA (an important regulator of fatty acid oxidation) possibly through the activation of PPARα which has been shown to occur during fasting.

In the fasted heart, fatty acid oxidation has been shown to provide up to 90% of the myocardial ATP (Kantor et al. 2001 and Suzuki et al. 2002). In our studies we also saw a significant increase in fatty acid oxidation rates coupled with a significant decrease in glucose oxidation rates. Cardiac fatty acid utilization is controlled, in part, by the regulation of expression of genes involved in fatty acid uptake and oxidation (Barger et al. 2000). One mechanism by which this expression regulation may occur is through PPARα, a lipid-activated nuclear receptor that induces the transcription of a number of genes involved in the control of lipid metabolism (Barger et al. 2000 and Campbell et al. 2002). PPARα increases the expression of a number of enzymes involved in fatty acid transport and utilization such as fatty acid transport protein (FATP), fatty acyl translocase (FAT/CD36), acyl CoA synthetase (ACS), muscle-specific carnitinepalmitoyl transferase-1 (CPT-1), acyl dehydrogenase (both MCAD and LCAD) and 3-ketoacyl-CoA thiolase (3-KAT) (Motojima et al. 2000, van Bilsen

et al. 1997, van der Lee et al. 2000, Brandt et al. 1998, Djouadi et al. 1999, Gulick et al. 1994 and Barger et al. 2001). However, the expression changes of MCD, ACC and AMPK during fasting have not been fully characterized. Young et al. in 2001 demonstrated a PPARα induced increase of expression and activity of MCD. Additionally, Campbell et al. (2002) showed a decrease in MCD expression and activity in PPARα knockout transgenic mice; therefore, these data imply PPARα's role in the regulation of MCD. Since PPARα has been shown to induce genes involved in the fatty acid metabolism, it is possible that this increase may occur, in part, due to the PPARα regulated expression of genes for MCD (as shown by Campbell et al. 2002 and Young et al. 2001) as well as ACC and AMPK (although no previous literature addresses this), all of which play a role in the regulation of malonyl CoA levels. We, thus, hypothesized that the increase in fatty acid oxidation noted during fasting was coupled to an increase in the expression of PPARα, which would be linked to an alteration in expression levels of MCD, AMPK and ACC. The first step in determining whether this was true was to use nutritionally deprived rats and demonstrate an increase in cardiac fatty acid oxidation.

Two groups of rats were chosen at random and assigned to either the fasted group or the control group. Fasted rats were nutritionally deprived for 72 hours whereas the control group was allowed to eat *ad libitum* during this period. In order to maintain a controlled environment, all rats were housed individually. At the end of the 72 hour period rats were sacrificed and hearts were perfused for measurement of levels of

glucose and fatty acid oxidation. In the fasted rats, cardiac fatty acid oxidation rates significantly increased relative to the controls, while glucose oxidation rates decreased significantly. These results are in accordance with that which has been published previously in the literature (Van der Lee et al. 2001 and Suzuki et al. 2002) and thus, this confirms that our model of fasting and heart perfusion render metabolic results comparable to those previously published. Additionally, our results showed an increase in the acetyl CoA contribution to the TCA cycle from acetyl CoA derived from fatty acid oxidation in the fasted group relative to controls, thus suggesting hearts from the fasted group demonstrated increased reliance on palmitate oxidation than on glucose oxidation.

In order to explain how this increase in fatty acid oxidation occurs during fasting, the expression levels of PPARα were determined in the fasted and control rat hearts. PPARα is lipid-activated nuclear receptor that encodes for transcription of fatty acid oxidation enzymes and proteins involved in cellular fatty acid import and oxidation (Finck et al. 2002). Previous studies examining the effects of fasting have demonstrated an increase in the expression of PPARα in fasted hearts relative to control hearts (Van der Lee et al. 2001). Therefore, in our studies, we examined the expression of cardiac PPARα through immunoblot analysis. In our fasted group, there was a significant increase of expression of cardiac PPARα relative to the control group. Therefore, the increase in fatty acid oxidation noted in the heart during fasting may be attributed to the increase in PPARα expression. In order to elucidate the

mechanism by which this increase occurred, we decided to examine whether the expression level of enzymes involved in the regulation of malonyl CoA levels changed during fasting. This seemed logical since malonyl CoA is a potent inhibitor of carnitine palmitoyltransferase-1 (CPT-1), the enzyme that transports acyl CoA into the mitochondria for fatty acid oxidation (McGarry et al. 1978 and Saggerson et al. 1986).

It has been suggested that during fasting, expression and activity levels of MCD are increased due to PPARα specific activation (Young et al. 2001). Additionally, Campbell et al. (2002) showed that in transgenic PPARα knockout mice, MCD expression and activity decreased relative to control mice. Therefore, we examined whether there was an increase in MCD expression and activity in the fasted hearts. We found there to be no alteration in the expression level of MCD in the fasted hearts relative to control; however, when the MCD activity was examined, we found there to be an increase in MCD activity in fasted rats relative to control. This data is supported by previously published data showing that in fasted rats, MCD activity increases; however, the total MCD protein levels are unchanged (Dyck et al. 2000). Our data suggest that the increase in fatty acid oxidation noted during our fasting study is not due to an increase of the expression of MCD. Thus, the increase in MCD activity may be through a number of different mechanisms such as phosphorylation (Dyck et al. 2000); however, further experimentation will be required to determine whether this is the case in our experiments.

It is possible that the increase of PPARα expression noted during our fasting study was not as high as the expression elicited in the Young et al. (2001) study. In their study, the activation of PPARα using the activator WY-14643 may be greater than that which we elicited by fasting induced expressional increase. Thus, the increase of PPARα we noted in fasting may not be enough to induce the transcriptional control of MCD; however, further experimentation will have to be performed to determine whether or not this is the case.

Another enzyme that is involved in the regulation of malonyl CoA levels is ACC (McGarry et al. 1977, Awan et al. 1993 and Saddik et al. 1993) whose activity results in a decrease in fatty acid oxidation. Therefore, we proposed that during fasting, there may be a PPARα-induced decrease in ACC expression, thus resulting in the increase in fatty acid oxidation. Our results demonstrated no significant difference in protein levels of ACC between the fasted and control groups. Additionally, the activity of ACC was examined through determination of phosphorylation status (phosphorylation decreases the activity of ACC) (Saddik et al. 1993 and Kudo et al. 1995). We demonstrate that there was no change in ACC activity between the control and fasted rats. This data is supported by previous studies that showed fasting does not increase ACC activity levels in muscle (Winder et al. 1995). Therefore, the changes in fatty acid oxidation during fasting were not associated with levels of expressional change of ACC or the activity of the enzyme.

Another enzyme that could potentially be involved in the alteration of cardiac fatty acid oxidation noted during fasting is AMPK, activation of which increases fatty acid

oxidation rates in the heart (Kudo et al. 1995). Therefore, we examined levels of AMPK expression and activity (as shown through AMPK phosphorylation). We did not note any significant change in AMPK expression or phosphorylation between the fasted and control group, indicating that the alteration in fatty acid oxidation noted during fasting was not due to an increase in AMPK expression.

Taken together, the lack of expressional change noted in MCD, ACC and AMPK levels between the fasted and control group indicate that these enzymes are not responsible for alterations in fuel substrate usage during fasting. It is possible that PPARα does regulate the expression of MCD, ACC and AMPK at some point during the fasting period; however, the regulation could be transient and thus our experiment did not detect it. For example, it is possible that the initial increase in cardiac fatty acid oxidation rates following the onset of fasting may be regulated by PPARα regulation of MCD, ACC and AMPK transcription (further experimentation of a time-course of the effects of fasting would be required to determined this), but 72 hours into the fasting period, the sustained increase in fatty acid oxidation rates may be due to PPARα regulation of other enzymes involved in fatty acid oxidation. Published data suggest that PPARα levels increase during fasting (Leone et al. 1999) and that PPARα has been shown to influence the utilization of fatty acids through gene expression. Genes regulated by PPARα include fatty acid transport protein (FATP), fatty acyl translocase (FAT/CD36), acyl CoA synthetase (ACS), muscle-specific carnitine palmitoyltransferase-1 (CPT-1), acyl dehydrogenase (both MCAD and

LCAD) and 3-ketoacyl-CoA thiolase (3-KAT) (Motojima et al. 2000, van Bilsen et al. 1997, van der Lee et al. 2000, Brandt et al. 1998, Djouadi et al. 1999, Gulick et al. 1994 and Barger et al. 2001).

The question still remains as to how the increase in fatty acid oxidation occurs during fasting if it is not due to an expressional increase of MCD, ACC or AMPK or and activity alteration of ACC or AMPK. Levels of malonyl CoA have been shown to be inversely correlated to rates of fatty acid oxidation within the heart (McGarry et al. 1989). Therefore, we examined levels of malonyl CoA in the fasted and control hearts and noted no significant change in the levels of malonyl CoA between these groups. We thus speculated on why this may occur. There are two possible reasons why we noted no change in whole heart levels of malonyl CoA in the fasted hearts versus controls. The first reason is that malonyl CoA levels are not responsible for the alteration of fatty acid oxidation levels noted in the fasted heart. The second possibility is that there is compartmentalization of malonyl CoA occurring in the myocytes with only small amount actually having access to CPT-1 for regulation. This possibility seems much more feasible. However, detecting these changes in malonyl CoA compartmentalization is very difficult and, to our knowledge, no group has developed a technique to determine these types of changes.

Malonyl CoA acts by inhibiting the carrier protein, CPT-1 which is a key rate-limiting enzyme involved in fatty acid oxidation (McGarry et al. 1989). Therefore, we proposed that the increase in fatty acid oxidation may be due to the decrease in levels of malonyl CoA, thereby decreasing the inhibition on CPT-1 to allow for increased

levels of fatty acid oxidation. When we noted no change in malonyl CoA levels, I turned to the literature to explain these results.

The expression of a number of different genes involved in fatty acid oxidation have been show to be increased due to PPARα activation. One of these enzymes is muscle-specific CPT-1 (Brandt et al. 1998). Therefore, since we are seeing an increase in PPARα expression during fasting, this could be resulting in an increase in CPT-1 expression. This increase could explain, in part, why we are seeing an increase in fatty acid oxidation in fasted hearts without any change in malonyl CoA levels. The increase in fatty acid oxidation could be due to a greater ability to transport fatty acids into the mitochondria by CPT-1 with no change in the regulation of the individual transporters (by malonyl CoA), thus resulting in an increase in fatty acid carriage into to mitochondria for oxidation (possible up-regulation of β-oxidation enzymes by PPARα will be explained later in this discussion).

Another result that is supported by the literature is that in fasted group, we note a significant increase in the level of free fatty acid uptake, as measured during the perfusion period, relative to control hearts. The equation used to determine the fatty acid uptake assumes the findings of Saddik et al. (1991) suggesting that the majority of free fatty acids that are incorporated into endogenous lipid stores end up in TG stores as opposed to other neutral lipids such as phospholipids, cholesterol esters and mono and diacylglycerol stores. Thus, in order to determine the cardiac fatty acid uptake we considered the fatty acid oxidation rates and incorporation of palmitate into endogenous TG stores during the perfusion period. We saw a significant increase in

fatty acid uptake and fatty acid oxidation rates in the fasted relative to control hearts, but we noted no significant change between groups of the amount of fatty acid incorporation into endogenous TG stores. The mechanism by which this increase in fatty acid oxidation rates may occur in conjunction with increased fatty acid uptake could be through the increase of PPARα that we are noting in the fasted hearts. PPARα has been shown to increase the fatty acid transport uptake through the induction of genes such as FATP, FAT/CD36 and FABP (Motojima et al. 1998, van Bilsen et al. 1997 and Van Der Lee et al. 2000). Therefore, the increase in fatty acid uptake noted in the fasted hearts could be due to the PPARα-induced expression of these genes. Up-regulation of these above-mentioned genes would result in an increase in fatty acid uptake, and this increase in uptake could be driving the increase in fatty acid oxidation rates we saw in fasted rats. However, if this were the case, we would probably have noted an increase in fatty acid incorporation into TG stores since all routes of fatty acid use would have more free fats to use due to the increase in intracellular fatty acids available. Since we noted no change in fatty acid incorporation into endogenous TG stores between the fasting and control groups, a more viable possibility of why there is a significant increase in fatty acid oxidation rates during fasting could be due to PPARα's regulation on β-oxidation enzymes. Up-regulation of β-oxidation enzymes could result in an increase in the catabolism of the up-taken fats, thus causing a 'pulling' of fats into the oxidation pathway rather than the esterification route (for anabolic TG formation). This is detailed below.

The medium chain, long chain and very-long chain acyl dehydrogenases (MCAD, LCAD, VLAD) and 3-ketoacyl-CoA thiolase (KAT) are all mitochondrial oxidation regulating enzymes whose expression is effected by PPARα (Djouadi et al. 1999, Gulick et al. 1994 and Van Der Lee et al. 2000). In our fasted rats, the increase in PPARα expression we are noting could be resulting in an increase in the expression of these enzymes which could be attributing to the increase in fatty acid oxidation rates that we are noting during fasting. It is possible, although speculative, that the up-regulation of mitochondrial fatty acid oxidation during fasting is resulting in a 'pulling' of fatty acids into the cell for oxidation. This is evidenced in our data showing an increase in fatty acid uptake in fasted hearts. However, the increase in uptake that we are noting is not coupled with an increase in fatty acid incorporation into endogenous TG stores relative to the control hearts. This suggests that enzymes associated with the esterification of fatty acids are not affected during fasting as greatly as those involved in cardiac fatty acid oxidation. Again, this is highly speculative but may provide some explanation for our findings.

A final possibility as to why there is an increase of fatty acid oxidation during fasting could be due to PPARα s' regulation of glucose oxidation. Wu et al. in 1999 demonstrated that PDK4 is activated by PPARα ligands. PDK4 is an enzyme which phosphorylates and inactivates pyruvate dehydrogenase (PD). PD converts pyruvate created through glycolysis to acetyl CoA to be used in the TCA cycle. Thus, the increase in PPARα that is being noted in the fasted tissues may be resulting in an

increase in PDK4 activity, thus leading to an decrease in PD activity which, in turn, would result in a decrease in glucose oxidation such as we are noting in the fasted group. This is only speculative but makes logical sense when considering our results with respect to glucose oxidation. This finding of Wu et al. (1999) is contradicted by Hopkins et al. (2001) whose study showed there to be only marginal changes in PDK4 expression in PPARα over-expressing transgenic mice. Hopkins et al. (2001) attributed the increase in fatty acid oxidation noted in PPARα over-expressing mice to decreased pyruvate flux through PD due to negative feedback on PD by fatty acid oxidation reaction products rather than due to PDK4 phosphorylation of PD, thereby questioning PPARα's direct role in the regulation of cardiac glucose oxidation such as suggested by Wu et al. (1999).

Therefore, there are many different mechanisms by which fasting could result in alterations in cardiac metabolism. PPARα is involved in the regulatory control of a number of different parts of the cardiac lipid utilization pathway. However, based on the results of our experiments whereby we examined the expression levels of MCD, ACC and AMPK, all of which regulate levels of malonyl CoA, it is unlikely that the increase in fatty acid oxidation we are noting during fasting is due to increased expression of these enzymes. This is supported by our data that showed no significant change in malonyl CoA levels between groups; however, as mentioned previously, our experimental protocol did not account for malonyl CoA compartmentalization that could be occurring. Additionally, based on our results, it is unlikely that during

fasting, PPARα regulates the expression of MCD, ACC or AMPK since no change of expression of MCD, ACC or AMPK was noted when PPARα expression was increased through fasting. Other enzymes have been suggested to play a role in the increase of fatty acid transport, utilization and oxidation through PPARα-mediated expression, and these enzymes may be responsible for the increase in fatty acid oxidation we noted during fasting.

REFERENCES

Awan MM, Saggerson ED. Malonyl-CoA metabolism in cardiac myocytes and its relevance to the control of fatty acid oxidation. *Biochem J.* 1993 Oct 1;295:61-6.

Barger PM, Kelly DP. PPAR signaling in the control of cardiac energy metabolism. *Trends Cardiovasc Med.* 2000 Aug;10(6):238-45.

Brandt JM, Djouadi F, Kelly DP. Fatty acids activate transcription of the muscle carnitine palmitoyltransferase I gene in cardiac myocytes via the peroxisome proliferator-activated receptor alpha. *J Biol Chem.* 1998 Sep 11;273(37):23786-92.

Campbell FM, Kozak R, Wagner A, Altarejos JY, Dyck JR, Belke DD, Severson DL, Kelly DP, Lopaschuk GD. A role for peroxisome proliferator-activated receptor alpha (PPARalpha) in the control of cardiac malonyl-CoA levels: reduced fatty acid oxidation rates and increased glucose oxidation rates in the hearts of mice lacking PPARalpha are associated with higher concentrations of malonyl-CoA and reduced expression of malonyl-CoA decarboxylase. *J Biol Chem.* 2002 Feb 8;277(6):4098-103.

Carling D, Clarke PR, Zammit VA, Hardie DG. Purification and characterization of the AMP-activated protein kinase. Copurification of acetyl-CoA carboxylase kinase and 3-hydroxy-3-methylglutaryl-CoA reductase kinase activities. *Eur J Biochem.* 1989 Dec 8;186(1-2):129-36.

Djouadi F, Brandt JM, Weinheimer CJ, Leone TC, Gonzalez FJ, Kelly DP. The role of the peroxisome proliferator-activated receptor alpha (PPAR alpha) in the control of cardiac lipid metabolism. *Prostaglandins Leukot Essent Fatty Acids.* 1999 May-Jun;60(5-6):339-43.

Dyck JR, Berthiaume LG, Thomas PD, Kantor PF, Barr AJ, Barr R, Singh D, Hopkins TA, Voilley N, Prentki M, Lopaschuk GD. Characterization of rat liver malonyl-CoA decarboxylase and the study of its role in regulating fatty acid metabolism. *Biochem J.* 2000 Sep 1;350 Pt 2:599-608.

Escher P, Braissant O, Basu-Modak S, Michalik L, Wahli W, Desvergne B. Rat PPARs: quantitative analysis in adult rat tissues and regulation in fasting and refeeding. *Endocrinology.* 2001 Oct;142(10):4195-202.

Finck BN, Lehman JJ, Leone TC, Welch MJ, Bennett MJ, Kovacs A, Han X, Gross RW, Kozak R, Lopaschuk GD, Kelly DP. The cardiac phenotype induced by PPARalpha overexpression mimics that caused by diabetes mellitus. *J Clin Invest.* 2002 Jan;109(1):121-30.

Gulick T, Cresci S, Caira T, Moore DD, Kelly DP. The peroxisome proliferator-activated receptor regulates mitochondrial fatty acid oxidative enzyme gene expression. *Proc Natl Acad Sci U S A.* 1994 Nov 8;91(23):11012-6.

Hardie DG. Regulation of fatty acid and cholesterol metabolism by the AMP-activated protein kinase. *Biochim Biophys Acta.* 1992 Feb 12;1123(3):231-8.

Hopkins TA, Sugden MC, Holness MJ, Kozak R, Dyck JR, Lopaschuk GD. Control of cardiac pyruvate dehydrogenase activity in peroxisome proliferator-activated receptor-{alpha} transgenic mice. *Am J Physiol Heart Circ Physiol.* 2003 Jul;285(1):H270-H276.

Kantor P, Lopaschuk GD, Opie L. Myocardial Energy Metabolism. Heart Physiology and Pathophysiology, Fourth Edition. 543-569. 2001. Edited by Kurachi Y, Terzic A, Cohen M, and Sperelakis N. Copyright © 2001 by Academic Press.

Kudo N, Gillespie JG, Kung L, Witters LA, Schulz R, Clanachan AS, Lopaschuk GD. Characterization of 5'AMP-activated protein kinase activity in the heart and its role in inhibiting acetyl-CoA carboxylase during reperfusion following ischemia. Biochim Biophys Acta. 1996 May 31;1301(1-2):67-75.

Leone TC, Weinheimer CJ, Kelly DP. A critical role for the peroxisome proliferator-activated receptor alpha (PPARalpha) in the cellular fasting response: the PPARalpha-null mouse as a model of fatty acid oxidation disorders. *Proc Natl Acad Sci U S A*. 1999 Jun 22;96(13):7473-8.

McGarry JD, Mannaerts GP, Foster DW. A possible role for malonyl-CoA in the regulation of hepatic fatty acid oxidation and ketogenesis. *J Clin Invest.* 1977 Jul;60(1):265-70.

McGarry JD, Woeltje KF, Kuwajima M, Foster DW. Regulation of ketogenesis and the renaissance of carnitine palmitoyltransferase. *Diabetes Metab Rev.* 1989 May;5(3):271-84.

Motojima K, Passilly P, Peters JM, Gonzalez FJ, Latruffe N. Expression of putative fatty acid transporter genes are regulated by peroxisome proliferator-activated receptor alpha and gamma activators in a tissue- and inducer-specific manner. *J Biol Chem*. 1998 Jul 3;273(27):16710-4.

Saddik M, Lopaschuk GD. Myocardial triglyceride turnover and contribution to energy substrate utilization in isolated working rat hearts. *J Biol Chem.* 1991 May 5;266(13):8162-70.

Saddik M, Gamble J, Witters LA, Lopaschuk GD. Acetyl-CoA carboxylase regulation of fatty acid oxidation in the heart. *J Biol Chem.* 1993 Dec 5;268(34):25836-45.

Saggerson D. Carnitine palmitoyltransferase in extrahepatic tissues. *Biochem Soc Trans.* 1986 Aug;14(4):679-81.

Sim AT, Hardie DG. The low activity of acetyl-CoA carboxylase in basal and glucagon-stimulated hepatocytes is due to phosphorylation by the AMP-activated protein kinase and not cyclic AMP-dependent protein kinase. *FEBS Lett.* 1988 Jun 20;233(2):294-8.

Suzuki J, Shen WJ, Nelson BD, Selwood SP, Murphy GM Jr, Kanehara H, Takahashi S, Oida K, Miyamori I, Kraemer FB, Kanefara H. Cardiac gene expression profile and lipid accumulation in response to starvation. *Am J Physiol Endocrinol Metab.* 2002 Jul;283(1):E94-E102.

van Bilsen M, de Vries JE, Van der Vusse GJ. Long-term effects of fatty acids on cell viability and gene expression of neonatal cardiac myocytes. *Prostaglandins Leukot Essent Fatty Acids.* 1997 Jul;57(1):39-45.

van Bilsen M, van der Vusse GJ, Reneman RS. Transcriptional regulation of metabolic processes: implications for cardiac metabolism. *Pflugers Arch.* 1998 Dec;437(1):2-14.

van der Lee KA, Vork MM, De Vries JE, Willemsen PH, Glatz JF, Reneman RS, Van der Vusse GJ, Van Bilsen M. Long-chain fatty acid-induced changes in gene expression in neonatal cardiac myocytes. *J Lipid Res.* 2000 Jan;41(1):41-7.

Van der Lee KA, Willemsen PH, Samec S, Seydoux J, Dulloo AG, Pelsers MM, Glatz JF, Van der Vusse GJ, Van Bilsen M. Fasting-induced changes in the expression of genes controlling substrate metabolism in the rat heart. *J Lipid Res.* 2001 Nov;42(11):1752-8.

Winder WW, MacLean PS, Lucas JC, Fernley JE, Trumble GE. Effect of fasting and refeeding on acetyl-CoA carboxylase in rat hindlimb muscle. *J Appl Physiol.* 1995 Feb;78(2):578-82.

Wu P, Inskeep K, Bowker-Kinley MM, Popov KM, Harris RA. Mechanism responsible for inactivation of skeletal muscle pyruvate dehydrogenase complex in starvation and diabetes. *Diabetes*. 1999 Aug;48(8):1593-9.

Young ME, Goodwin GW, Ying J, Guthrie P, Wilson CR, Laws FA, Taegtmeyer H. Regulation of cardiac and skeletal muscle malonyl-CoA decarboxylase by fatty acids. *Am J Physiol Endocrinol Metab*. 2001 Mar;280(3):E471-9.

CHAPTER 4.

Cardiac *in vivo* Gene Therapy: A Cautionary Tale

My role in this work involved performing all gene transfer surgeries, perfusions and biochemical experiments, except for those mentioned below. Heart preparations for histological analysis were contracted to the Pathology department at the University of Alberta Hospital, who fixed, embedded and sliced the hearts for analysis. The adenovirus was made and propagated by Amy Barr, who also created the GFP construct. Judith Altarejos prepared the transgene for caAMPK. I performed some of the cardiac myocyte isolations with the help of Lynn Eisner, who performed the rest.

CHPATER 4

Cardiac *in vivo* Gene Therapy: A Cautionary Tale

Abstract

Intracoronary gene delivery has been suggested to homogenously infect more than 30% of cardiac myocytes. Therefore, we wished to use this technique to infect the heart with trangenes coding for enzymes involved in the regulation of fatty acid oxidation such as MCD and AMPK in order to elucidate the effect of these enzymes on metabolism. Rat hearts were infected *in vivo* via the coronary arteries with either an adenovirus containing the gene for green fluorescent protein (GFP) or constitutively active 5'AMP-activated protein kinase co-expressing green fluorescent protein (caAMPK-GFP). However, subsequent perfusion showed no change in fatty acid metabolism between the Ad-GFP and Ad-caAMPK infected groups. Thus, we needed to confirm that the efficiency of myocyte infection was similar to that previously published. An examination of the intracoronary technique showed that in whole-heart homogenates, GFP was being expressed in both the Ad-GFP and Ad-caAMPK-GFP infected groups. We also performed intracoronary gene deliveries using the transgene coding for Akt and immunoblotted whole heart homogenates to

demonstrate an increase in Akt expression. When cardiac myocyte isolation was performed to quantify infection, only 0.2 ± 0.03% of the myocytes were actually infected. Even with the addition of histamine (to increase endothelial cell permeability), only 0.8 ± 0.08% of the cardiac myocytes were infected. When hearts infected with GFP were fixed and sliced for identification of the location of GFP expression, a marked expression of GFP in the endothelial layer of the vasculature in both the myocardium and epicardium was observed. Thus, we decided to employ an alternate gene delivery technique whereby the virus containing the transgene was directly injected into a targeted area of the myocardium through the direct myocardial injection technique. Results from these experiments demonstrated an increase in the percentage of myocytes infected to 5.1 ± 0.3%, while heart slices revealed the expression of the GFP transgene in the cardiac myocytes. Taken together, our data imply that the intracoronary gene delivery technique does not infect cardiac myocytes with the efficiency previously suggested and that most of the virus infects the coronary vasculature. In addition, out data also imply that the virus may not even be gaining access to the myocardium since very few endothelial cells of the myocardial vasculature are infected relative to the endothelial cells in the epicardial vasculature. The direct injection technique, while able to infect an increased percentage of myocytes, does not allow for the homogenous gene delivery previously promised by the intracoronary technique. Thus, in summary, results from the *in vivo* study suggest that caution must be taken when considering these *in vivo* gene delivery techniques

due to the low efficiency of myocyte infection rendered from these methods of delivery.

INTRODUCTION

In vivo cardiac gene transfer holds the promise of facilitating the elucidation of the function of the delivered gene within the proper context of its physiological function. Much insight can be gained from the overexpression of wild-type genes or by the suppression of other genes by using dominant-negative constructs. Cardiac gene therapy has been suggested for treatment of cardiovascular diseases such as heart failure and ischaemic heart disease, with initial studies examining gene therapy for treatment of such diseases demonstrating initial promise (Hajjar et al. 1998 and Laham et al. 1998).

Barr et al. (1994) published on the efficiency of the intracoronary gene delivery technique as an efficient means of infecting cardiac myocytes. These results were supported by Hajjar et al. (1998) and the promise that intracoronary gene delivery was an efficient means of homogenously infecting the cardiac myocytes was introduced into the literature. With the ability to modify the genetic blueprint of the myocytes to render different functional and metabolic effects, the possibility for a variety of different transgenes to be expressed *in vivo* has become a very attractive scientific tool.

Certain cardiovascular diseases are associated with alterations in cardiac metabolism. An example being diabetes and / or ischemia where levels of fatty acid oxidation increase dramatically and this increase is associated with functional

deficiency (Kannel et al. 1976 and Lopaschuk et al. 1994). Therefore, if enzymes involved in regulating levels of fatty acid oxidation in the heart could be targeted and their activity altered, the levels of fatty acid oxidation within the heart could be modified. This modification could have potential implications in the treatment of diabetes and ischemic heart disease.

There are different techniques by which cardiac *in vivo* gene therapy can be achieved. The two most commonly used techniques are the intracoronary technique and the direct myocardial injection technique (Hajjar et al. 1998 and Acsadi et al. 1991). There are both advantages and disadvantages associated with each technique; however, we were attracted to the intracoronary gene delivery technique since it has been suggested to render efficient gene delivery homogenously throughout the myocardium (Hajjar et al. 1998) and these aspects of delivery were necessary for our experiments. (Refer to Chapter 1 for full explanation of techniques - their benefits, drawbacks and their uses).

Two enzymes that are intimately involved in the regulation of fatty acid oxidation are MCD and AMPK, the activities of which control fatty acid oxidation via altering malonyl CoA levels (Kudo et al. 1996 and Dyck et al. 1998). Therefore, if the over-expression or decreased expression of these enzymes could be achieved *in vivo*, determination of the alterations in cardiac metabolism elicited by this over-expression could allow us to confirm that metabolic alteration can be achieved through genetic manipulation of the cardiac myocytes. Previous *in vitro* experiments in our laboratory have demonstrated an increase in fatty acid oxidation levels in cultured cardiac

myocytes infected with an adenovirus vector containing the constitutively active transgene for AMPK co-expressing green fluorescent protein (GFP) (Ad-caAMPK-GFP) (unpublished data) and thus, it is proposed that the *in vivo* delivery of the same gene will render similar metabolic results.

Thus, we hypothesized that the intracoronary *in vivo* gene delivery technique would efficiently infect cardiac myocytes. Using this technique, we would deliver a constitutively active AMPK gene co-expressing GFP which we hypothesized would result in an increase in fatty acid oxidation relative to control hearts.

Preparation of Recombinant Adenovirus

The adenovirus for Ad-GFP, Ad-caAMPK-GFP and Ad-Akt was prepared as described in Chapter 2.

Animals

Male Sprague-Dawly rats (250-300g) were used for all viral deliveries.

Surgical Procedure

The thoracotomy, preparation of hearts for viral delivery, and post-surgical care of the animals is described in detail in Chapter 2.

Intracoronary Gene Delivery

In vivo intracoronary gene delivery virus to heart in the absence (Ad-GFP, Ad-caAMPK-GFP and Ad-Akt) and presence (Ad-GFP) of histamine was performed as described in Chapter 2.

Direct Myocardial Injection of Virus

Cardiac gene delivery via the direct injection of Ad-GFP into the myocardium was performed as described in Chapter 2.

Perfusions of Infected Hearts

Hearts infected intracoronarily with Ad-GFP and Ad-caAMPK-GFP were perfused and analyzed for function and metabolic changes, as described in Chapter 2. The perfusion buffer contained in mM: NaCl 118, $NaHCO_3$ 25, KCl 4.7, KH_2PO_4 1.2, $MgSO_4$ 1.66, $CaCl_2$ 2.5, palmitate 0.4 and glucose 5 (as well as 100 μU/L of insulin).

Assessment of Cardiac Protein Expression

Infected hearts were pulverized, homogenized and immunoblotted for the presence of GFP, c-myc (which identifies the presence of caAMPK) and Akt, as described in Chapter 2.

Cardiac Myocyte Isolation

Infected hearts from all delivery groups underwent cardiac myocyte isolation and visualized for quantification of the percentage of myocytes infected via the various gene delivery techniques (intracoronary with and without histamine and direct injection), as described in Chapter 2.

***In situ* visualization of GFP expression**

Prior to cardiac myocyte isolation, hearts infected via the intracoronary technique (in the presence and absence of histamine) and the direct injection technique were visualized *in situ* for determination of GFP expression, as described in Chapter 2.

Preparation of Heart Slices for GFP Fluorescence Analysis

Infected hearts from the intracoronary technique with histamine and the direct injection technique were fixed, embedded, sliced and visualized for qualification and determination of location of GFP fluorescence, as described in Chapter 2.

Statistics

Data was analyzed using either Student-Neumman-Keuls test for groups where there was no significant difference between standard deviations or the Welch's Test for unequal variance for groups where there was significant difference between standard deviations. Values are shown as mean ± the standard error of the mean (SEM). The data were analyzed using the statistical program Instat 2.01. Two-tailed values were deemed significant when $p<0.05$.

Intracoronary perfusion Data Ad-GFP (n=4) vs. Ad-caAMPK-GFP (n=7)

Hearts infected with Ad-GFP and Ad-caAMPK-GFP via the intracoronary gene delivery technique in the absence of histamine were perfused 5 days (120 hours) following infection. There was no significant difference in functional perfusion parameters (Table 4.1), palmitate oxidation rates or glucose oxidation rates (Figure 4-1) between the Ad-GFP and Ad-caAMPK-GFP groups.

Determination of Myocardial GFP content

Immunoblotting was performed on whole heart homogenates to confirm the expression of GFP in infected hearts following perfusion. Figure 4-2 shows infected hearts that were homogenized, standardized and immunoblotted for GFP presence. Positive control (GFP protein tagged with a 2 kDa his-protein) and uninfected control were used to show the presence of GFP within the cells. All infected hearts showed the presence of GFP, while the uninfected control showed no presence of the 27 kDa GFP protein All infected hearts (infected with Ad-GFP and Ad-caAMPK-GFP) showed presence of GFP.

Determination of Myocardial c-myc (showing caAMPK content)

Hearts that were infected with Ad-GFP (1 heart examined from this group) and Ad-caAMPK-GFP (3 hearts examined from this group) (tagged with the c-myc protein for

identification purposes) were homogenized, standardized and immunoblotted for presence of c-myc, which would indicate the presence of the expressed caAMPK. Hearts were immunoblotted and compared to uninfected tissues as well as a positive control (cells infected *in vitro* with the Ad-caAMPK-GFP virus). The presence of c-myc was not detected in any of the infected tissues (Figure 4-3).

Myocardial Akt Protein Content

The intracoronary delivery of Ad-Akt1 was performed to ensure that the immunoblot results showed an increase in Akt levels (Figure 4-4) similar to those already presented in the literature (Figure 4-5). We performed the intracoronary delivery of Ad-Akt using the same virus, concentration of virus and method of delivery as the results presented in the literature (Taniyama et al. 2002). We observed an increase in the protein level of Akt in the infected tissue relative to the uninfected control similar to that observed by Taniyama et al. 2002).

Comparison of GFP Expression in Hearts Infected with Ad-GFP via Intracoronary Delivery (without and with histamine) or Direct Myocardial Injection

Infected hearts were crushed, homogenized and standardized for protein content. These tissues were then immunoblotted to demonstrate the relative GFP expression in the three delivery groups. Figure 4-6 shows the relative amounts of GFP in the hearts

from the intracoronary techniques (absence and presence of histamine) and the direct myocardial injection technique.

Cardiac myocyte isolation

Intracoronary Delivery without Histamine

In order to examine the efficiency of gene delivery techniques to directly infect the cardiac myocytes, cardiac myocytes were isolated from the left ventricle of hearts infected with Ad-GFP via the intracoronary delivery technique in the absence of histamine. Hearts were subjected to collagenase digestion and myocytes were isolated and visualized to quantify the percentage of myocytes infected from this gene delivery method (Figure 4-7). A total of 3 hearts were isolated and visualized. The percentage of myocytes expressing GFP was $0.2 \pm 0.03\%$.

Intracoronary Delivery with Histamine

Cardiac myocytes were isolated from the left ventricle of hearts infected using the histamine intracoronary delivery technique. The hearts were subjected to collagenase digestion and the myocytes were visualized and quantified to determine the percentage of myocytes infected. Figure 4-8 is a picture taken from one of the hearts and represents the number of myocytes infected in the hearts from this delivery technique. A total of 4 hearts were studied and the mean percentage of myocytes infected from this technique was $0.8 \pm 0.08\%$.

Direct injection

Hearts from rats infected with Ad-GFP via 10 direct injection sites into the myocardium of the left ventricle were subjected to collagenase digestion and a portion of the left ventricle was removed and further subjected to collagenase digestion. The cardiac myocytes were isolated and visualized. Pictures were taken of the cardiac myocytes from these hearts and the cells were counted in order to determine the percentage of myocytes infected in the left ventricle of the direct injection infected heart (Figure 4-9). A total of 3 hearts were studied and the percentage of myocytes infected in the left ventricle was 5.1 ± 0.3%.

Following the initial collagenase digestion, the hearts, which had already had a portion of the left ventricle removed for secondary collagenase digestion to determine the % of myocytes in the entire ventricle, were visualized *in situ* to determine whether there were any other injection sites. Injection sites that were visualized in each heart were removed and subjected to secondary collagenase digestion. These isolated myocytes were quantified for the infection efficiency surrounding the injection site (Figure 4-10). A total of 36.4 ± 2.9% of the myocytes demonstrated expression of GFP in this isolated area of the ventricle (n=3).

Comparison of Techniques

Figure 4-11 compares the efficiency of myocyte infection in the entire left ventricle from the various gene delivery techniques studied. In the presence of histamine, the intracoronary technique increased the efficiency of myocyte infection by 4 fold

(p=0.0015), while delivering of virus directly into the myocardium increased the percentage of infected myocytes by 25 fold compared to the intracoronary technique without histamine (p=0.0035). The results quantifying the percentage of myocytes infected from all techniques are summarized in Table 4.2.

In situ Heart Fluorescence Microscopy

Prior to secondary collagenase digestion, the infected hearts were visualized *in situ* to examine the pattern of myocyte infection in the hearts from the different delivery techniques. Figures 4-12 and 4-13 are representative pictures taken of hearts that were infected by the intracoronary and direct injection technique, respectively. Figure 4-12 shows some myocytes expressing GFP; however, the figure also shows there to be significant GFP expression in a coronary vessel. Figure 4-13 shows myocytes expressing GFP. No vasculature is noted to be expressing GFP as is the case with the intracoronary picture (Figure 4-12). Additionally, Figure 4-14 shows the pattern of GFP expression surrounding the injection site following direct injection of Ad-GFP The purpose of this picture is to show the localization of infection to injection site following direct myocardial injection. Finally, a segment of the aorta from an intracoronary delivery heart was isolated and visualized for fluorescence. Figure 4-15 shows the marked GFP expression in all layers of the aortic vasculature wall.

Localization of GFP Fluorescnce in Slices from GFP Infected Hearts

Hearts infected via the intracoronary delivery technique in the presence of histamine were examined for GFP fluorescence in the epicardial segment of the heart. Infected hearts demonstrated the presence of extensive GFP fluorescence in the coronary vasculature (Figure 4-16A). In order to confirm this fluorescence was due to GFP and not background, uninfected control hearts were also prepared, sliced and visualized for fluorescence. Figure 4-16B demonstrates the lack of fluorescence in the control coronary vasculature.

Hearts infected via the intracoronary delivery technique in the presence of histamine were examined for GFP fluorescence in the myocardial segment of the heart. Infected hearts demonstrated the presence of GFP fluorescence in the microvasculature (Figure 4-17). Endothelial cells in the myocardium were the only cell type demonstrating fluorescence in the slices that were visualized (total of n=3 hearts were sliced and visualized).

Hearts infected via the direct injection delivery technique were examined for GFP fluorescence in the heart slices. Dramatic myocyte GFP fluorescence was noted in all infected hearts in areas surrounding the injection site. Figure 4-18 shows the infection within the myocardium of the gene delivery hearts. No fluorescence was noted in the epicardium of the infected hearts.

Surgical mortality

All delivery techniques used the same method of surgery to expose the heart for gene delivery. A total of 47 rats were used for the gene delivery studies, with 4 animals perishing during the study. For the intracoronary delivery in the absence of histamine, a total of 24 rats underwent viral delivery and 2 of these animals died. For the intracoronary delivery in the presence of histamine, a total of 11 animals were operated on and 1 of these animals died. The direct injection delivery technique study used 12 animals and 1 of these animals died following delivery. Table 4.3 shows the experimental fate of the infected hearts following various gene delivery techniques as well as the mortality noted from each technique.

Table 4.1

Perfusion Functional Parameters of Hearts Infected by Intracoronary Delivery of Ad-GFP and Ad-caAMPK-GFP

	GFP Infected (n=4)	AMPK Infected (n=7)
Heart Rate (bpm)	290 ± 9	293 ± 15
Peak Systolic Pressure (mmHg)	112 ± 8	116 ± 5
Developed Pressure (mmHg)	37 ± 7	45 ± 6
Cardiac Output (ml/min)	30 ± 7	32 ± 2

Values are mean ± SE (n=4 Ad-GFP and n=7 Ad-caAMPK-GFP).

No significant differences were noted between groups.

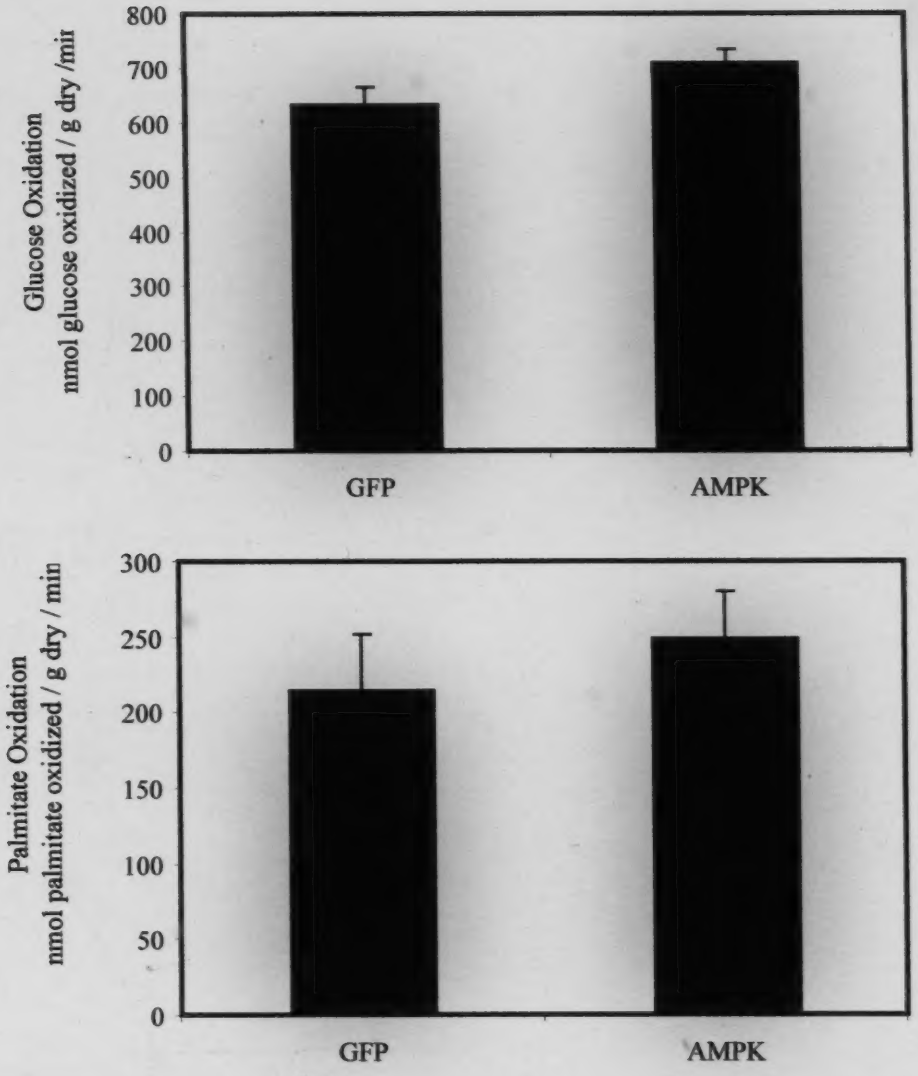

Figure 4-1.Glucose and palmitate oxidation rates in isolated working hearts from Ad-GFP and Ad-caAMPK-GFP infected hearts. Values are mean ± SE (n=4 Ad-GFP and n=7 Ad-caAMPK-GFP). No significant differences were noted between groups.

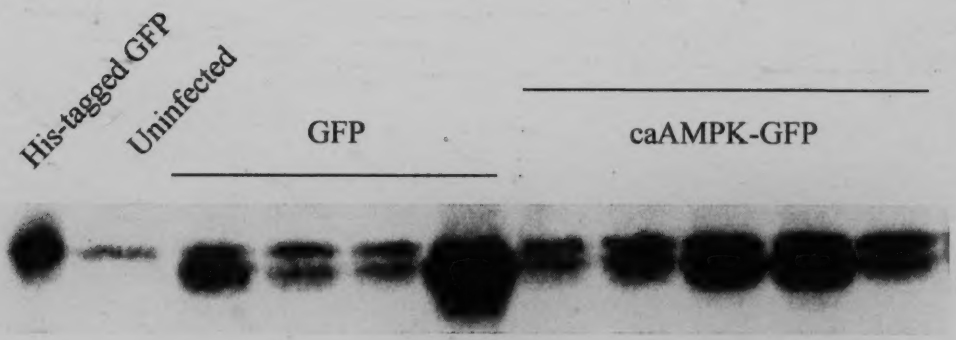

Figure 4-2. Immunoblot of Ad-GFP and Ad-caAMPK-GFP infected hearts following perfusion. A positive control (His-tagged GFP protein) and negative control (uninfected control heart) were used to determine the expression of GFP in all infected tissues. All infected hearts demonstrated GFP expression.

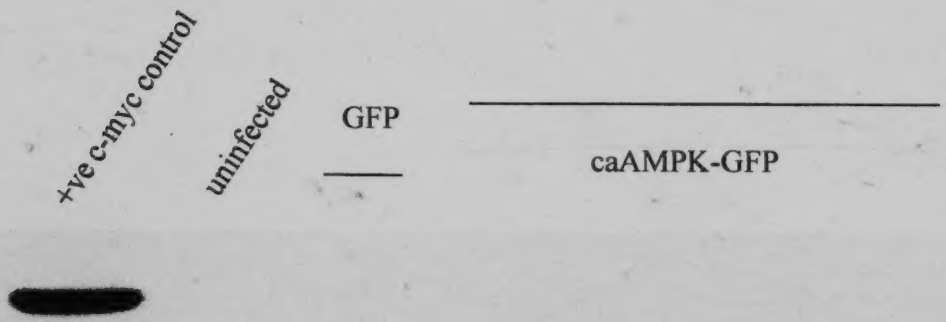

Figure 4-3. Immunoblot determination of the expression of c-myc (protein tag used to identify the presence of caAMPK expression) in Ad-GFP and Ad-caAMPK-GFP infected hearts. A positive control (cells infected with Ad-caAMPK-GFP *in vitro*) was compared with the uninfected and infected hearts. No infected hearts demonstrated c-myc expression.

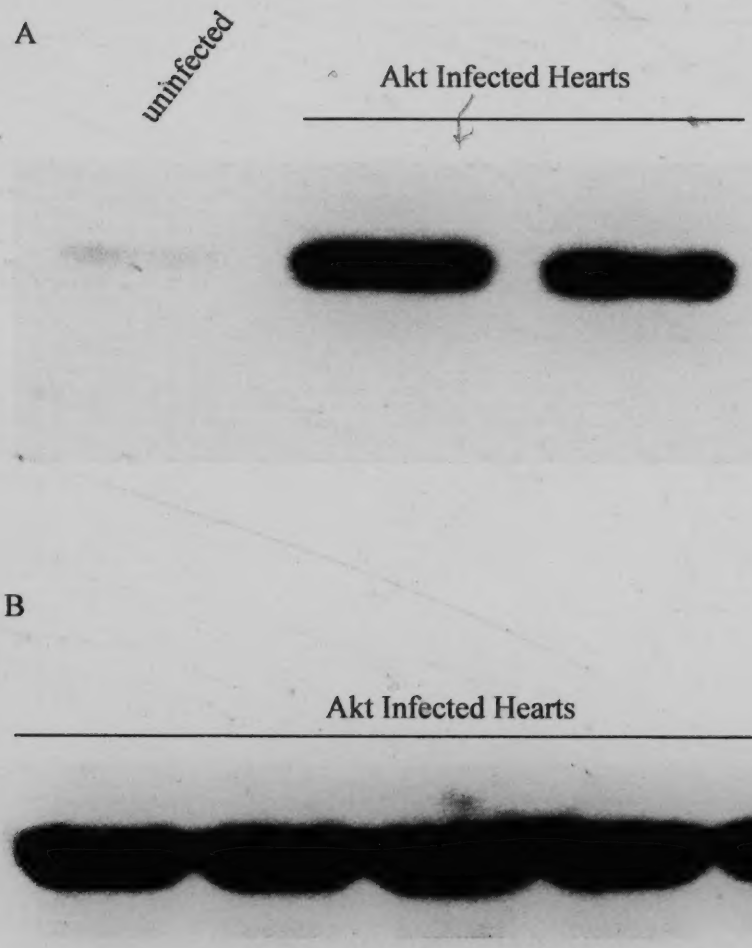

Figure 4-4. Akt expression in hearts infected with Ad-Akt1. Infections were performed by using the intracoronary gene delivery technique by replicating Taniyama et al. (2002) procedure to determine whether a similar increase in Akt could be noted (relative to Taniyama et al. 2002). Blot (A) shows the expression of Akt in two infected Ad-Akt hearts relative to an uninfected control. Blot (B) shows all 5 Ad-Akt infected hearts with the first 2 lanes being the infected hearts from Blot (A).

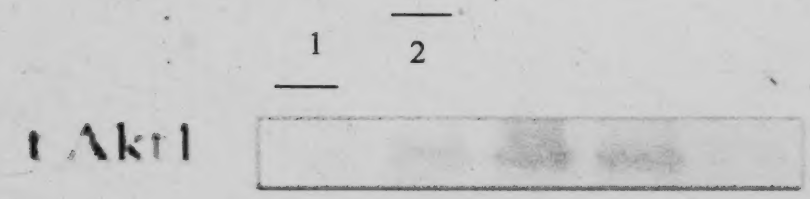

Figure 4-5. Immunoblot results of Akt expression following intracoronary delivery of Ad-Akt1 (taken from the paper of Taniyama et al. 2002). Lane 1 shows an uninfected heart and compares the Akt levels to an infected heart (lane 2) after 3 days of recovery time following the gene delivery.

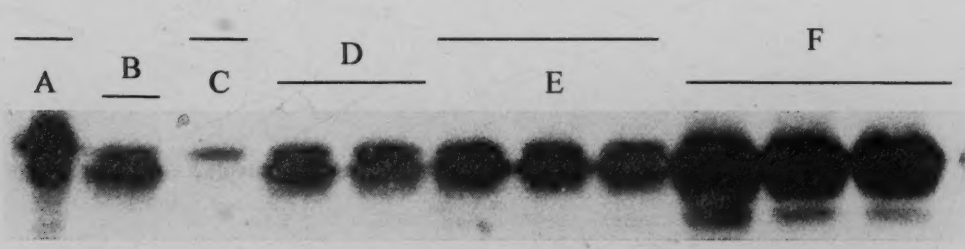

Figure 4-6. Immunoblot of hearts infected with Ad-GFP using different gene delivery techniques. Under lane (A):positive control His-tagged GFP protein control. Under lane (B): Ad-GFP positive control tissue. Under lane (C): uninfected control. Lanes under (D): 2 hearts infected by the intracoronary technique in the absence of histamine. Lanes under (E): 3 hearts infected by the intracoronary technique in the presence of histamine. Lanes under (F): 3 hearts infected by direct injection myocardial injection.

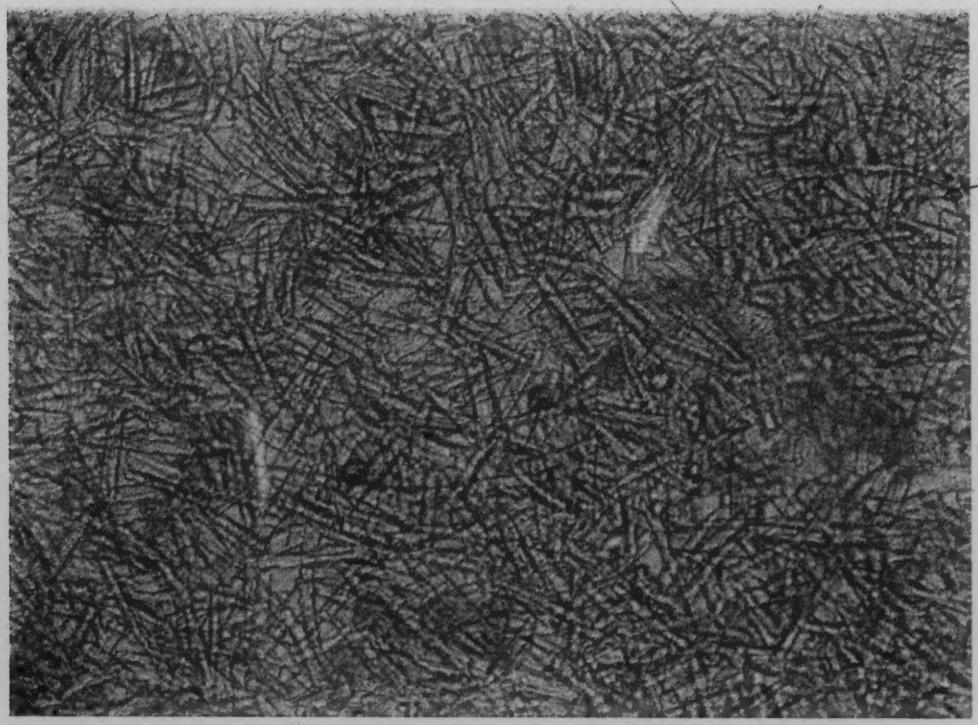

Figure 4-7. Myocytes isolated from the left ventricle of a heart infected via the intracoronary gene delivery technique (without histamine). Following primary and secondary collagenase digestion of the heart, myocytes were visualized for GFP expression. Both infected and non-infected myocytes were counted and the percentage of myocytes infected was determined.

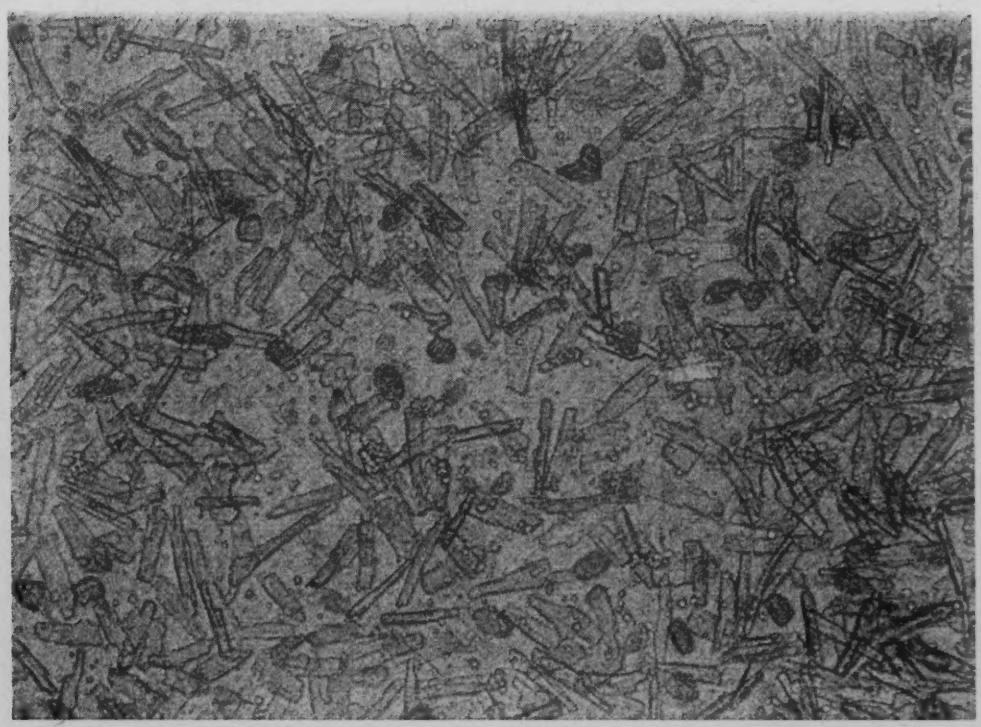

Figure 4-8. Myocytes isolated from the left ventricle of a heart infected using the intracoronary technique (in the presence of histamine). Following primary and secondary collagenase digestion of the heart, myocytes were visualized for GFP expression. Both infected and non-infected myocytes were counted and the percentage of myocytes infected was determined.

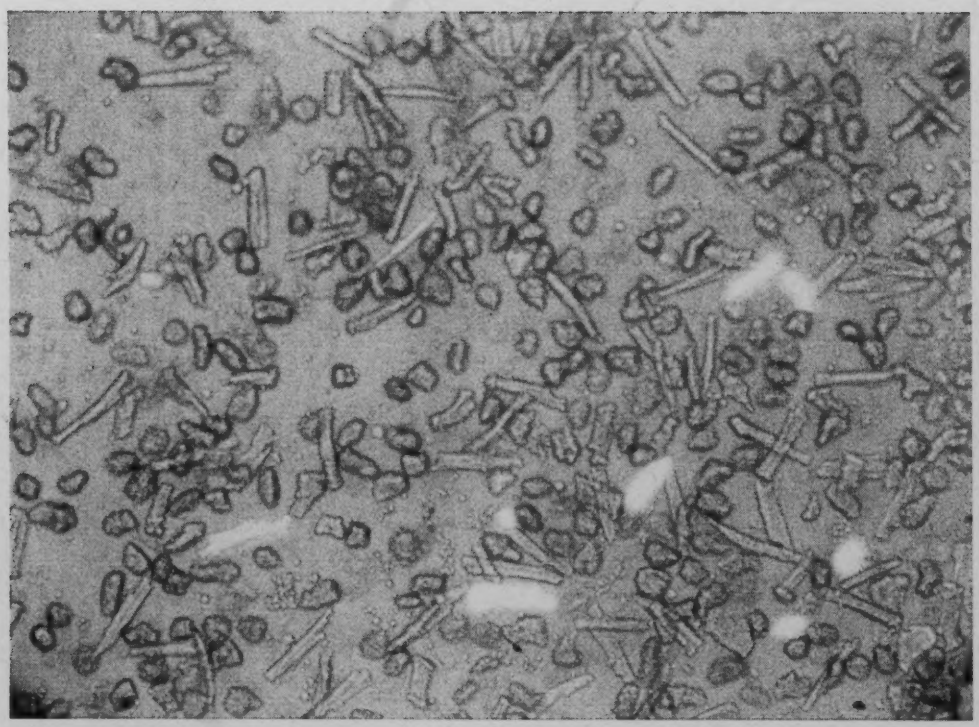

Figure 4-9. Myocytes isolated from the left ventricle of a heart infected via direct myocardial injection. Following primary and secondary collagenase digestion of the heart, myocytes were visualized for GFP expression. Both infected and non-infected myocytes were counted and the percentage of myocytes infected was determined.

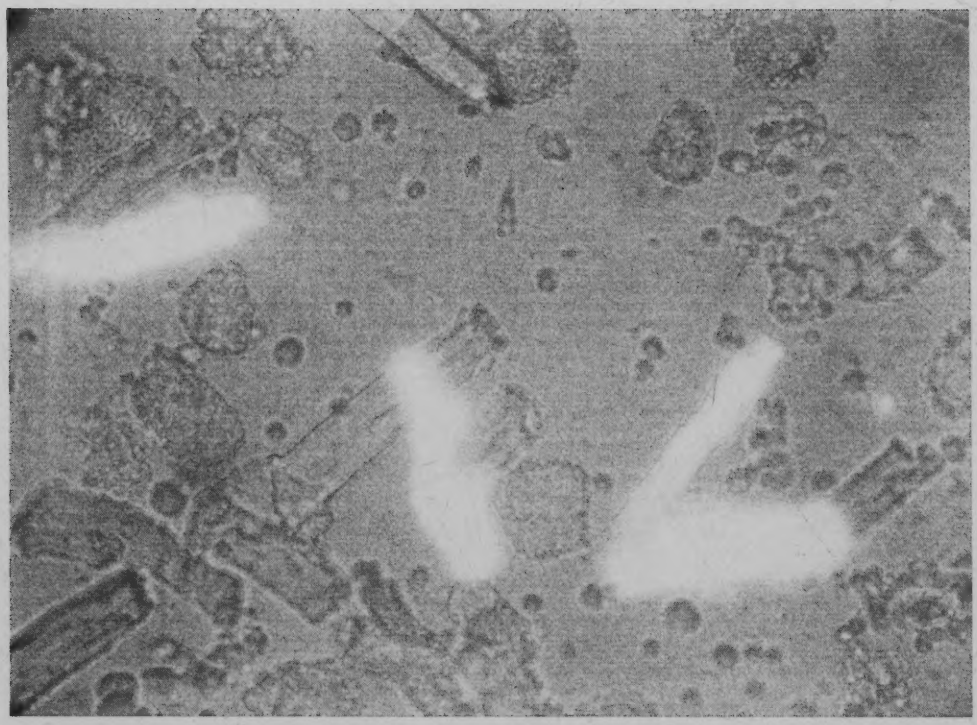

Figure 4-10. Myocytes isolated from a visually confirmed area that was infected via the direct myocardial injection gene delivery technique (visualized *in situ* and then cut-out). *In situ* visualization of the heart showed the location of viral injection. The area analyzed was approximately 3 mm around the infection area. Myocytes were isolated and visualized for fluorescence.

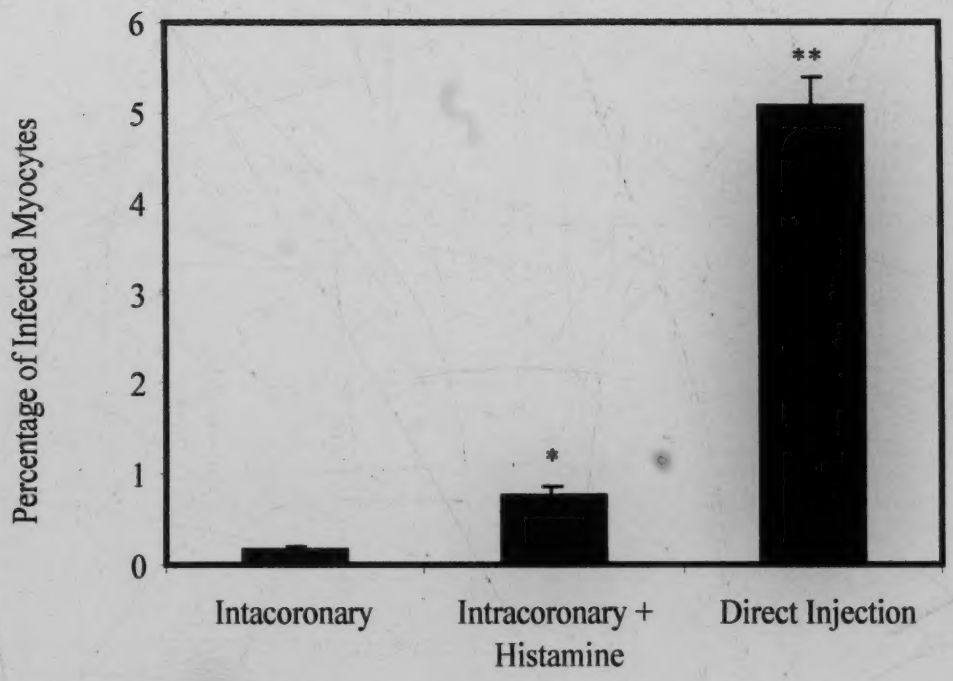

Figure 4-11. Comparison of efficiency of gene delivery techniques by quantifying the percentage of myocytes infected. Hearts infected via the intracoronary technique in the absence and presence of histamine (n=4 and n=3, respectively) and hearts from the direct injection technique (n=3) were subjected to collagenase digestion and the percentage of infected myocytes was determined.

*Significantly different from intracoronary technique (no histamine) group.

** Significantly different from intracoronary technique both in the absence and presence of histamine.

Table 4.2

Percentage of Myocytes Infected - Comparison of Gene Delivery Techniques.

	Percentage of Infected Myocytes
Intracoronary Delivery without Histamine (n=3)	0.20 ± 0.03
Intracoronary Delivery with Histamine (n=4)	0.80 ± 0.08 *
Direct Injection (whole left ventricle) (n=3)	5.1 ± 0.3 **
Direct Injection (injection site) (n=3)	36.4 ± 2.9 ***

Values are mean ± SE of the 'n' numbers shown in brakets

Significantly different from intracoronary technique (without histamine).

** Significantly different from intracoronary techniques (both without and with histamine).

*** Significantly different from intracoronary technique (without histamine) and direct injection (whole left ventricle).

Figure 4-12. *In situ* visualization of a heart infected with Ad-GFP through the intracoronary technique (with histamine). Following primary collagenase digestion, a section of the heart was visualized for the location of GFP expression.

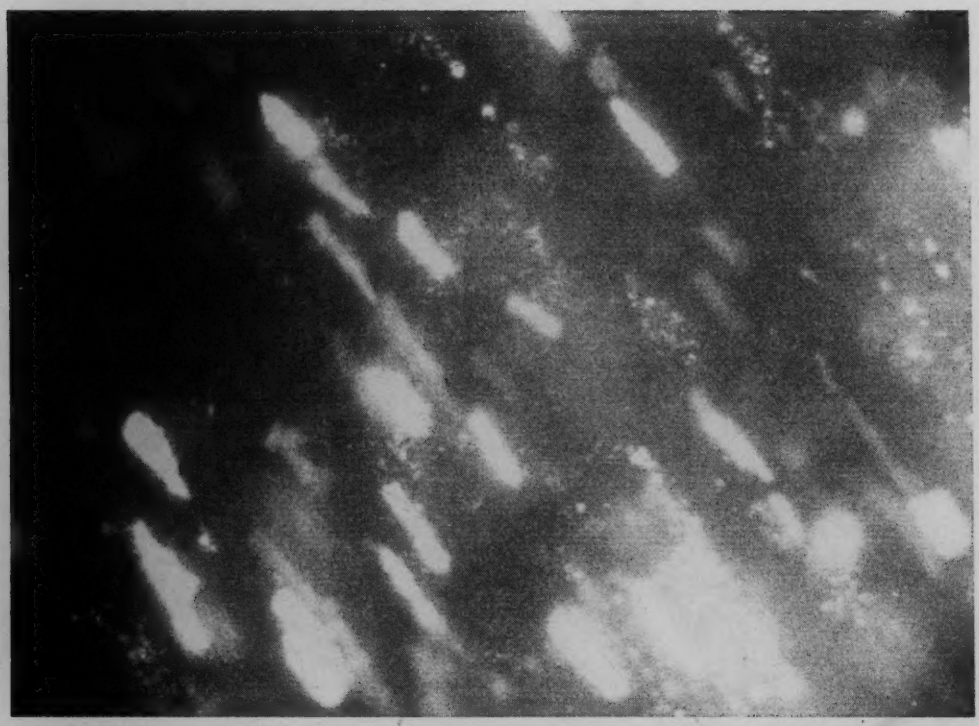

Figure 4-13. *In situ* visualization of myocytes infected with Ad-GFP following direct myocardial injection. Following primary collagenase digestion, a section taken from the left ventricle of an infected heart was visualized for GFP expression. This picture shows myocytes expressing GFP.

Figure 4-14. *In situ* visualization of site directly injected with Ad-GFP. Following primary collagenase digestion, the heart's surface was visualized for evidence of GFP expression. This picture shows the injection site and the area of GFP surrounding the injection site.

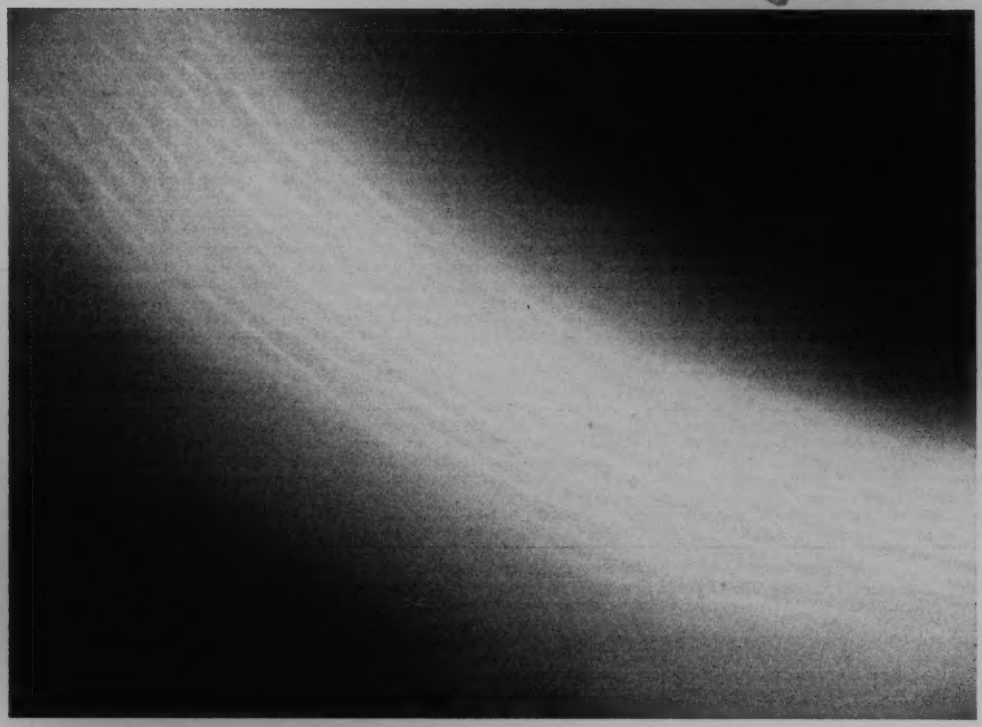

Figure 4-15. *In situ* visualization of aorta. Fluorescence in an aortic segment was examined from a heart infected with Ad-GFP via the intracoronary gene delivery technique in the absence of histamine.

A

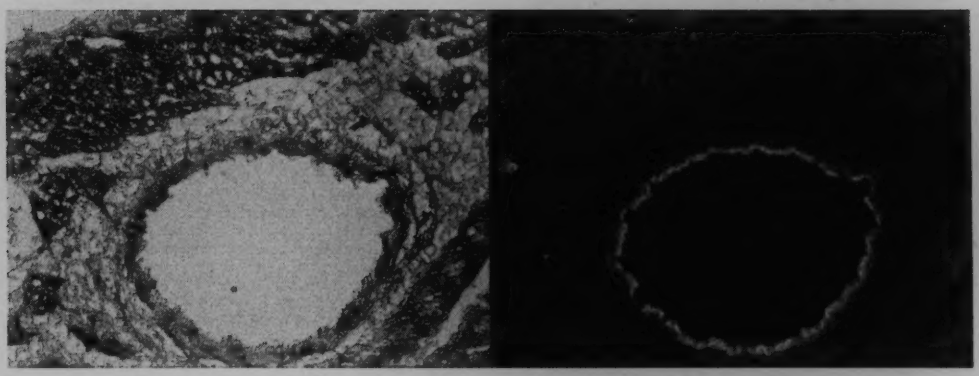

B

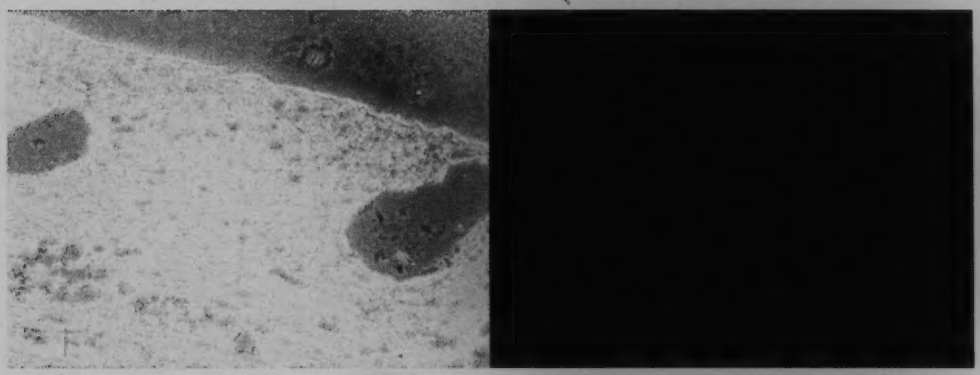

Figure 4-16. Heart slices taken from intracoronary infected heart and control (uninfected) hearts. (A) Heart slice taken from a heart infected via the intracornary delivery of Ad-GFP (in the presence of histamine). The left picture is a phase contrast and the picture on the right shows the same picture visualized for fluorescence. The GFP expression can be noted in the vessel wall of this epicardial coronary vessel. (magnification x 100). (B) Epicardium of control heart (uninfected with virus). The picture on the left is the phase contrast visualization of the epicardial vessel while the picture on the right shows the fluorescence visualization of the same picture. (magnification x 100).

Figure 4-17. Heart slice taken from a heart infected via the intracoronary technique (in the presence of histamine). These pictures visualize a section of the myocardium via phase contrast (left) and fluorescence (right). The picture shows a cell fluorescing in the myocardium. (magnification x 400).

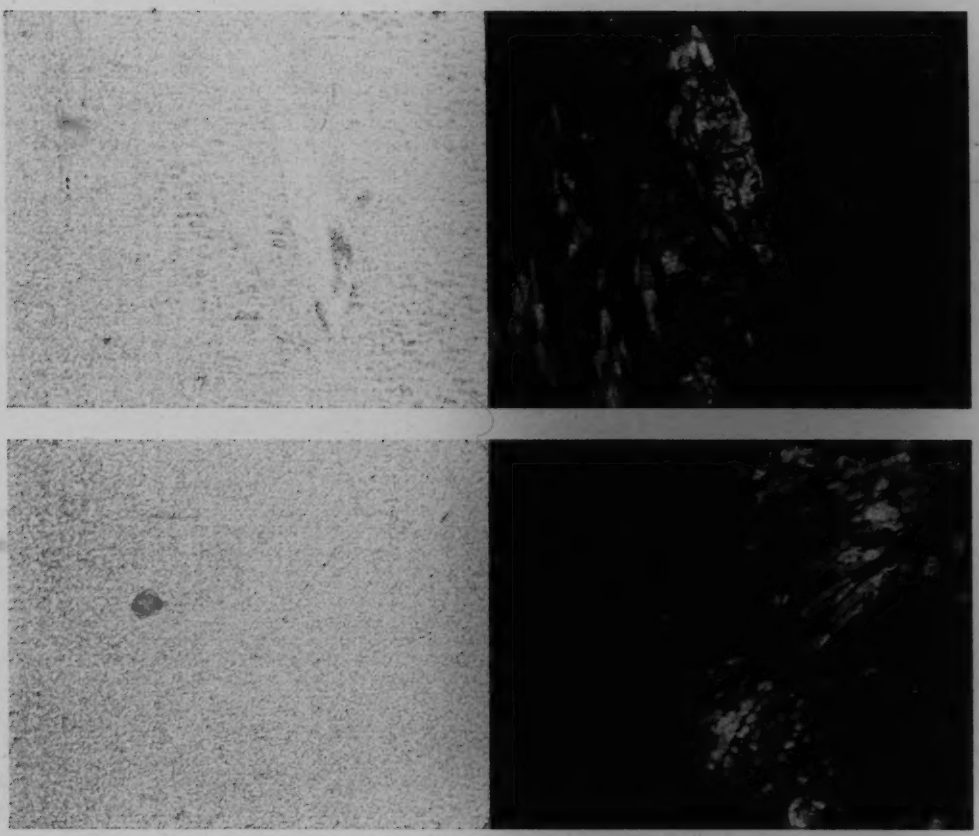

Figure 4-18. Slices taken from hearts infected via the direct myocardial injection technique. Slices were visualized for GFP fluorescence in the areas of the myocardium and epicardium. The fluorescence was visualized in the area where the viral injections were administered. These areas of the myocardium demonstrate substantial myocyte fluorescence indicating efficient viral infection of the myocardium where the virus was injected. The pictures on the left are phase contrast of the fluorescent pictures (right) so that the area of infection could be shown. The phase contrast pictures show that the areas of th e heart fluorescing are the cardiac myocytes in the myocardium. (magnification x 100).

Table 4.3

Experimental Fate of Hearts Infected Through Different Gene Delivery Techniques

	I	I + H	DI
Perfused	11	0	0
Immunoblotted	8	3	4
Collagenase Digestion	3	4	3
Sliced	0	3	4
Mortality	2	1	1

Number of hearts from each delivery group that was used for various experiments. I represents the hearts from the intracoronary technique in the absence of histamine. I + H represents the hearts infected via the intracoronary technique in the presence of histamine. DI represents the hearts infected via the direct myocardial injection technique. The number of rats that died in association with the various gene delivery techniques is represented via the mortality numbers.

DISCUSSION

The initial purpose of this project was to determine whether the delivery of genes coding for specific enzymes in the regulation of malonyl CoA levels could alter the fuel usage in the heart, as shown though cardiac perfusion and analysis. Using an intracoronary gene delivery technique originally documented by Barr et al. (1994), we first set out to determine whether we could efficiently deliver transgenes coding for constitutively active 5'AMP-activated protein kinase (caAMPK) directly to the myocyte. It was expected that efficient gene delivery to the cardiac myocytes via intracoronary gene delivery would occur in the amounts previously published (Hajjar et al. 1998).

The efficiency of gene delivery to the myocytes via the intracoronary delivery technique has been reported to be greater than 30% (Barr et. al 1994 and Hajjar et al. 1998) and other groups have referenced these numbers in their own experiments (Miao et al. 2000). However, when the perfusion results comparing GFP vs. caAMPK-GFP gene delivery showed no significant difference in cardiac fuel usage, it firstly had to be confirmed that the gene of interest was being expressed and, secondly, where it was being expressed.

AMPK is a stress kinase that has been shown to increase fatty acid oxidation in the heart (Saddik et al. 1993). Therefore, by delivering a constitutively active AMPK to the rat hearts via intracoronary gene delivery and then perfusing of these hearts,

determination of fatty acid oxidation rates in these hearts compared to control GFP delivery was performed. No difference in fatty acid oxidation rates was noted between groups. The first step in determining why there was no alteration in fatty acid oxidation during perfusion of the infected hearts was to confirm the expression of caAMPK in the hearts. Since the control gene was GFP and the experimental gene, caAMPK, co-expressed GFP, expression could be confirmed though immunoblotting of whole-heart homogenates and confirming the presence of GFP in the infected hearts. The immunoblot results demonstrated GFP in both the GFP and caAMPK-GFP infected hearts while no GFP was noted in the uninfected control. This confirmed that the virus was infecting cells in the heart and the gene was being translated to the protein. However, immunoblotting for c-myc revealed that c-myc was not being detected (c-myc was the tag used on the constitutively active AMPK gene since caAMPK can not be detected by available AMPK antibodies). This did not necessarily mean that caAMPK was not being expressed. It did, however, mean that caAMPK was not being detected in the infected tissues by immunoblot analysis.

GFP examination revealed the presence of this protein in all infected hearts, as would be expected. Thus, rather than determine why there was no detection of caAMPK through such means as testing other c-myc antibodies, or performing AMPK activity assays, the next step was to confirm that it was the myocytes that were the cardiac cell-type being infected. Since it is the cardiac myocytes that primarily oxidize fatty acids, confirmation that these cells were being infected was performed before further examination of caAMPK expression.

A powerful tool in the realm of cardiac *in vivo* gene delivery is the ability to isolate cardiac myocytes from the heart and examine them for GFP fluorescence. This technique of cardiac myocyte isolation is commonly used for electrophysiological analysis of cardiac myocytes (Shimoni et al. 1998). However, this technique has not been used for *in vivo* gene delivery experiments until recently. Prior confirmation of efficiency of myocyte infection was performed through heart slicing, staining, and visualizing the reporter gene of interest (ie. β-galactosidase) (Shohet et al. 2000 and Hajjar et al. 1998). Therefore, heart slices were stained to show the location of this protein. However, since the reporter gene used in our studies was GFP, which requires light rather than staining for identification, the ability to isolate the myocytes and visualize fluorescence in these cells is an experimental tool that has been rarely used to determine the efficiency of myocyte infection.

Neyroud et al. (2002) published data examining the efficiency of gene delivery to the myocytes following intracoronary gene delivery. This group utilized a technique whereby myocytes were isolated and quantified for gene expression. Their results showed <1% infection to the myocytes following the intracoronary delivery. This efficiency was far less than what had been previously published (30-50%) (Barr et al. 1994 and Hajjar et al. 1998). This efficiency of infection Neyroud et al. (2000) demonstrated correlates with the efficiency that our experiments showed. Although there was a different reporter gene used in our studies, it is arguable that GFP analysis following cardiac myocyte isolation allows for more precise quantification of infection since other cell-types in the heart were not being considered in the

quantification of myocyte expression such as may have been done in prior experiments.

It has been widely suggested by other groups that the endothelial barrier hinders efficient gene delivery to the myocytes through the intracoronary delivery technique (Shohet et al. 2000 and Ikeda et al. 2002). In order to overcome this barrier, different techniques that are aimed at disrupting the endothelial barrier have been used to increase the myocyte delivery efficiency. Shohet et al. (2000) published a novel technique whereby the adenoviral vector was attached to albumin coated microbubbles and intracoronary delivery of the microbubble-viral solution was performed in the presence of echocardiographic bursts. This technique allowed for disruption of the endothelial barrier since the cardiac-directed echocardiographic bursts destroyed the microbubbles, which in turn pulled the endothelial cells apart and allowed the virus entry to the myocytes. This technique, although elegant and efficient, was not a feasible technique for our laboratory since it required large amounts of virus for each animal. The microbubble technique required at least 2 ml of high-titer virus per animal, and half of this virus is lost during attachment of the virus onto the microbubble shell. Additionally, the large amounts of virus being delivered *in vivo* threatened the animals with hepatotoxicity since the liver is an organ that has no endothelial barrier and, as such, would be greatly infected by the delivered virus. This large amount of virus could also elicit a significant immune response and this risk was not one that attracted our laboratory to this technique.

Another method that addresses the endothelium as a barrier hindering efficient myocardial gene delivery is one published by Ikeda et al. (2002). This group suggests another means of disrupting the endothelium so that the virus can have greater access for infection to the myocytes. Their method of disrupting the endothelium with histamine, an endothelial disruptive agent, was initially shown to be efficient for gene delivery. Greelish et al. (1999) and Ikeda et al. (2002) incorporated this idea into their intracoronary gene delivery technique. The groups demonstrated that, in hamster models, the use of histamine increased the viral delivery of genes to cardiac myocytes. Therefore, since we demonstrated that the standard intracoronary delivery of genes to the heart was inefficient in terms of myocyte infection, we determined whether histamine could increase the efficiency of gene delivery to the cardiac myocyte.

Ikeda et al. (2000) and Svensson et al. (1999) use of histamine to disrupt the endothelium involved slightly different techniques of surgery; however, the idea of coronary perfusion of the virus was the same. Svensson et al. (1999) delivered histamine for 3 minutes through the coronary arteries to allow sufficient time for the histamine to disrupt the endothelium. In our studies, histamine was administered in the same way as the virus was delivered (cross-clamping) and then, following a 3 minute recovery period to allow the histamine to have its effects, the virus was delivered. It was hoped that including histamine into the delivery protocol would result in an increase of myocardial infection relative to the intracoronary technique in the absence of histamine. Since the purpose of administering the histamine was first

and foremost to determine whether it could increase the infection efficiency of viral delivery to the cardiac myocytes, the hearts were not perfused but were analyzed for presence of GFP and quantification of the percentage of myocytes infected in the left ventricle. Immunoblot analysis revealed that the presence of GFP in the infected hearts was similar to the amounts seen without histamine in the delivery protocol. However, when the hearts were examined to determine the percentage of cardiac myocytes infected, the number of myocytes infected had increased by 4-fold when histamine was added to the intracoronary protocol. However, the histamine only increased the number of infected myocytes from 0.20 ± 0.03% to 0.80 ± 0.08%. Therefore, even in the presence of an endothelial disruptive agent, the percentage of infected myocytes was still below 1%, a number presumed too low to determine any kind of alteration of fuel usage due to experimental gene delivery.

Based on these initial results, the focus of the project, which was initially to examine the effect on fuel usage in hearts that had been infected with a gene involved in cardiac metabolism, had switched to examining different methods of cardiac *in vivo* gene delivery so that the initial project could, at some future point, be undertaken.

As previously mentioned, groups had published on the success of the basic intracoronary gene transfer technique (delivery without histamine). Ken Walsh's group in Boston recently published a paper (Taniyama et al. 2002) examining the effect of Akt delivery on the heart. Although focus of the studies presented in the paper were not in the scope of our experiments, it was thought that a comparison of the gene delivery efficiency, as demonstrated by immunoblots of whole-heart

homogenates, would allow us to confirm that the surgeries were being performed in a similar manner that would result in similar efficiency of cardiac myocyte infection. Therefore, since we had the specific virus employed in that study, the paper's techniques were repeated precisely to determine whether or not our infection efficiencies were similar to those already presented in the literature. A second set of intracoronary deliveries was performed which mimicked Dr. Walsh's methods precisely. Similar to their studies, we demonstrated an increase in Akt levels in the infected hearts. These results demonstrated that our delivery technique was being performed in the same way as other groups who were examining the effects of gene delivery following intracoronary gene delivery.

Based on these results, we demonstrated that the intracoronary gene delivery technique was not infecting the percentage of myocytes that was being widely quoted in the literature. However, the infected hearts examined for presence of the protein coded for by the gene demonstrated the presence of the protein in the amount that has previously been documented (Taniyama et al. 2002). Since immunoblot analysis examines for the presence of the desired protein in whole heart homogenates, the possibility that the gene was actually being expressed in another cell-type in the heart besides the myocytes needed to be considered. Since the main hindrance to gene delivery to the heart through the intracoronary route is the endothelial barrier, we thought it possible that the vasculature of the heart was expressing the gene, rather than the cardiac myocytes. We therefore analyzed whether endothelial cells from infected hearts expressed GFP. Hearts infected by intracoronary gene delivery in the

presence of histamine were fixed, sliced, and visualized for the location of GFP fluorescence.

The idea that the vasculature was being infected preferentially was substantiated through *in situ* visualizations of infected hearts following intracoronary delivery of virus in the presence of histamine. When a small segment of the left ventricle was visualized *in situ*, myocytes were seen to be fluorescing. However, the fluorescence in the myocytes appeared to be outweighed by the fluorescence in vascular structures, presumably coronary arterioles. Additionally, when we analyzed a segment of the aorta (taken distal to the site of the cross-clamp) for GFP fluorescence *in situ*, the segment brightly fluoresced through all vasculature layers. Despite the mention that the aorta does not express the viral transgene (Hajjar et al. 1998), our data suggests otherwise.

We also examined whole heart slices to determine whether reporter gene fluorescence was present in the vasculature tissue. Hearts were fixed in formalin, embedded in paraffin, sliced and visualized to determine the location of GFP fluorescence. The three layers of the heart were all examined. By far the majority of the fluorescence was noted in the epicardial and myocardial vasculature. In the epicardium, larger coronary arterioles fluoresced brightly relative to control hearts. Additionally, in the myocardium, only endothelial cells surrounding capillaries expressed the GFP protein. All the heart slices visualized from 3 different infected hearts, the only cell-type that was fluorescing were those associated with the vasculature. Endothelial cells of the vasculature demonstrated fluorescence far greater

than any other cardiac cell-types. In all the slices visualized, no cardiac myocytes fluoresced. This does not necessarily imply that there was no infection of myocytes. It did, however, mean that the infection efficiency was too low to note any infection in these cell-types. This data, therefore, substantiated our quantification of myocyte infection from studies examining isolated cardiac myocytes. It also supported our theory that the cells of the vasculature were expressing the reporter gene preferentially over the cardiac myocytes. This expression in the vasculature-related cells would also explain why there was presence of GFP in whole-heart homogenates since the homogenates would contain these endothelial cells.

At this point of the study, our results suggested that the intracoronary technique was not an efficient means of infecting the cardiac myocytes, since our initial aim was to infect the myocytes rather than the coronary vasculature. Other groups had apparently greater success with the technique (Barr et al. 1994 and Hajjar et al. 1998) and were quoting great success of myocyte infection (>30%) using similar and smaller amounts and titer of virus that our laboratory used. However, as more data was published concerning the intracoronary gene delivery, it became apparent that other groups were experiencing difficulties in gene delivery efficiency similar to our group. Neyroud et al. (2002) found there to be <1% gene delivery efficiency to the myocytes and this observation of lower delivery efficiency was echoed by Wright et al. (2001).

Early studies noting high delivery efficiency used ß-galactosidase as a reporter gene while our experiments used GFP (Barr et al. 1994 and Hajjar et al. 1998).

Therefore, it could be suggested that these differences in reporter gene could account for the discrepancy of efficiency. However, Neyroud et al. (2000) examined both ß-galactosidase and GFP and reported efficiency of infection similar to ours. Additionally, Wright et al. (2001) also examined ß-galactosidase as a reporter gene to demonstrate infection and their findings were also similar to ours. Therefore, it was not necessarily the different reporter gene that was leading to the discrepancy in myocyte infection efficiencies. It is also of particular interest that no group, with the exception of Hajjar et al. (1998), has been able to demonstrate an infection efficiency anywhere as high as Barr et al. (1994) original estimation of >30% myocyte infection from intracoronary virus delivery. Although we do not choose to comment on the efficiency of infection noted by the other groups, we do choose to offer an explanation of why so little infection was noted in the myocytes following intracoronary delivery in our laboratory.

The heart slices used to determine the location of GFP fluorescence demonstrated a high level of infection in the coronary arterioles, identified as such due to the thick layer of vascular smooth muscle surrounding the vessel. Additionally, the aorta that was visualized *in situ* showed marked GFP fluorescence. However, smaller vessels in the myocardium demonstrated only sporadic GFP fluorescence. Thus, we suggest that the administered virus is not actually gaining access through the coronaries to the area of the myocytes following intracoronary delivery. A study examining the infection efficiency of myocytes following the *ex vivo* delivery of a re-circulating viral solution though Langendorff perfusion of rabbit hearts demonstrated a high level of myocyte

infection (Donahue et al. 1997). This study determined that efficient delivery of virus to myocytes occurred using re-circulation of virus model. Although a number of different parameters were examined that will be later addressed in this discussion, the study demonstrated good efficiency of delivery and this idea supports our presumption that the virus is infecting vasculature tissue before it reached the area of the myocardium which is essential for myocyte infection. Our studies, that were performed *in vivo* through an intracoronary clamp technique, did not allow for re-circulation of buffer and, perhaps, not even myocardial perfusion of the virus. This may be one reason why efficient myocyte infection did not occur despite performing the cardiac *in vivo* gene delivery in the same fashion as other groups that showed greater infection efficiency of myocytes (Hajjar et al. 1998). Other parameters that could be affecting the efficiency of viral delivery could be the time that the virus accessed the heart. Since the model of gene therapy we used is an *in vivo* technique, only a short clamping time can be allowed since the heart's blood outflow is prevented during the delivery due to aortic clamping. Hajjar et al. (1998), which developed the cross-clamping technique from the Barr et al. (1994) original procedure, states that only 10 seconds of clamping is necessary for gene delivery. It was actually this protocol that was used to determine the infection efficiency of >32%. The titer of virus used for these experiments (2×10^{10}) were within 2 fold of ours (3.85×10^{10}) and, therefore, it is not the concentration of virus that could be leading to the discrepancy of infection efficiency. Additionally, our gene deliveries were performed using a greater time for maintenance of the clamp during delivery.

Our group maintained the clamp for at least one minute. However, even studies published by Donahue et al. (1997) which, as previously mentioned, utilized an *ex vivo* viral re-circulation model, showed that exposure of the heart to the virus through the coronary arteries for an exposure time less than 5 minutes, results in less than 3% gene delivery. Donahue's quantification of gene delivery efficiency to the myocytes was similar to ours, as well as many other groups. Therefore, the time of virus exposure to the heart appears to have substantial effect on the efficiency of gene delivery. Donahue's study showed, using the *ex vivo*, re-circulation, intracoronary viral delivery model, that at least 45 minutes of virus exposure to the heart is required before 30% of the myocytes are infected. In short, previous quantifications of cardiac *in vivo* myocyte infection seemed overly optimistic relative to the percents our group showed. Recently, other groups that have also been examining the intracoronary gene delivery technique for gene delivery efficiency to cardiac myocytes have shown results similar to ours (Wright et al. 2001 and Neyroud et al. 2000).

The intracoronary delivery technique was initially attractive not only because of its supposedly high efficiency of delivery to the myocytes, but also because of the homogeneity of delivery to the myocardium. However, we also considered another gene delivery technique published that has demonstrated efficiency of delivery to the myocytes. This technique involves direct injection of the virus into the myocardium. This was actually the first technique described for *in vivo* gene therapy to the heart (Acsadi et al. 1991). The technique was used to deliver genes to the heart after preliminary studies demonstrated that skeletal muscle readily took-up the injected

genetic information and thus, it was proposed that other striated muscle, such as the heart, may actually uptake the virus as well. It was originally shown by Acsadi et al. (1991) that directly injecting genetic material into the myocardium resulted in expression of that genetic information. Groups subsequently have employed this technique since it allows for introduction of the genetic material directly into the target cells of interest without infecting the vascular component of the heart, such as has been demonstrated with the intracoronary technique (Kornowski et al. 2000). Directly injecting the virus into the myocardium has been critiqued because it offers only a focal expression of the transgene around the injection area, although this approach demonstrates expression of that gene of interest within the target myocytes (Pellegrini et al. 1998). Therefore, since our efficiency of infecting myocytes via the intracoronary technique had not been overly successful, we injected the virus directly into the myocardium and compare the efficiency of delivery to the intracoronary technique.

In order to perform a controlled experiment so that the efficiency of the delivery techniques could be directly compared, the method of surgery was the same in both groups. The amount of virus directly injected into the left ventricle was 50% of that perfused through the whole heart for the intracoronary technique. For the intracoronary technique, 200 µl of Ad-GFP (3.85×10^{10} pfu/ml) was perfused through the heart which would, in theory, allow for half, 100 µl, of this viral solution to enter the left coronary artery to infect the myocardium of the left ventricle. Therefore, we proposed using a similar amount of virus to the intracoronary techniques so that the

results could be directly compared. 10 µl of virus was directly injected into 10 different sites of the left ventricle, resulting in a total of 100 µl injected into the left myocardial wall.

The hearts were examined for presence and location of the GFP protein, and quantification of myocyte expression of GFP. Heart homogenates taken from the left ventricle were immunoblotted for presence of GFP and these hearts demonstrated marked GFP expression, greater than that in the intracoronary delivery groups (in the absence and presence of histamine). Some of these hearts were also subjected to cardiac myocyte isolation procedures in order to quantify the percentage of myocytes infected via this direct injection technique. Left ventricular segments were isolated and the myocytes were removed for visualization. The percentage of myocytes expressing GFP was determined to be 5.1 ± 0.3%. Additionally, following the removal of a segment of the left ventricle for quantification of the percentage of myocytes infected in the whole left ventricle, the heart was visualized *in situ* to determine whether there were any additional areas that demonstrated GFP fluorescence. Areas that demonstrated fluorescence were removed and subjected to further collagenase digestion to determine the percentage of myocytes infected directly around the injection area. When the heart was visualized *in situ* and an injection area was noted, it was dissected out of the heart to an accuracy of 3mm around the injection site. This therefore allowed for a 9 mm^2 segment (surface area) to be subjected to further to collagenase digestion. The individual myocytes were visualized and quantified for fluorescence and it was shown that directly around the

injection site, 36.4 ± 2.9% of the myocytes were infected. Finally, hearts that were directly injected with virus were fixed, embedded, sliced and visualized for location of GFP fluorescence. All GFP fluorescence occurred in the myocardium and the myocytes clearly demonstrated GFP presence. No areas of the epicardium demonstrated GFP fluorescence. It was apparent that the area that was infected in the myocardium was directly surrounding the injection site since the myocyte GFP fluorescence appeared in patches.

Therefore, our results showed an increase of efficiency of myocyte infection through the direct injection of virus into the myocardium as compared with the intracoronary delivery technique (both in the absence and presence of histamine). The percentage of myocytes infected increased by a factor of 25 when using the direct injection technique. Additionally, our heart-slice results demonstrated that the expression of GFP appeared only in the myocytes in the myocardium, the area that the virus was injected into, and not in the vasculature such as had been noted during intracoronary delivery.

In terms of efficiency of viral delivery to the myocytes, the direct injection technique appears to be superior to the intracoronary delivery technique. However, it has been mentioned that the direct injection technique only allows for focal expression of the gene around the area that the virus is injected (Acsadi et al. 1991 and Pellegrini et al. 1998) and, therefore, its use in examining functional and metabolic changes in the heart due to delivery of genes coding for enzymes involved in cardiac metabolism is questionable. This is because in order for changes in

metabolism to be noted, in theory, myocytes from all areas of the heart need to be infected. This was initially why the intracoronary technique was so appealing to our group. However, the overall percentage of myocytes infected in the left ventricle was far greater when using the direct injection technique.

Despite this increase, there was still only approximately 5% of myocytes infected in the whole left ventricle. When the percentage of myocytes from directly around the injection area was determined approximately 35% were infected. This number of infected myocytes was far more promising; however, achieving this percentage overall would require injecting more areas of the left ventricle. Pellegrini et al. (1998) estimated that myocytes within 1-2 mm around the injection site are infected. Therefore, in order to achieve homogenous, efficient gene delivery to the whole left ventricle using direct injection into the myocardium would theoretically require injecting virus into the left ventricle within every 2-3 mm. This, although appealing as a means of infecting the whole heart, is not overly feasible since the injection of virus into the heart results in areas of tissue damage around the injection site (Guzman et al. 1993 and French et al. 1994). Thus, if all areas of the left ventricle were infected, the necrosis could be substantial and the effects on the heart could be detrimental. Therefore, although the direct injection technique used was effective at increasing the percentage of myocytes infected relative to the intracoronary techniques, the percentage of myocytes infected (~5%) is still too low to determine any kind of metabolic change induced by the delivery of genes involved in cardiac metabolism (such as AMPK).

Therefore, we still have no technique of gene delivery that could allow us to examine the effects of delivering genes for AMPK and MCD *in vivo* to alter cardiac fatty acid oxidation. Thus, although this study was effective in terms of determining the percentage of myocytes infected from different *in vivo* gene delivery techniques and possibly cautioning other groups to their use, it was not successful for determination of the metabolic effects of over-expressing AMPK in the heart.

SUMMARY

We hypothesized that viral delivery to the heart via the well-documented intracoronary gene delivery technique would result in an efficiency of infection similar to that already published. However, when we quantified the efficiency of cardiac myocyte infection via cardiac myocyte isolation, the efficiency of infection was far lower than previously published. Therefore, since the first objective of the study was not achieved, we were unable to perform subsequent experiments to examine whether our second hypothesis that over-expressing AMPK and MCD in hearts would result in increased fatty acid oxidation rates.

Thus, we continued to examine different cardiac gene delivery techniques to examine the efficiency of cardiac myocyte infection rendered from delivery of genes via these various techniques. We determined that the most efficient gene delivery technique was the direct injection technique that infected myocytes in the area of the injection site to the myocardium. Hearts infected by the intracoronary technique in the presence and absence of histamine did not demonstrate efficient myocardial infection, rather infection was noted primarily in the cells of the vasculature.

It is hoped that the results from this study will caution other groups to the use of these delivery techniques since the efficiency of myocyte infection achieved through these *in vivo* gene delivery techniques may be lower than desired for examination of the effects of certain delivered transgenes.

REFERENCES

Acsadi G, Jiao SS, Jani A, Duke D, Williams P, Chong W, Wolff JA. Direct gene transfer and expression into rat heart in vivo. *New Biol.* 1991 Jan;3(1):71-81.

Barr E, Carroll J, Kalynych AM, Tripathy SK, Kozarsky K, Wilson JM, Leiden JM. Efficient catheter-mediated gene transfer into the heart using replication-defective adenovirus. *Gene Ther.* 1994 Jan;1(1):51-8.

Donahue JK, Kikkawa K, Johns DC, Marban E, Lawrence JH. Ultrarapid, highly efficient viral gene transfer to the heart. *Proc Natl Acad Sci* USA. 1997 Apr 29;94(9):4664-8.

Dyck JR, Barr AJ, Barr RL, Kolattukudy PE, Lopaschuk GD. Characterization of cardiac malonyl-CoA decarboxylase and its putative role in regulating fatty acid oxidation. *Am J Physiol.* 1998 Dec; 275(6 Pt 2):H2122-9.

French BA, Mazur W, Geske RS, Bolli. Direct *in vivo* gene transfer into porcine myocardium using replication-deficient adenoviral vectors. *Circulation.* 1994 Nov;90(5):2414-24.

Greelish JP, Su LT, Lankford EB, Burkman JM, Chen H, Konig SK, Mercier IM, Desjardins PR, Mitchell MA, Zheng XG, Leferovich J, Gao GP, Balice-Gordon RJ, Wilson JM, Stedman HH. Stable restoration of the sarcoglycan complex in dystrophic muscle perfused with histamine and a recombinant adeno-associated viral vector. *Nat Med.* 1999 Apr;5(4):439-43.

Guzman RJ, Lemarchand P, Crystal RG, Epstein SE, Finkel T. Efficient gene transfer into myocardium by direct injection of adenovirus vectors. *Circ Res.* 1993 Dec;73(6):1202-7.

Hajjar RJ, Schmidt U, Matsui T, Guerrero JL, Lee KH, Gwathmey JK, Dec GW, Semigran MJ, Rosenzweig A. Modulation of ventricular function through gene transfer *in vivo*. *Proc. Natl. Acad. Sci. USA*. 1998 Apr 28;95(9):5251-6.

Hardie DG. Regulation of fatty acid and cholesterol metabolism by the AMP-activated protein kinase. *Biochim Biophys Acta.* 1992 Feb 12;1123(3):231-8.

Ikeda Y, Gu Y, Iwanaga Y, Hoshijima M, Oh SS, Giordano FJ, Chen J, Nigro V, Peterson KL, Chien KR, Ross J Jr. Restoration of deficient membrane proteins in the cardiomyopathic hamster by *in vivo* cardiac gene transfer. *Circulation*. 2002 Jan 29;105(4):502-8.

Kannel WB, McGee D, Gordon T. A general cardiovascular risk profile: the Framingham Study. *Am J Cardiol.* 1976 Jul;38(1):46-51.

Kornowski R, Fuchs S, Epstein SE, Branellec D, Schwartz B. Catheter-based plasmid-mediated transfer of genes into ischemic myocardium using the pCOR plasmid. *Coron Artery Dis.* 2000 Dec;11(8):615-9.

Kudo N, Gillespie JG, Kung L, Witters LA, Schulz R, Clanachan AS, Lopaschuk GD. Characterization of 5'AMP-activated protein kinase activity in the heart and its role in inhibiting acetyl-CoA carboxylase during reperfusion following ischemia. *Biochim Biophys Acta.* 1996 May 31;1301(1-2):67-75.

Laham RJ, Simons M, Tofukuji M, Hung D, Sellke FW. Modulation of myocardial perfusion and vascular reactivity by pericardial basic fibroblast growth factor: insight into ischemia-induced reduction in endothelium-dependent vasodilatation. *J Thorac Cardiovasc Surg.* 1998 Dec;116(6):1022-8.

Lopaschuk GD, Belke DD, Gamble J, Itoi T, Schonekess BO. Regulation of fatty acid oxidation in the mammalian heart in health and disease. *Biochim Biophys Acta.* 1994 Aug 4;1213(3):263-76.

Miao W, Luo Z, Kitsis RN, Walsh K. Intracoronary, adenovirus-mediated Akt gene transfer in heart limits infarct size following ischemia-reperfusion injury *in vivo*. *J Mol Cell Cardiol*. 2000 Dec;32(12):2397-402.

Neyroud N, Nuss HB, Leppo MK, Marban E, Donahue JK. Gene delivery to cardiac muscle. *Methods Enzymol.* 2002;346:323-34.

Pellegrini C, O'Brien T, Yap J, Jeppsson A, Tazelaar HD, McGregor CG. Systematic evaluation of distribution of transgene expression after adenovirus-mediated gene transfer to the transplanted heart. *Transpl Int.* 1998;11(5):373-7.

Saddik M, Gamble J, Witters LA, Lopaschuk GD. Acetyl-CoA carboxylase regulation of fatty acid oxidation in the heart. *J Biol Chem.* 1993 Dec 5;268(34):25836-45.

Shimoni Y, Light PE, French RJ. Altered ATP sensitivity of ATP-dependent K+ channels in diabetic rat hearts. *Am J Physiol.* 1998 Oct;275(4 Pt 1):E568-76.

Shohet RV, Chen S, Zhou YT, Wang Z, Meidell RS, Unger RH, Grayburn PA. Echocardiographic destruction of albumin microbubbles directs gene delivery to the myocardium. *Circulation.* 2000 Jun 6;101(22):2554-6.

Svensson EC, Marshall DJ, Woodard K, Lin H, Jiang F, Chu L, Leiden JM. Efficient and stable transduction of cardiomyocytes after intramyocardial injection or intracoronary perfusion with recombinant adeno-associated virus vectors. *Circulation.* 1999 Jan 19;99(2):201-5.

Taniyama Y, Walsh K. Elevated myocardial Akt signaling ameliorates doxorubicin-induced congestive heart failure and promotes heart growth. *J Mol Cell Cardiol.* 2002 34:1241-7.

Wright MJ, Wightman LM, Latchman DS, Marber MS. *In vivo* myocardial gene transfer: optimization and evaluation of intracoronary gene delivery *in vivo*. *Gene Ther*. 2001 Dec;8(24):1833-9.

CHAPTER 5 – DISCUSSION AND CONCLUSIONS

CHAPTER 5 – Discussion and Conclusions

The ability to alter cardiac metabolism has many experimental and clinical applications. Through nutritional deficiency and *in vivo* gene transfer experimental models, we set out to determine if cardiac metabolic rates could be altered since it may have potential use for the treatment of diabetes and ischaemic heart disease (both of which are associated with alterations in cardiac metabolism (Kannel et al. 1976 and Lopaschuk et al. 1994)). Nutritional deficiency has been shown to elicit an increase in fatty oxidation and MCD activity and expression (Van der Lee et al. 2001 and Young et al. 2001). Through the *in vivo* cardiac delivery of transgenes coding for the MCD protein, we sought to mimic the effects of metabolic gene expression seen during fasting without any nutritional deficiency. The first step in this study determined the alterations in cardiac metabolism induced by a 72 hour period of fasting. Specifically, we examined the expression of genes involved in the regulation of malonyl CoA levels such as AMPK, ACC and MCD. Our data from the fasting study demonstrated an increase in both the rate of cardiac fatty acid oxidation and MCD activity such as had been previously shown (Van der Lee et al. 2001 and Young et al. 2001). However, we noted no changes in the expression of MCD, AMPK or ACC. The next step was delivering a transgene coding for constitutively active AMPK (caAMPK), whose over-expression *in vitro* (using an adenovirus vector for this transgene) to cultured myocytes had elicited an increase in fatty acid oxidation (unpublished data – studies performed by Judith Altarejos). Although our goal was to examine the effects

of over-expressing MCD *in vivo*, we began by delivering the caAMPK due to the initial success of infection of the cultured myocytes.

Whereas *in vitro* infection simply requires incubating cells in culture with the virus, *in vivo* gene transfer is more technically challenging. The success of delivering genes to the heart *in vivo* has been documented by Hajjar et al. (1998). This group modified an earlier intracoronary gene delivery technique designed by Barr et al. (1994). Both Hajjar and Barr's group quantified the success of this technique in terms of efficiency of myocyte infection to be greater than 30% (Barr et al. 1994 and Hajjar et al. 1998). Thus, we used the technique published by Hajjar et al. (1998) to infect rat hearts with the genes coding for green fluorescent protein (GFP) and caAMPK (co-expressing GFP).

Five days following the gene delivery, we determined the metabolic rates of glucose and palmitate within these hearts through the isolated working heart model (Lopaschuk et al. 1997). Perfusion results demonstrated no change in either glucose or palmitate oxidation. Thus, the next step of the study was to determine the efficiency of myocyte infection from the intracoronary delivery of recombinant adenovirus. When we isolated myocytes and visualized them for GFP fluorescence, our results showed that less than 1% of myocytes were infected from intracoronary gene delivery, a percentage far lower than shown by other groups (Barr et al. 1994 and Hajjar et al. 1998). Therefore, this study switched from examining *in vivo* delivery of genes involved in the regulation of cardiac metabolism, to one where we examined the efficiency of different gene transfer models.

The fasting study was another approach to modify metabolic gene expression. Since the *in vivo* gene delivery study was diverging from the objective due to the inefficiency of gene delivery from the intracoronary technique, we decided to further examine the nutritionally deprived hearts with respect to PPARα, MCD, ACC (total and phosphorylated) and AMPK (total and phosphorylated) expression levels. Additionally, we examined triacylglycerol and fatty acid levels in the hearts and plasma. Full discussion of the effects of fasting and the role of PPARα in regulating alterations in fatty acid oxidation is provided in Chapter 3. Additionally, Chapter 4 discusses the *in vivo* gene transfer techniques examined. It is hoped that the results obtained from the *in vivo* study will allow for the development of an appropriate gene delivery technique so that the initial objective of examining the cardiac metabolic effects of over-expressing MCD and caAMPK can be performed in future experiments.

Limitations

- Although we determined the expression levels of MCD, ACC and AMPK in the fasting study, we did not examine the transcription levels of the genes. Since PPARα is a transcription factor, changing levels of transcription of these enzymes would be detected via mRNA levels, not expression levels.
- We did not perform a time-course of the effects of fasting. Rather, we used a 72 hr fasting period and examined the effects of this nutritional deficiency on cardiac metabolism.

- Our results showed that alterations in cardiac metabolism do not occur in association with alterations in malonyl CoA levels. However, our studies examining the levels of this CoA ester determine levels in whole heart homogenates. This technique does not allow for determination of malonyl CoA compartmentalization. It is possible that the levels of malonyl CoA available to regulate CPT-1 transport of acyl CoA alters during fasting but we are not detecting this change due to our protocol.
- We did not perform a time-course for the expression of GFP following *in vivo* gene transfer. Rather, we based our recovery time / expression period on previously published data showing the time-course of expression of genes delivered via the adenovirus vector (see Chapter 1 for explanation of the adenovirus as a gene delivery vector).
- It is possible that our quantification of infected myocytes is an underestimation. Some myocytes may be infected with small amounts of virus and/or only expressing small amounts of GFP. Since our quantification technique required visualizing myocytes for fluorescence, those expressing only small amounts of GFP may not be being detected due to low levels of fluorescence. However, our quantification of the percentage of myocytes infected via the intracoronary technique is in accordance with recently published data (see Chapter 4 – Discussion for full explanation).
- Aortic clamping, although suggested to be efficient for intracoronary gene transfer (see Chapter 1 for explanation of why clamping is used), may not

allow for full coronary perfusion of the virus. This may explain why we are noting all the expression in the larger coronary arteries.

Future Directions

- Examine the mRNA levels of MCD, ACC and AMPK in the fasted hearts to determine whether the transcription levels of these enzymes are altered relative to control hearts.
- Examine the direct myocardial injection technique further to determine whether more injection sites allow for greater infection without high levels of necrosis which could affect the functional capabilities of the infected hearts.
- Examine the area around the direct injection site to determine the distance around injection site that the transgene is expressed.
- The use of the mouse as the *in vivo* model for direct myocardial injection may allow for greater efficiency of myocyte infection. Since the mouse heart is smaller, the use of the same amount of virus per animal would theoretically allow for greater infection. (other groups are currently examining this). Additionally, our lab has the ability to perform working heart experiments on mice hearts so that metabolic alterations induced by the delivery of transgenes could be determined using the mouse model for gene therapy.

- Groups examining the intracoronary technique have evolved the technique to include cardioplege and cooling (Hoshijima et al. 2002). The basis for their technique is that through histamine administration, cooling and cardioplegia, hamster hearts can be stopped and cardiac metabolism slowed while the virus is being perfused retrogradely though the carotid artery. We did try this technique on our rat models (data not shown) and all animals died following the procedure. However, the examination of this technique using hamster models may allow us to determine the increase in efficiency of infection.
- The titer of virus we are using could be increased. This would allow for greater concentration of virus to be delivered without altering the volume which would be especially effective with the direct myocardial injection technique.
- Once an efficient gene transfer technique has been developed, continue examining the effects of over-expressing MCD and AMPK in the heart. Also, determining the effects on cardiac metabolism following delivery of genes coding for the dominant negative constructs for MCD and AMPK would be a great complimentary experiment to the over-expression.

REFERENCES

Barr E, Carroll J, Kalynych AM, Tripathy SK, Kozarsky K, Wilson JM, Leiden JM. Efficient catheter-mediated gene transfer into the heart using replication-defective adenovirus. *Gene Ther.* 1994 Jan;1(1):51-8.

Hajjar RJ, Schmidt U, Matsui T, Guerrero JL, Lee KH, Gwathmey JK, Dec GW, Semigran MJ, Rosenzweig A. Modulation of ventricular function through gene transfer *in vivo*. *Proc. Natl. Acad. Sci. USA*. 1998 Apr 28;95(9):5251-6.

Hoshijima M, Ikeda Y, Iwanaga Y, Minamisawa S, Date MO, Gu Y, Iwatate M, Li M, Wang L, Wilson JM, Wang Y, Ross J Jr, Chien KR. Chronic suppression of heart-failure progression by a pseudophosphorylated mutant of phospholamban via *in vivo* cardiac rAAV gene delivery. *Nature Med.* 2002 Aug;8(8):864-71.

Kannel WB, McGee D, Gordon T. A general cardiovascular risk profile: the Framingham Study. *Am J Cardiol.* 1976 Jul;38(1):46-51.

Lopaschuk GD, Belke DD, Gamble J, Itoi T, Schonekess BO. Regulation of fatty acid oxidation in the mammalian heart in health and disease. *Biochim Biophys Acta.* 1994 Aug 4;1213(3):263-76.

Lopaschuk GD, Barr RL. Measurements of fatty acid and carbohydrate metabolism in the isolated working rat heart. *Mol Cell Biochem.* 1997 Jul;172(1-2):137-47.

Young ME, Goodwin GW, Ying J, Guthrie P, Wilson CR, Laws FA, Taegtmeyer H. Regulation of cardiac and skeletal muscle malonyl-CoA decarboxylase by fatty acids. *Am J Physiol Endocrinol Metab.* 2001 Mar;280(3):E471-9.